

Potomac Tributary Summary:  
A summary of trends in tidal water quality and  
associated factors, 1985-2022.

August 19, 2025

Prepared for the Chesapeake Bay Program (CBP) Partnership by the CBP  
Integrated Trends Analysis Team (ITAT)



*Citation:* Sullivan, B., Gootman, K., Gunnerson, A., Betts, S., Duran, G., Johnson, C., Mason, C., Perry, E., Bhatt, G., Keisman, J., Webber, J., Harcum, J., Lane, M., Devereux, O., Zhang, Q., Murphy, R., Karrh, R., Butler, T., Wei, Z. 2025. Potomac Tributary Summary: A summary of trends in tidal water quality and associated factors, 1985 - 2022. Chesapeake Bay Program, Annapolis MD.

*Authors:* Breck Sullivan (U.S. Geological Survey, USGS), Kaylyn Gootman (Environmental Protection Agency, EPA), Alex Gunnerson (USGS), Sarah Betts (Franklin and Marshall College), Gabriel Duran (Chesapeake Research Consortium), Cindy Johnson (Department of Environmental Quality), Chris Mason (USGS), Elgin Perry (Perry LLC.), Gopal Bhatt (Penn State), Jeni Keisman (USGS), Jimmy Webber (USGS), Jon Harcum (Tetra Tech), Mike Lane (Old Dominion University), Olivia Devereux (Devereux Consulting), Qian Zhang (University of Maryland Center for Environmental Science, UMCES), Rebecca Murphy (UMCES), Renee Karrh (Maryland Department of Natural Resources), Tom Butler (EPA), Vanessa Van Note (EPA), Zhaoying (Angie) Wei (UMCES).

Any use of trade, firm, or product names is for descriptive purposes only and does not imply endorsement by the U.S. Government.

## Contents

1. Purpose and Scope .....	4
2.1 Watershed Physiography .....	6
2.2 Land Use .....	7
2.3 Tidal Waters and Stations .....	9
3. Tidal Water Quality Status .....	11
4. Tidal Water Quality Trends .....	14
4.1 Surface Total Nitrogen .....	14
4.2 Surface Total Phosphorus .....	17
4.3 Surface Chlorophyll <i>a</i> : Spring (March-May) .....	19
4.4 Surface Chlorophyll <i>a</i> : Summer (July-September) .....	23
4.5 Secchi Disk Depth .....	27
4.6 Summer Bottom Dissolved Oxygen (June-September) .....	31
4.7 Surface Water Temperature .....	32
5. Factors Affecting Trends .....	35
5.1 Watershed Factors .....	35
5.1.1. Effects of Physical Setting .....	35
5.1.2. Estimated Nutrient and Sediment Loads .....	38
5.1.3. Expected Effects of Changing Watershed Conditions .....	40
5.1.4. Best Management Practices (BMPs) Implementation .....	43
5.1.5. Flow-Normalized Watershed Nutrient and Sediment Loads .....	44
5.2 Tidal Factors .....	45
5.2.1. Watershed and Estuarine Volume .....	46
5.2.2. Long-term Changes in Water Quality Longitudinal Profiles .....	51
5.3 Changing Environmental Conditions .....	56
5.3.1. Extreme Weather and Increased Precipitation .....	56
5.3.2. Warming Water Temperatures .....	61
5.3.3. Sea-Level Rise .....	63
5.3.4. Connecting to Living Resources .....	64
References .....	65
Appendix A: Glossary of Terms .....	72
Appendix B: Additional Plots .....	77

## 1. Purpose and Scope

The Potomac Tributary Summary outlines change over time for a suite of monitored tidal water quality parameters and associated potential drivers of those trends for the period 1985–2022 and provides a brief description of the current state of knowledge explaining these observed changes. Water quality parameters described include surface (above pycnocline) total nitrogen (TN), surface total phosphorus (TP), surface water temperature (WTEMP), spring (March-May) and summer (July-September) surface chlorophyll *a*, summer bottom (below pycnocline) dissolved oxygen (DO) concentrations, and Secchi disk depth (a measure of water clarity). Results for annual bottom TP, bottom TN, surface ortho-phosphate (PO<sub>4</sub>), surface dissolved inorganic nitrogen (DIN), surface total suspended solids (TSS), and summer surface DO concentrations are provided in an Appendix B. Drivers discussed include physiographic watershed characteristics, changes in TN, TP, and sediment loads from the watershed to tidal waters, expected effects of changing land use, and implementation of nutrient management and natural resource conservation practices. Factors internal to estuarine waters that also play a role as drivers are described including biogeochemical processes, physical forces such as wind-driven mixing of the water column and increase in rainfall intensity and volume, and biological factors such as phytoplankton biomass and the presence of submerged aquatic vegetation. Continuing to track water quality response and investigating these influencing factors are important steps to understanding water quality patterns and changes in the Potomac River. The intended audiences for this report include, but are not limited to, 1) technical managers within jurisdictions who use tidal water quality to inform management decisions, 2) local watershed organizations that are trying to understand these analyses and working to connect them to their local area(s), and 3) federal, state, and academic researchers. Figure 1 presents a conceptual model highlighting these intended audiences. Our goal is for the Tributary Summary documents to be sources of readily available background for change over time in tidal water quality observed with monitoring data. The intended purpose of the Tributary Summary documents is to help answer questions related to water quality, show how landscape factors drive water quality change over time, provide support for management decisions that may alter water quality trends and living resources conditions, and highlight where there may be information or knowledge gaps.

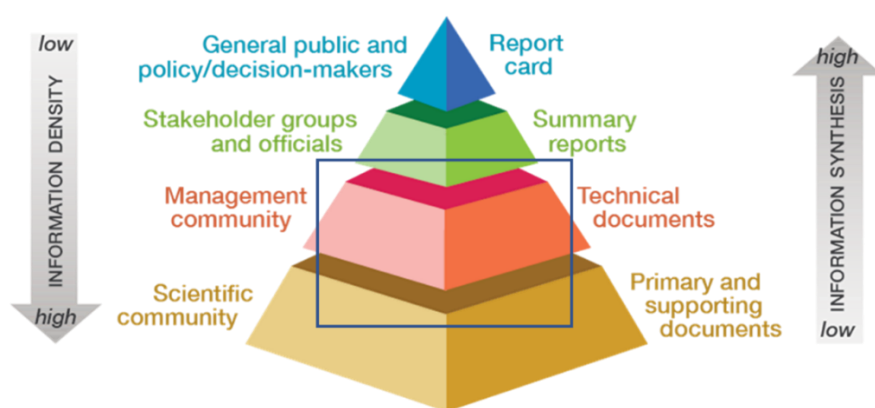


Figure 1: Conceptual model detailing different levels of information density and information synthesis. The intended audiences for the Tributary Summary documents are denoted by the blue box. Figure courtesy of the University of Maryland Center for Environmental Science Integration and Application Network (<https://ian.umces.edu/>).



## 2. Location

The Potomac River watershed covers approximately 12.5% of the Chesapeake Bay watershed. Its watershed is approximately 36,611 km<sup>2</sup> (Table 1) and spans parts of four states and Washington, D.C. (Figure 2). The tidal Potomac River begins just upstream of Washington, D.C. at the boundary of the Coastal Plain and Piedmont hydrogeomorphic regions (Bachman *et al.*, 1998) (Figure 2). Major tributaries to the Potomac River include Anacostia River, Antietam Creek, Cacapon River, Catoctin Creek, Conococheague Creek, Monocacy River, North Branch Potomac River, South Branch Potomac River, Occoquan River, Savage River, Seneca Creek, and Shenandoah River.

Table 1. Watershed areas, which includes tidal wetland area, for each of the 12 tributary or tributary groups for which Tributary Summaries have been produced. Each of the tributary summaries can be accessed at the following link:

<https://cast.chesapeakebay.net/Home/TMDLTracking#tributaryRptsSection>.

Tributary	Tributary Area (km <sup>2</sup> )
Virginia Mainstem	165,397
Maryland Mainstem	119,759
Potomac	37,457
James	31,147
York	12,530
Lower Eastern Shore	9,022
Rappahannock	6,729
Maryland Upper Eastern Shore	2,647
Patuxent	2,476
Choptank	1,845
Patapsco-Back	1,647
Maryland Upper Western Shore	1,523
Maryland Lower Western Shore	439
Source: Data are from the Chesapeake Assessment Scenario Tool (CAST)	

## 2.1 Watershed Physiography

The Potomac River watershed extends across five major physiographic regions, namely, Valley and Ridge, Piedmont, Coastal Plain, Blue Ridge, and Mesozoic Lowland (Bachman *et al.*, 1998) (Figure 2). The Piedmont physiography covers both carbonate and crystalline areas. The Coastal Plain physiography covers lowland, dissected upland, and upland areas. Implications of these physiographies for nutrient and sediment transport are summarized in Section 5.1.1.

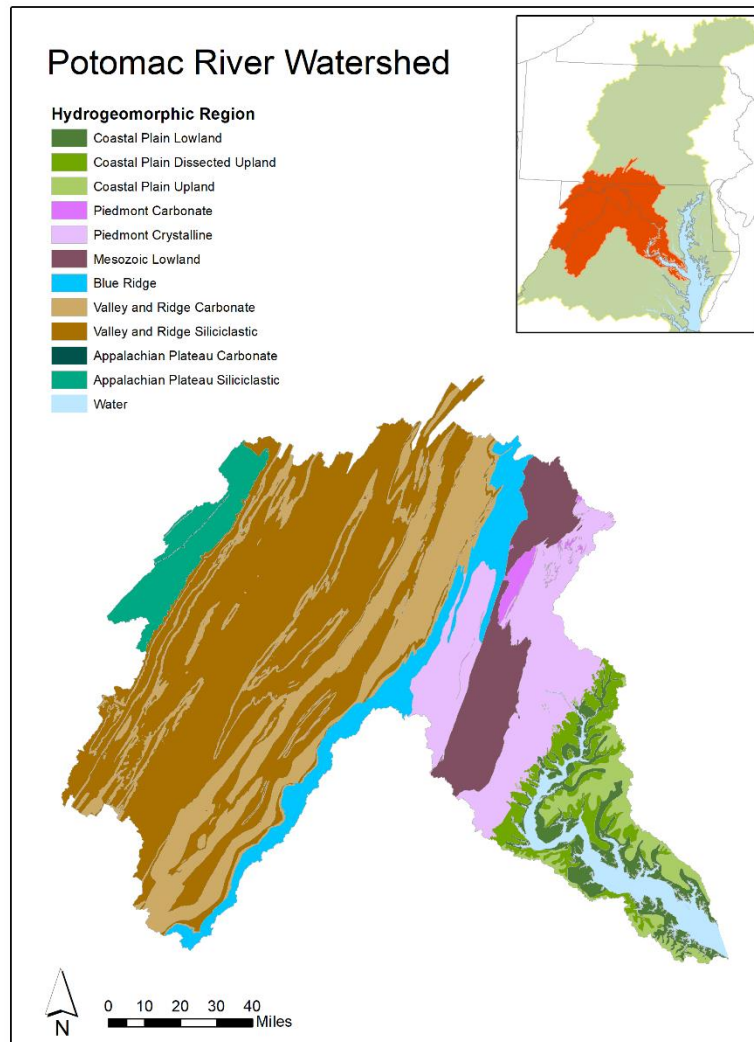


Figure 2. Distribution of physiography in the Potomac River watershed, shown in orange on the inset map. Base map credit Chesapeake Bay Program, [www.chesapeakebay.net](http://www.chesapeakebay.net), North American Datum 1983. Hydrogeomorphic region data credit: Brakebill, J.W. (ed) and Kelley, S.K. (ed), 2000, Hydrogeomorphic Regions in the Chesapeake Bay Watershed: U.S. Geological Survey data release, <https://doi.org/10.5066/P98WXDST>

## 2.2 Land Use

Land use in the Potomac River watershed is dominated (60%) by natural areas. Urban and suburban developed land areas have increased by 2,504 (71%) square kilometers since 1985, agricultural lands have decreased by 1,327 square kilometers, and natural lands have decreased by 1,170 square kilometers. The increase in developed area and decrease in agricultural area led to a greater proportion of developed land in the watershed, which increased from 10% in 1985 to 17% in 2022 (Figure 3). Since the 1970s, developed areas have expanded into previously natural and agricultural landscapes (Figure 4). The impacts of land development differ depending on the use from which the land is converted (Keisman et al., 2019; Ator et al., 2019). Implications of changing land use for nutrient and sediment transport are summarized in Section 5.1.4.

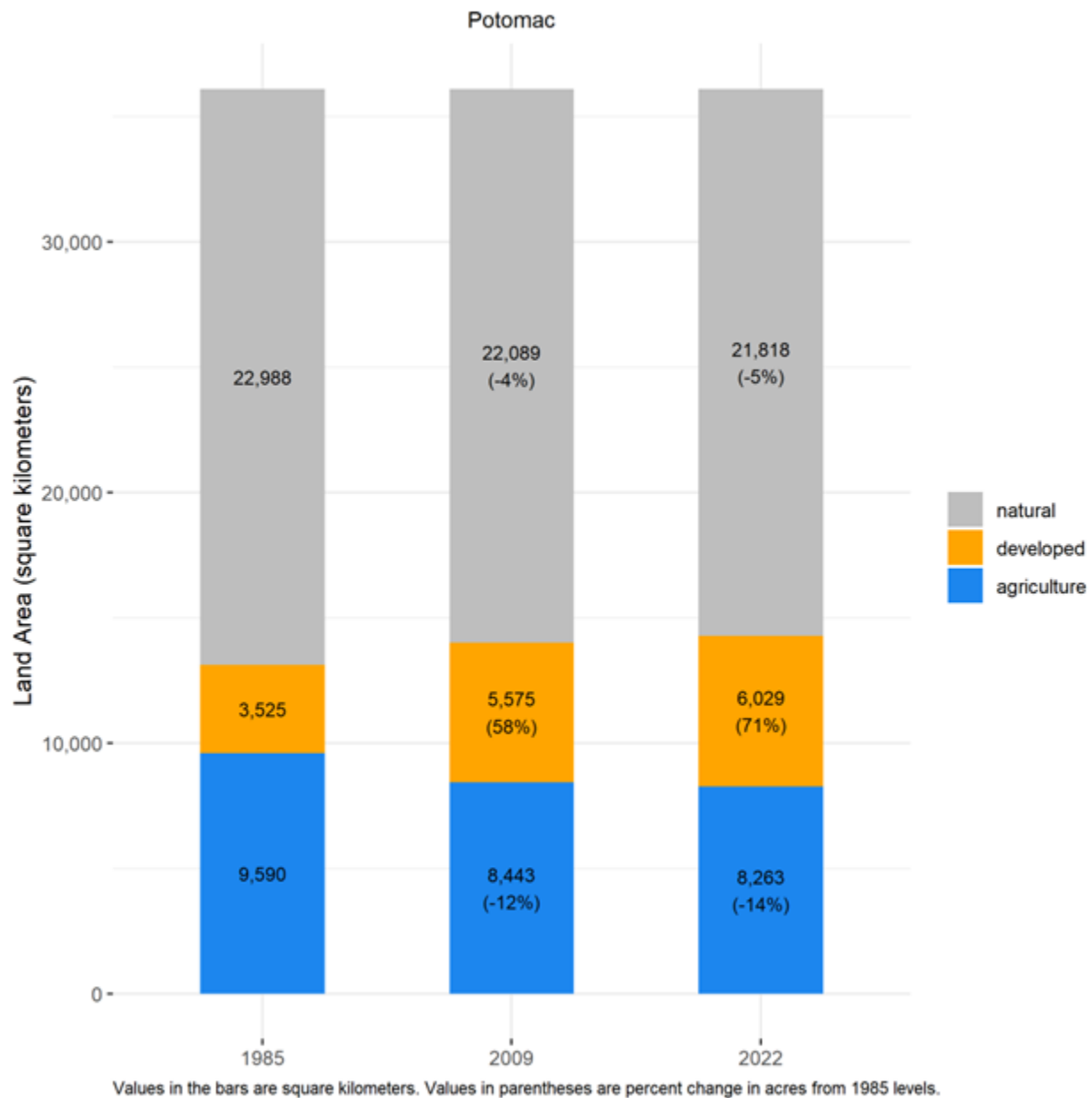


Figure 3. Distribution of land uses in the Potomac River watershed. Percentages are the percent change from 1985 for each source sector. (CAST; <https://cast.chesapeakebay.net/About/UpgradeHistory>, version Phase 6 - 7.6.0)

In general, prior to 1980, developed lands within the Potomac River watershed were concentrated in the Washington, D.C. metropolitan area which held 49% of the developed and semi-developed areas. Since then, developed lands have expanded to regions both further upstream into the watershed and further downstream into the tidal areas (Figure 4) (Arnold and Gibbons, 1996). Implications of changing land use for nutrient and sediment transport are summarized in Section 5.1.3.

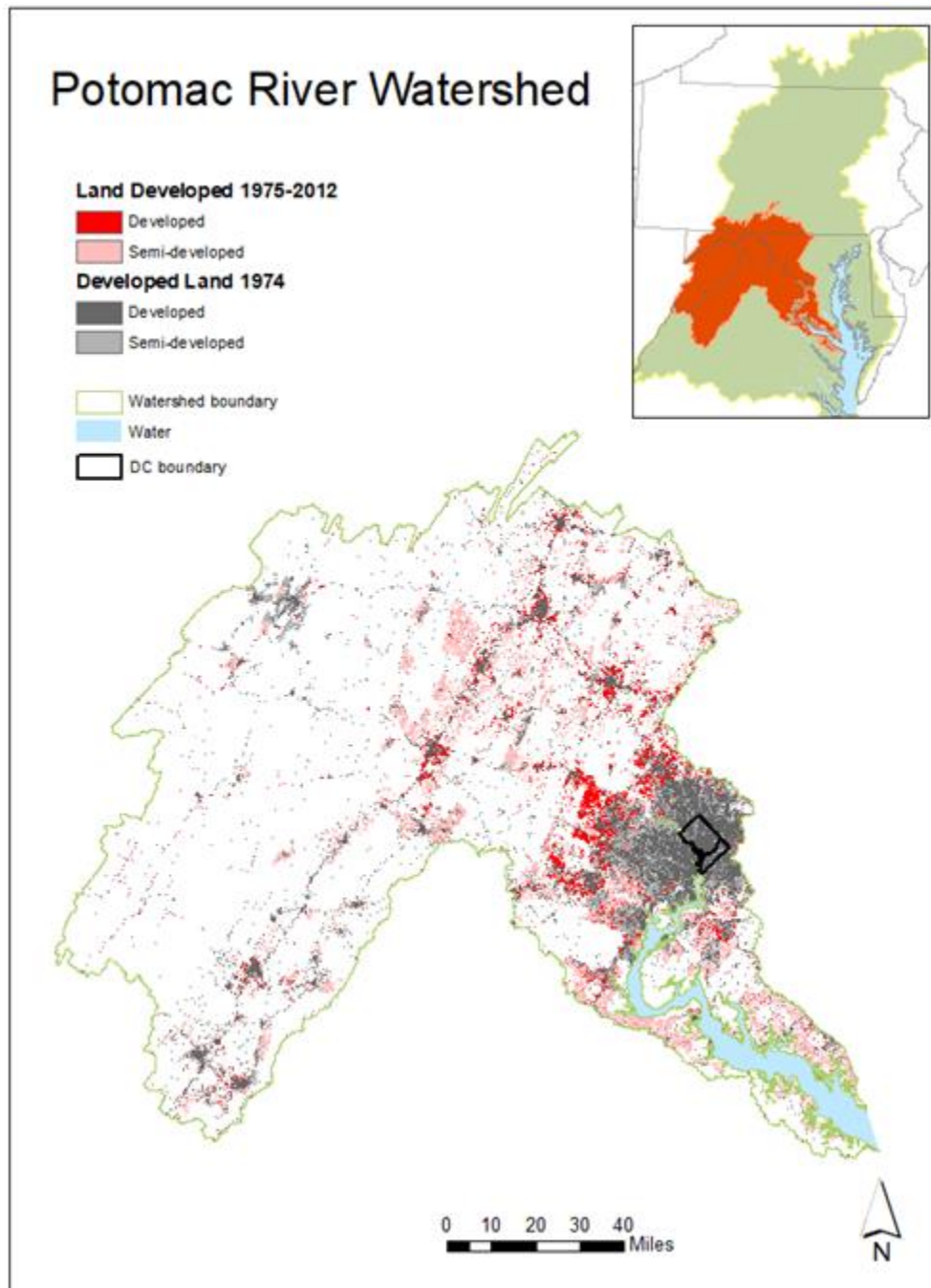


Figure 4. Distribution of impervious surface coverage in the Potomac River watershed, shown in orange on the insert map. Derived from the U.S. Geological Survey (USGS) National Land Cover Database (Dewitz, 2021). Base map credit Chesapeake Bay Program, [www.chesapeakebay.net](http://www.chesapeakebay.net), North American Datum 1983.

### 2.3 Tidal Waters and Stations

For the purposes of water quality standards assessment and reporting, the tidal portion of the Potomac River is divided into multiple split segments (U.S. Environmental Protection Agency, 2004): Tidal Fresh in Washington, District of Columbia (DC), Maryland (MD), and Virginia (VA) (POTTF\_DC, POTTF\_MD,

POTTF\_VA), Oligohaline in MD and VA (POTOH1\_MD, POTOH2\_MD, POTOH3\_MD, and POTOH\_VA), and Mesohaline in MD and VA (POTMH\_MD, POTMH\_VA) (Figure 5). Three tributaries of the Potomac are also represented, including the tidal fresh Anacostia River in Maryland (ANATF\_MD) and Washington, D.C. (ANATF\_DC), the tidal fresh Piscataway Creek (PISTF), and the tidal fresh Mattawoman Creek (MATTF) (Figure 5).

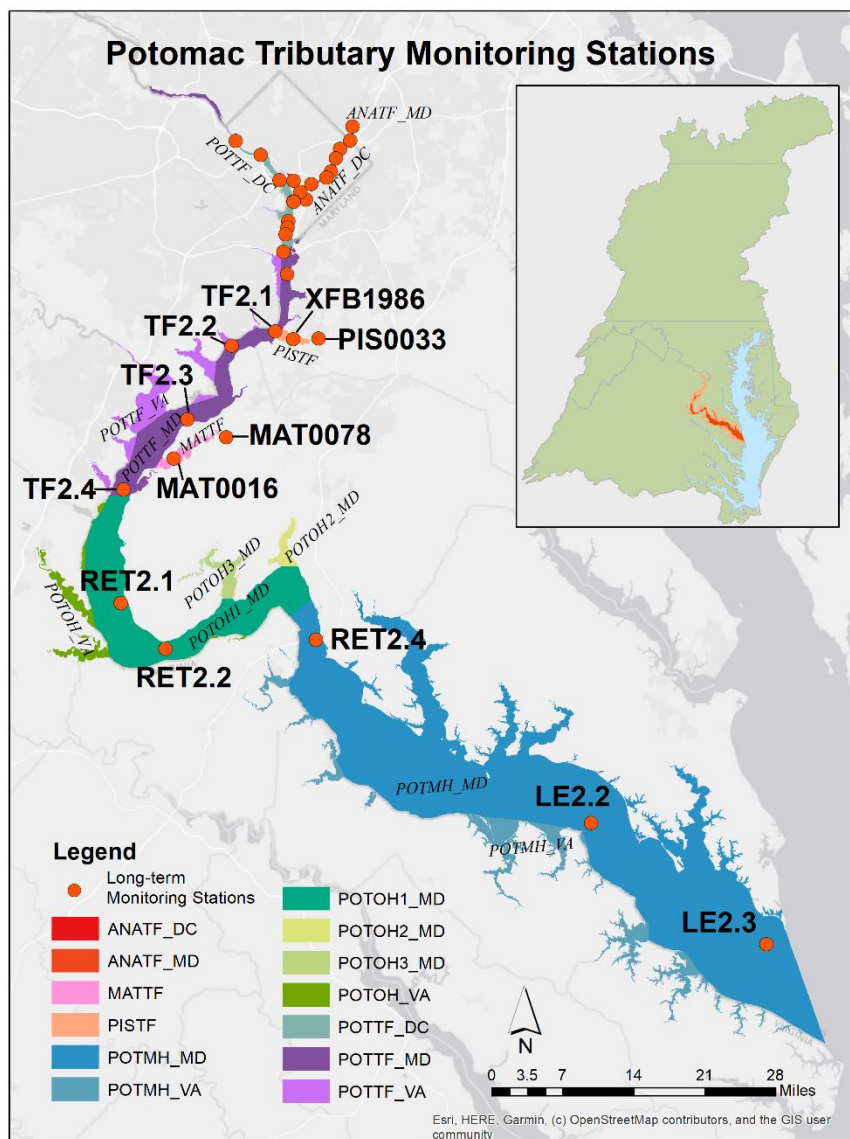


Figure 5. Map of tidal Potomac River segments and long-term monitoring stations. Base map credit Esri, HERE, Garmin, (c) OpenStreetMap contributors, and the GIS user community. World Geodetic System 1984. Any use of trade, firm, logos, or product names is for descriptive purposes only and does not imply endorsement by the U.S. Government.

Long-term trends in water quality are analyzed by the MD Department of Natural Resources at 13 stations extending from Piscataway Creek to the mouth of the Potomac River flowing into Chesapeake Bay and by D.C. Department of Energy and Environment at 18 stations (Figure 5). Water quality data at

these stations are also used to assess attainment of dissolved oxygen (DO) water quality criteria. All tidal water quality data analyzed for this report are available from the Chesapeake Bay Program Data Hub (Chesapeake Bay Program, 2018). Additional shallow-water monitoring that has been conducted in some embayments along the VA Potomac River shoreline and in some MD segments are included in the water quality criteria evaluation but not shown in the long-term trend graphics in subsequent sections because of their shorter duration (Maryland DNR, 2022; VIMS, 2022).

### 3. Tidal Water Quality Status

The Potomac River provides a direct example of the relevance of long-term water quality monitoring and the evaluation of long-term trends relative to environmental management goals. Multiple water quality standards were developed for the tidal waters of Chesapeake Bay to protect aquatic living resources (U.S. Environmental Protection Agency, 2003; Tango and Batiuk, 2013). These standards include specific criteria for dissolved oxygen (DO), chlorophyll a, and water clarity/underwater bay grasses. For the purposes of this report, a record of the evaluation results indicating whether different segments of this system have attained DO criteria over time (Zhang *et al.*, 2018b; Zhang *et al.*, 2018c; Hernandez Cordero *et al.*, 2020) are shown below (Figure 5). These results provide context for the importance of understanding water quality trends and the underlying drivers. More specifically, trends in the water quality parameters summarized in this report directly affect environmental management goals implemented by interested stakeholders within the watershed. For more information on water quality standards, criteria, and standards attainment, visit the CBP's "Chesapeake Progress" website at [www.chesapeakeprogress.com](http://www.chesapeakeprogress.com).

Attainment deficit is an approach used to document whether a particular criterion is met in a certain period, and if not, how far the segment is from meeting it. If the attainment deficit was zero, it means the criterion was fully met; if it was a negative number, it indicates how far the segment and designated use was from meeting the criterion during that period. The graphics in Figure 5 show that the Open Water (OW) criterion was at or near zero from the start of monitoring to the most recent assessment period covered by this report (2020-2022) in 10 segments, namely, MATTF, PISTF, POTMH\_MD, POTOH\_VA, POTOH1\_MD, POTOH2\_MD, POTOH3\_MD, POTTF\_DC, POTTF\_MD, POTTF\_VA. By contrast, the other segments (ANATF\_DC, ANATF\_MD, and POTMH\_VA) showed a high degree of variability with the former two segments rarely attaining the OW criterion. The Deep Water (DW) and Deep Channel (DC) criteria were applicable to only two segments: POTMH\_MD and POTMH\_VA. For POTMH\_MD, the DW attainment was generally worse than OW and the DC attainment was generally the worst among the three criteria. For POTMH\_VA, however, both DW and DC attainment had fairly small attainment deficit values. Mann-Kendall trend results indicated three statistically significant trends, i.e., a long-term improvement in POTOH1\_MD OW-DO and long-term declines in POTMH\_VA and POTTF\_VA OW-DO (Figure 6).



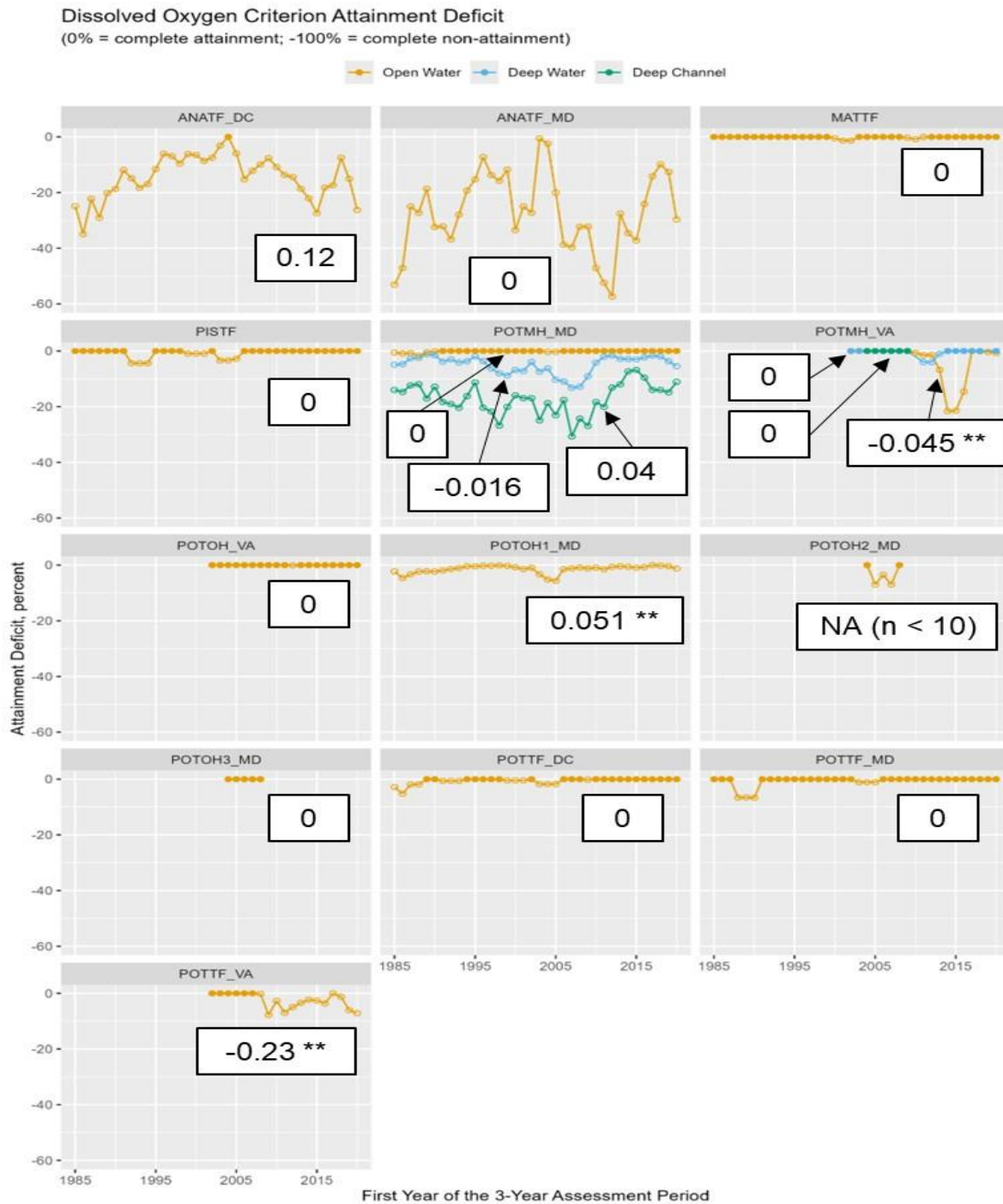


Figure 6. Attainment deficit for Open Water (30-day mean; June-September), Deep Water (30-day mean; June-September), and Deep Channel (Instantaneous; June-September) dissolved oxygen criteria for three-year assessment periods from the start of monitoring through the current (2020-2022) assessment period. A value of 0% indicates full attainment for a given criterion while negative values indicate percent non-attainment (deficit) for the segment and criterion being plotted. Numbers associated with a given line are the Sen Slope estimates. Trends significant at  $p < 0.05$  are indicated by \*\* or at  $p < 0.1$  by \*.



Comparing trends in station-level DO concentrations to the computed DO criterion status for a recent assessment period can reveal whether progress is being made towards attainment in a segment that is not meeting the water quality criteria, or conversely, whether conditions are degrading even if the criteria are currently being met. To illustrate this, the 2020-2022 attainment status for the OW and DC DO criteria based on a passed/failed assessment are overlain with the 1985-2022 trends in summer surface DO concentration and the 1985-2022 trends in bottom summer DO concentrations, respectively (Figure 7). The 30-day mean OW summer DO criterion status was mixed across the segments. Likewise, the trends in surface DO are mixed as well. The DC criterion was not met in the applicable segments, and only one station in that segment shows an increasing DO trend. This example shows the importance of establishing criteria and monitoring water quality conditions relative to established goals for those criteria. It also demonstrates the relevance of trend results in relation to criteria assessments.

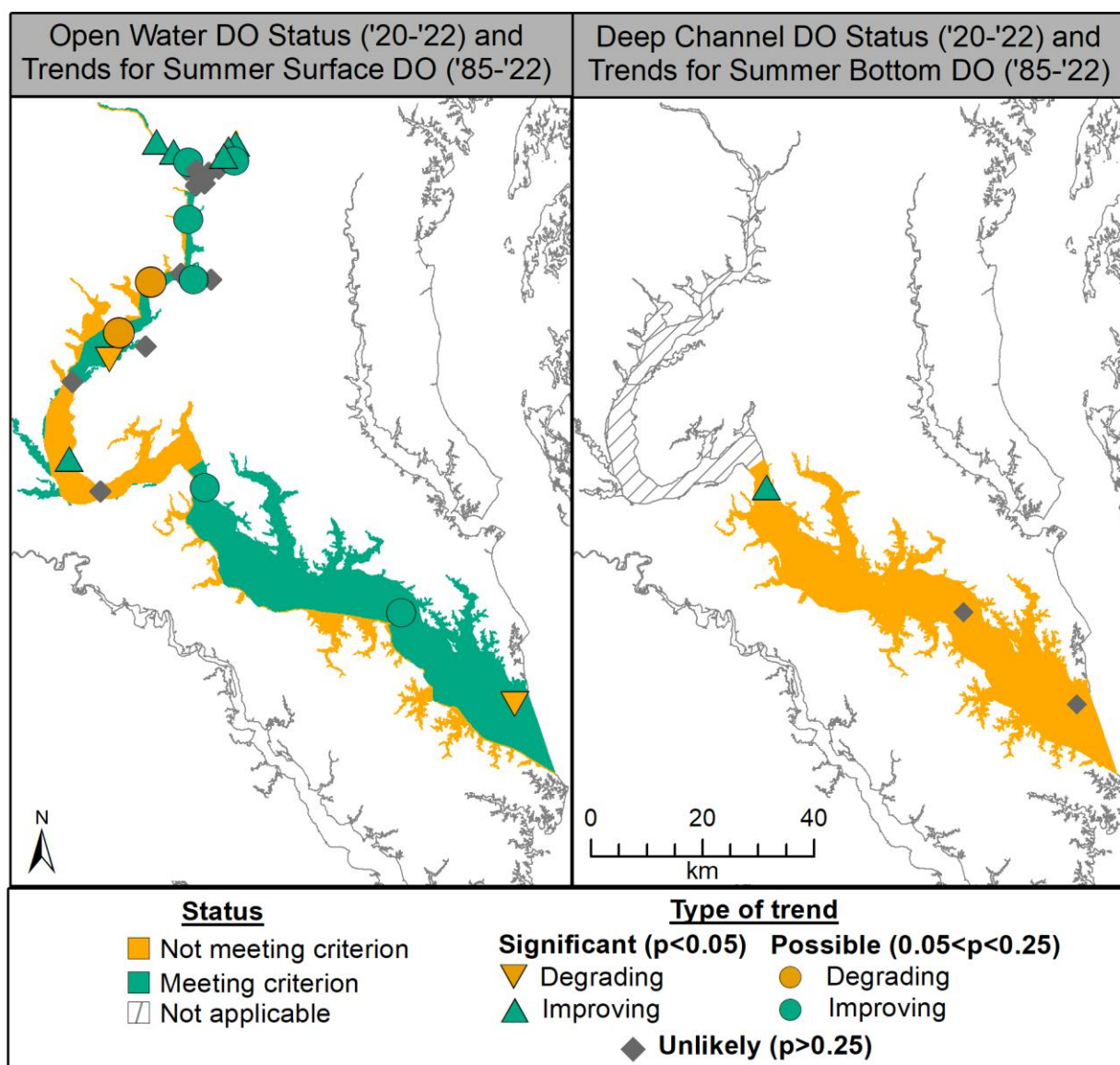


Figure 7. Pass-fail DO criterion status for 30-day OW summer DO and DC DO designated uses in Potomac River segments along with long-term trends in DO concentrations. Base map credit Chesapeake Bay Program, [www.chesapeakebay.net](http://www.chesapeakebay.net), North American Datum 1983. For more information on water quality standards, criteria, and standards attainment, visit the CBP's "Chesapeake Progress" website at [www.chesapeakeprogress.com](http://www.chesapeakeprogress.com).

## 4. Tidal Water Quality Trends

Tidal water quality trends were computed by fitting generalized additive models (GAMs) to the water quality observations that have been collected one or two times per month since the 1980s at the tidal stations labeled in Figure 5. Refer to Murphy *et al.* (2019) for more details on the GAM implementation that is applied each year by MD Department of Natural Resources for these stations in collaboration with the Chesapeake Bay Program and Virginia analysts.

Results shown below in each set of maps (e.g., Figure 8) include those generated using two different GAM functions fit to each station-parameter combination. The first approach involves fitting a GAM to the raw observations to generate a mean estimate of change over time at a given station, as observed in the estuary. The second approach involves including monitored river flow or *in situ* salinity (as an aggregated measure of multiple river flows) in the GAM to explain some of the variation in the water quality parameter. From the results of this second approach, "flow-adjusted" change over time gives a mean estimate of what the water quality parameter trend would have been if average river flows had been observed over the period of record. Note that depending on the location in the Potomac River, gaged river flow or salinity is used for this adjustment, but we refer to all of these results as "flow-adjusted" for simplicity.

To determine if there has been a change over time (i.e., a trend) at a particular station for a given parameter, we compute a percent change between the estimates at the beginning and end of a period of interest from the GAM fit. For each percent change computation, the level of statistical confidence was computed. Change was considered significant if  $p < 0.05$  and possible if the p-value is up to 0.25. That upper limit is higher than usually reported for hypothesis tests but allows us to provide a more complete picture of the results, identifying locations where change might be starting to occur and could be investigated further (Murphy et al., 2019). In addition to the maps of trends, for each parameter, there is a set of graphs (e.g., Figure 9) that include the raw observations (dots on the graphs) and lines representing the mean annual or seasonal GAM estimates, without flow-adjustment. The flow-adjusted GAM line graphs are not shown so that the figures better represent what living resources (e.g., fish species, submerged aquatic vegetation [SAV], blue crab [*Callinectes sapidus*]) actually experience.

### 4.1 Surface Total Nitrogen

Annual total nitrogen (TN) concentrations have declined from 1985 to 2022 at all 13 of the tidal Potomac stations, using both trends on concentration data alone and adjusting for flow (Figure 8). In the past 10 years, many of the tidal fresh and oligohaline stations show a decrease in TN concentrations.

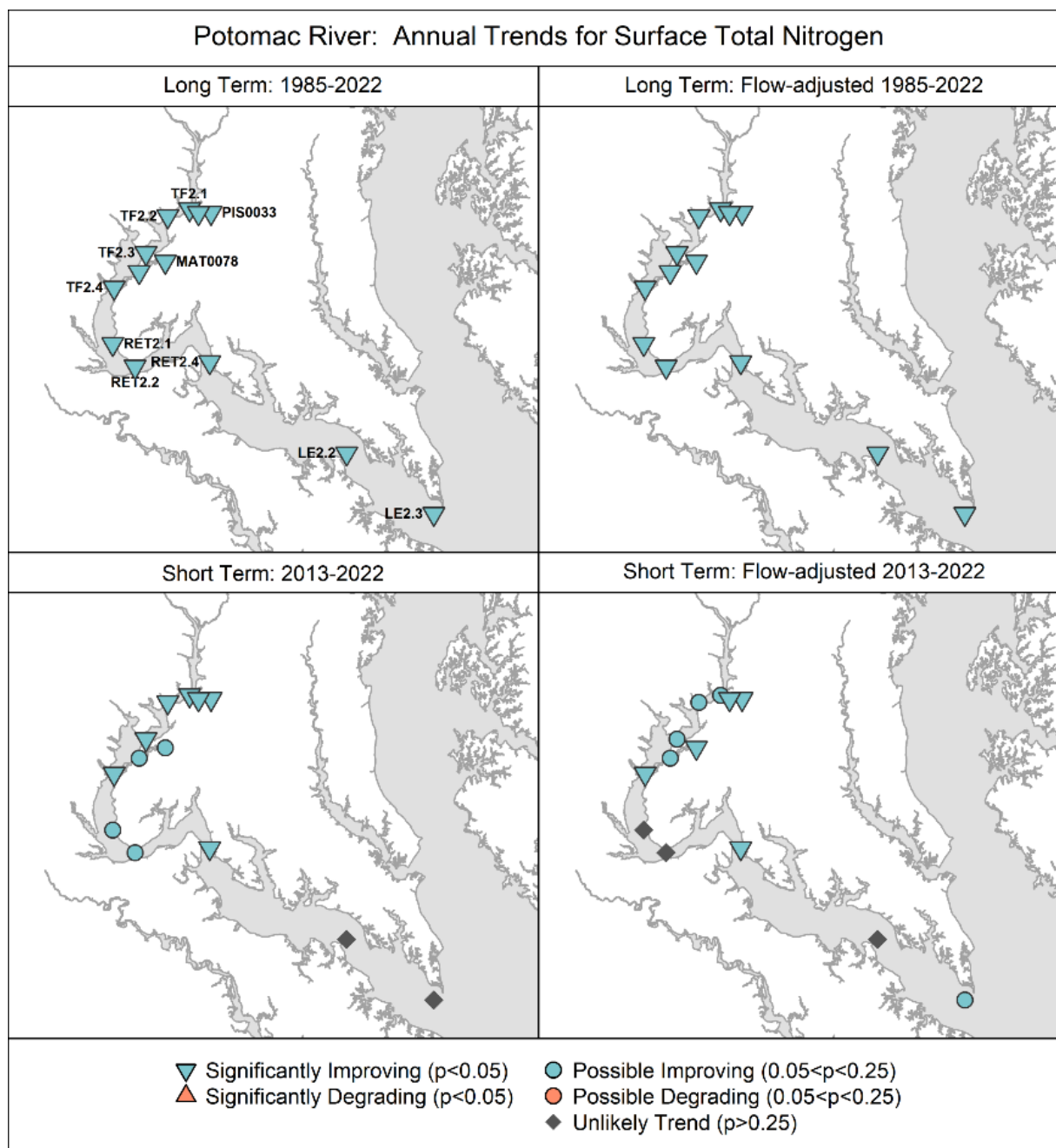


Figure 8. Flow-adjusted trends in surface TN concentrations as calculated using Generalized Additive Models (Murphy *et al.* 2019). Base map credit Chesapeake Bay Program, [www.chesapeakebay.net](http://www.chesapeakebay.net), North American Datum 1983. For more information on the tidal stations and Chesapeake Bay tidal water quality monitoring, refer to <https://www.chesapeakebay.net/what/programs/quality-assurance/tidal-water-quality-monitoring>.

The long-term decreasing TN trends are evident in both the data and the non-flow-adjusted mean annual GAM estimates presented in Figure 9. An upswing in TN in 2018 - 2019 is clear in some of these graphs as well, which can be attributed to higher river flows in those years, but TN at concentrations at most stations stabilize or decline starting in 2010 (Figure 9).

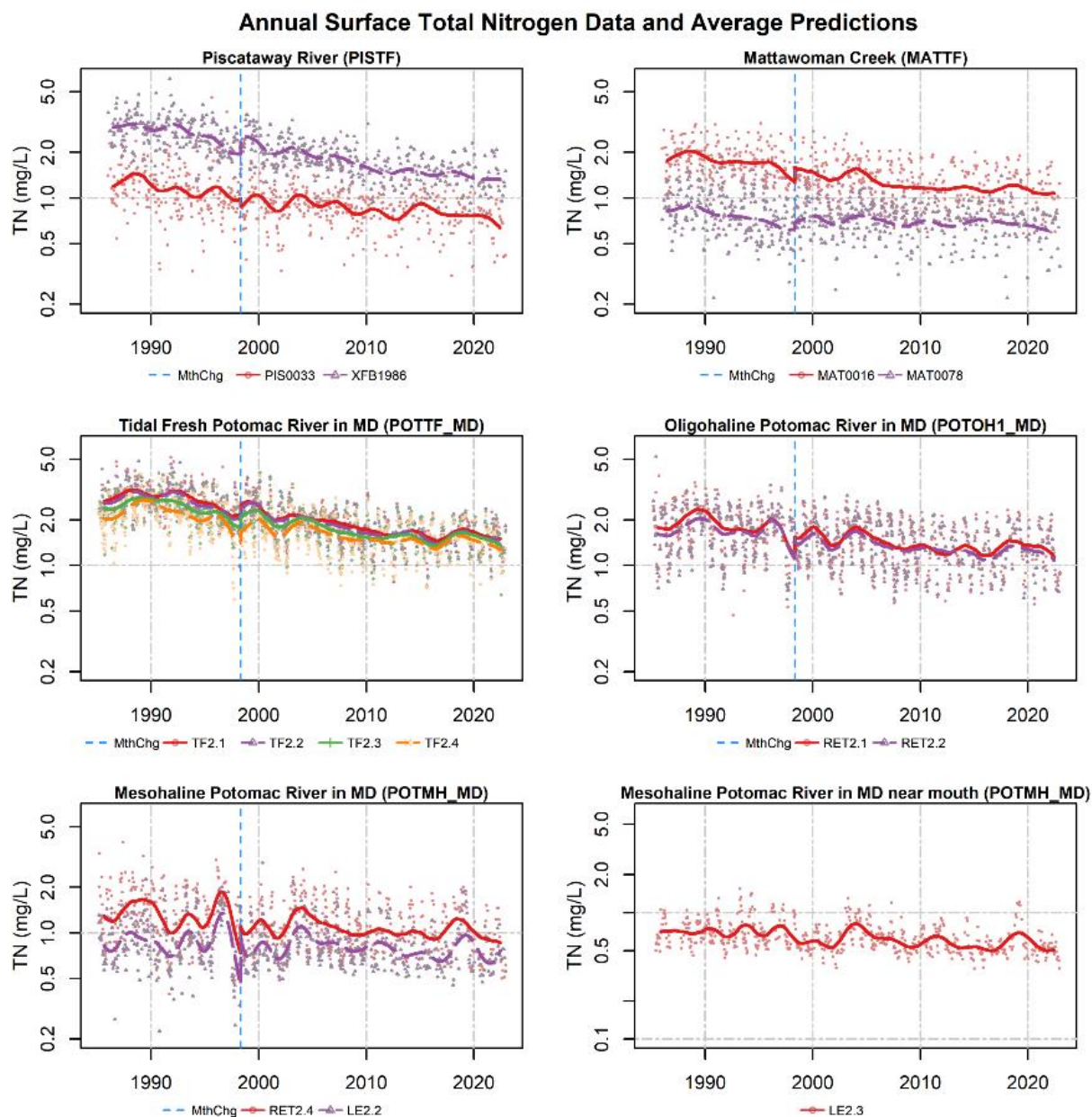


Figure 9. Surface TN concentration data (dots) and average long-term pattern generated from non-flow adjusted Generalized Additive Models (GAMs). Colored dots represent data corresponding to the monitoring station shown indicated in the legend; colored lines represent mean annual GAM estimates for the noted monitoring stations.



## 4.2 Surface Total Phosphorus

Surface total phosphorus (TP) concentrations are also improving at most stations over the long-term, both with and without flow-adjustment (Figure 10). In the short-term, most stations show unlikely trends. There is only one station showing significant improvement in the tidal fresh for flow-adjusted TP concentrations.

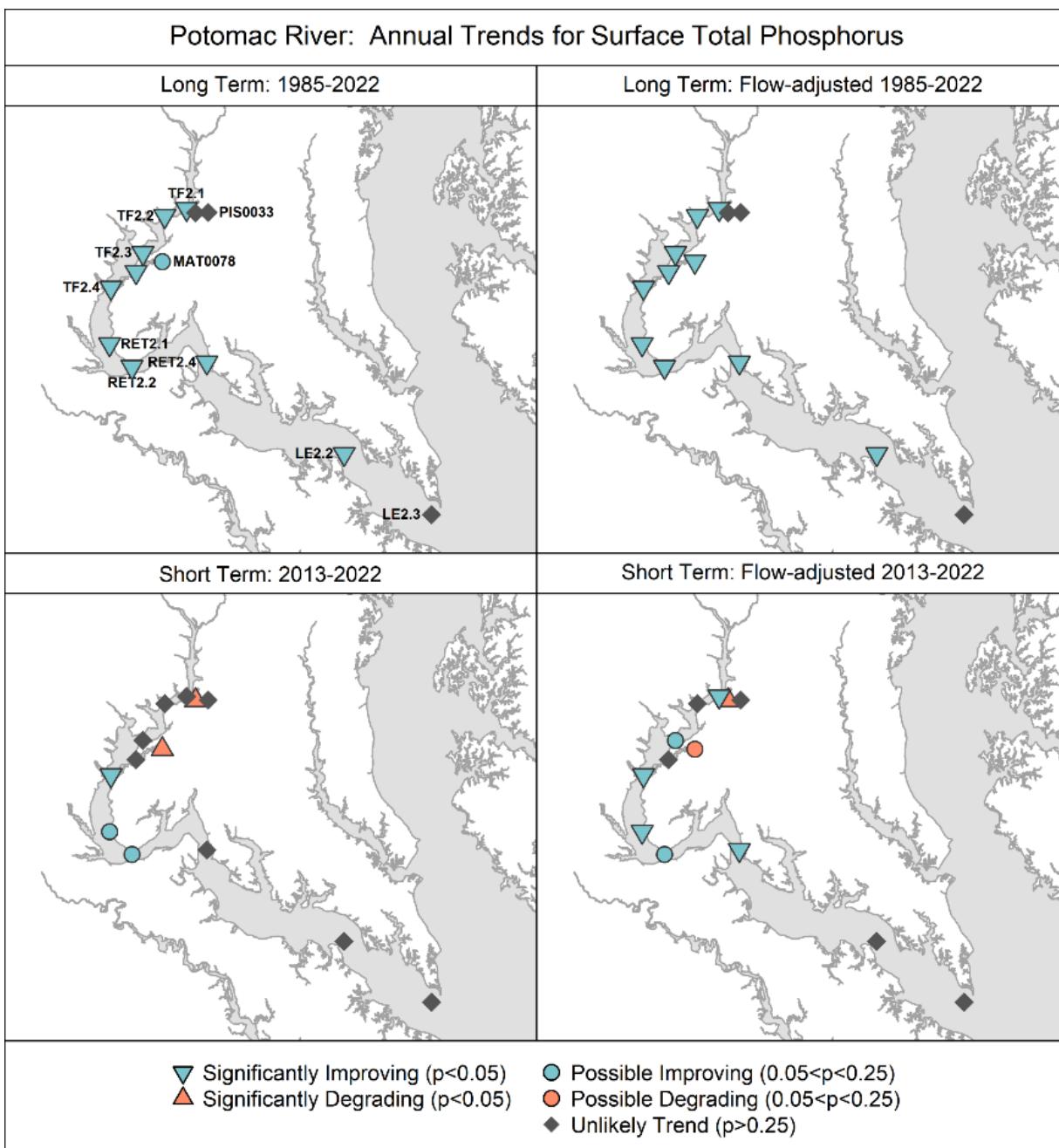


Figure 10. Flow-adjusted trends in surface TP concentrations as calculated using Generalized Additive Models (Murphy et al. 2019). Base map credit Chesapeake Bay Program, [www.chesapeakebay.net](http://www.chesapeakebay.net), North American Datum 1983. For more information on the tidal stations and Chesapeake Bay tidal water

quality monitoring, refer to <https://www.chesapeakebay.net/what/programs/quality-assurance/tidal-water-quality-monitoring>.

The most noticeable decrease in TP concentrations occurred at the mesohaline station (bottom left panel, Figure 11). Data and the non-flow-adjusted mean annual GAM estimates are mostly decreasing at other stations, with an increase in the last few years at the Piscataway Creek and Mattawoman Creek stations that has resulted in the degrading trends as show in Figure 10.

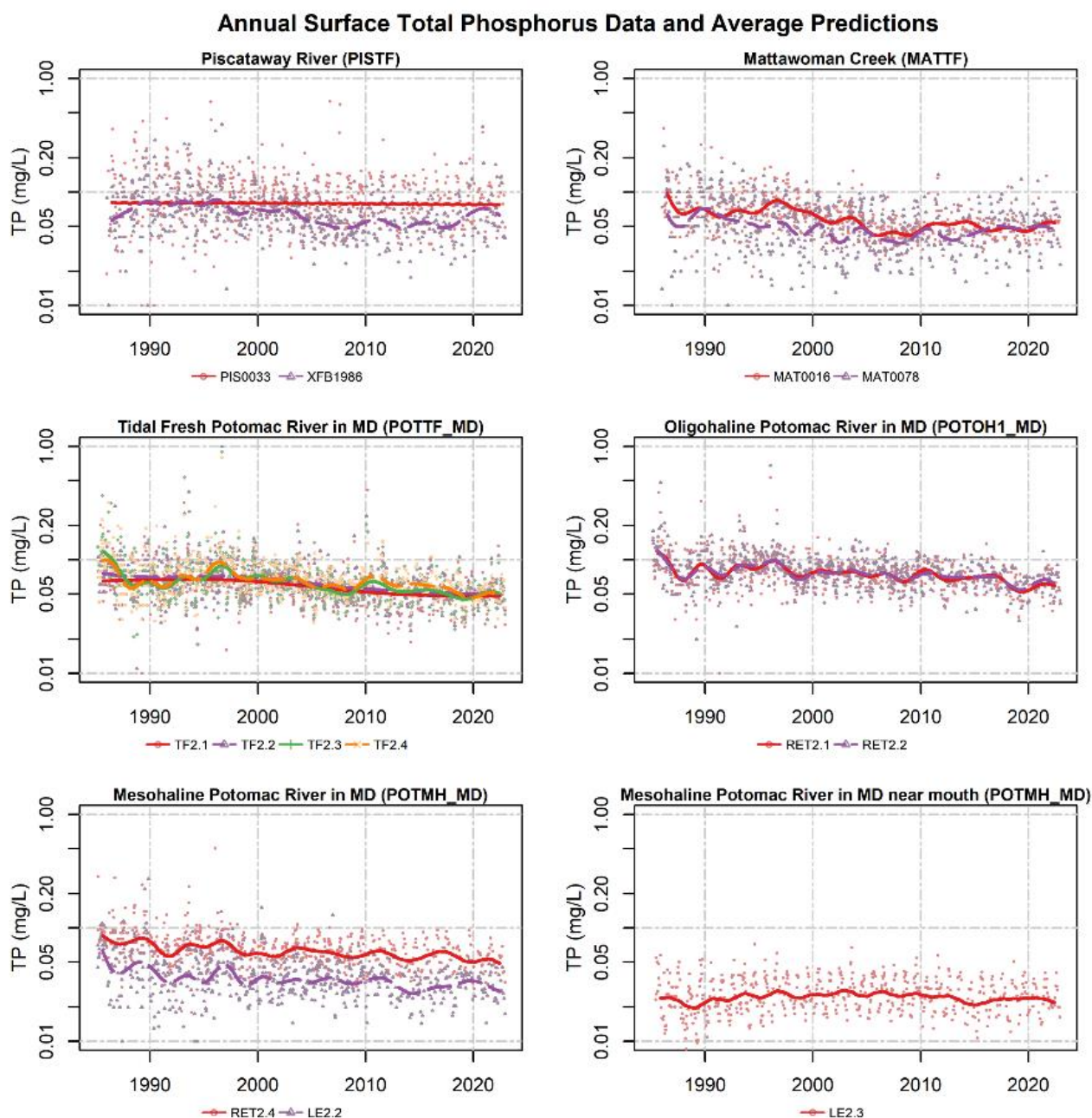


Figure 11. Surface TP concentration data (dots) and average long-term pattern generated from non-flow adjusted Generalized Additive Models (GAMs). Colored dots represent data corresponding to the

monitoring station shown indicated in the legend; colored lines represent mean annual GAM estimates for the noted monitoring stations.

#### 4.3 Surface Chlorophyll *a*: Spring (March-May)

Trends for chlorophyll *a* are split into spring and summer to analyze seasonal phytoplankton blooms that are commonly observed in different parts of Chesapeake Bay (Smith and Kemp, 1995; Harding and Perry, 1997). Spring trends (Figure 12) are possibly degrading downstream and significantly degrading in the tidal fresh in the long-term. In the short-term, most stations show unlikely trends, but for flow-adjusted chlorophyll *a* concentrations, most tidal fresh stations are significantly improving. Short-term trends computed for the Washington D.C. stations show mostly significantly improving spring chlorophyll *a*.

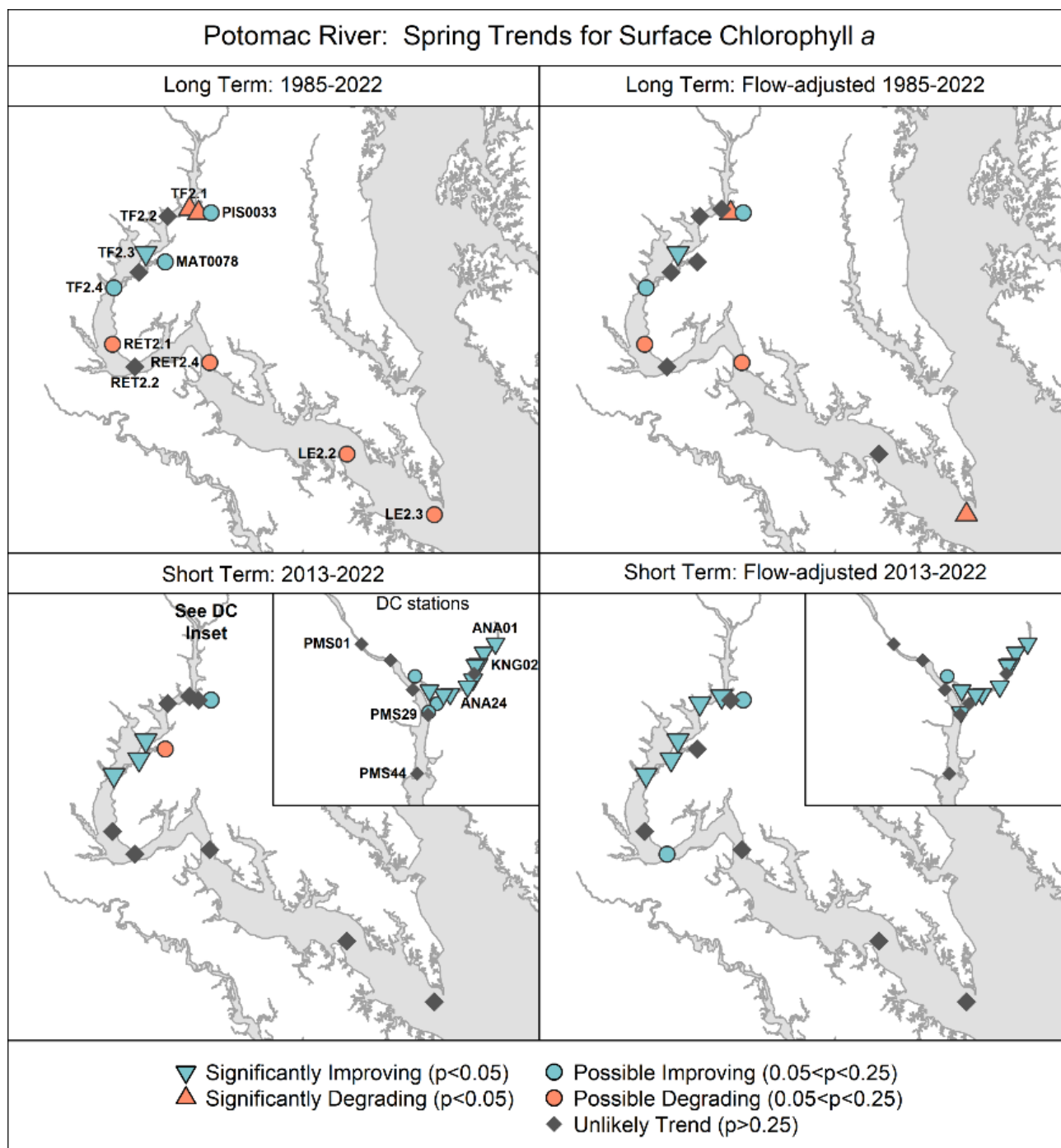


Figure 12. Flow-adjusted surface spring (March-May) chlorophyll *a* trends as calculated using Generalized Additive Models (Murphy et al. 2019). Base map credit Chesapeake Bay Program, [www.chesapeakebay.net](http://www.chesapeakebay.net), North American Datum 1983. For more information on the tidal stations and Chesapeake Bay tidal water quality monitoring, refer to <https://www.chesapeakebay.net/what/programs/quality-assurance/tidal-water-quality-monitoring>.

A high amount of variability exists in the long-term patterns of some of the chlorophyll *a* datasets and average spring GAM estimates (Figure 13a). A station in Piscataway Creek (PISTF) exhibits a clear



increase over time. Conversely, other stations in many of the graphs like the tidal fresh Potomac River (POTTF\_MD) and Oligohaline Potomac River in MD (POTOH1\_MD) show fluctuating concentrations of chlorophyll *a* in the long-term with an upswing in the last few years. Figure 13b shows the surface spring Chlorophyll *a* data and average short-term pattern generated from non-flow adjusted GAMs for the Washington D.C. stations. Most stations show a noticeable decline (Figure 13b).

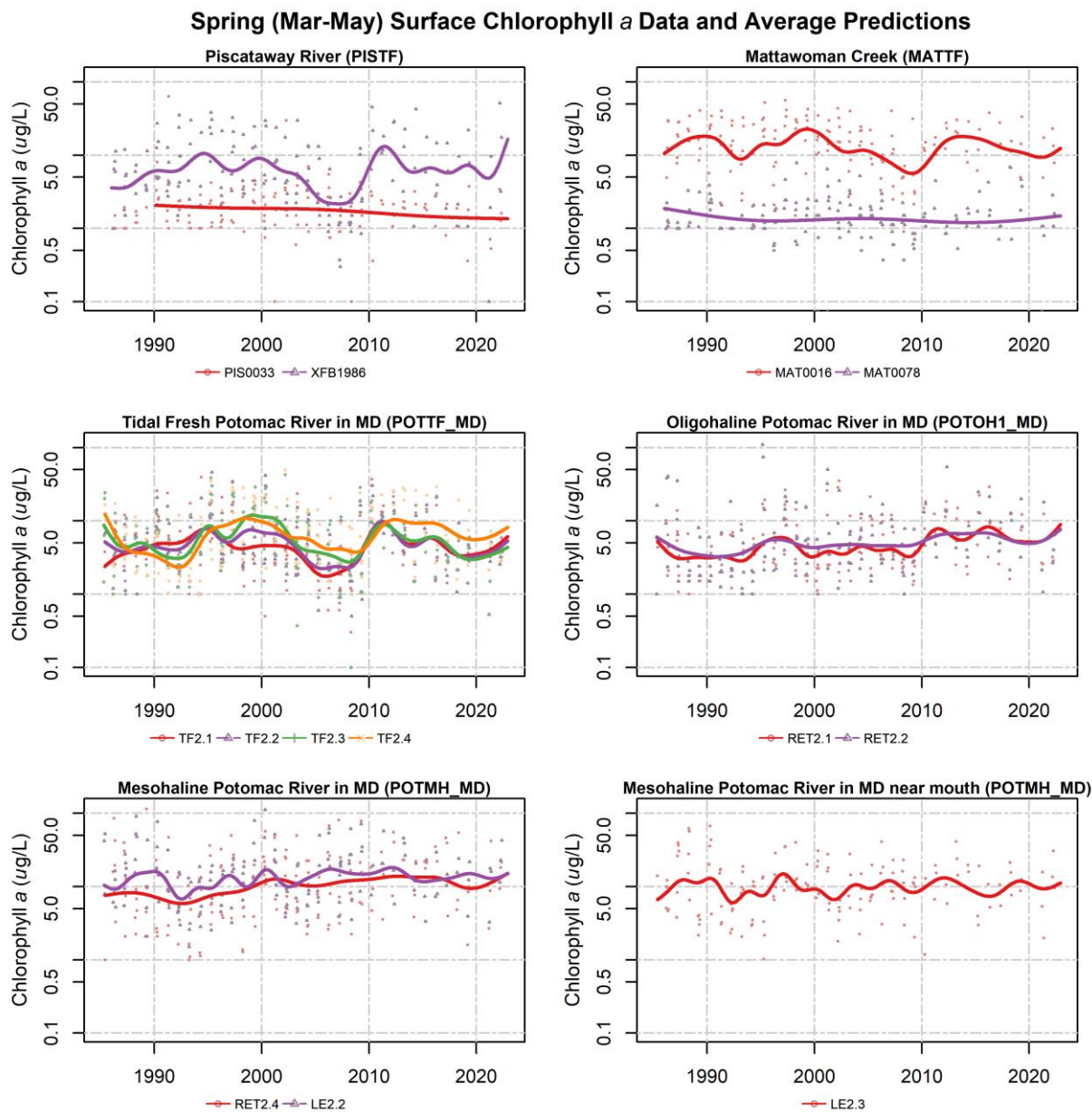


Figure 13a. Surface spring Chlorophyll *a* concentration data (dots) and average long-term pattern generated from non-flow adjusted Generalized Additive Models (GAMs). Colored dots represent March-May data corresponding to the monitoring station shown indicated in the legend; colored lines represent mean spring GAM estimates for the noted monitoring stations.

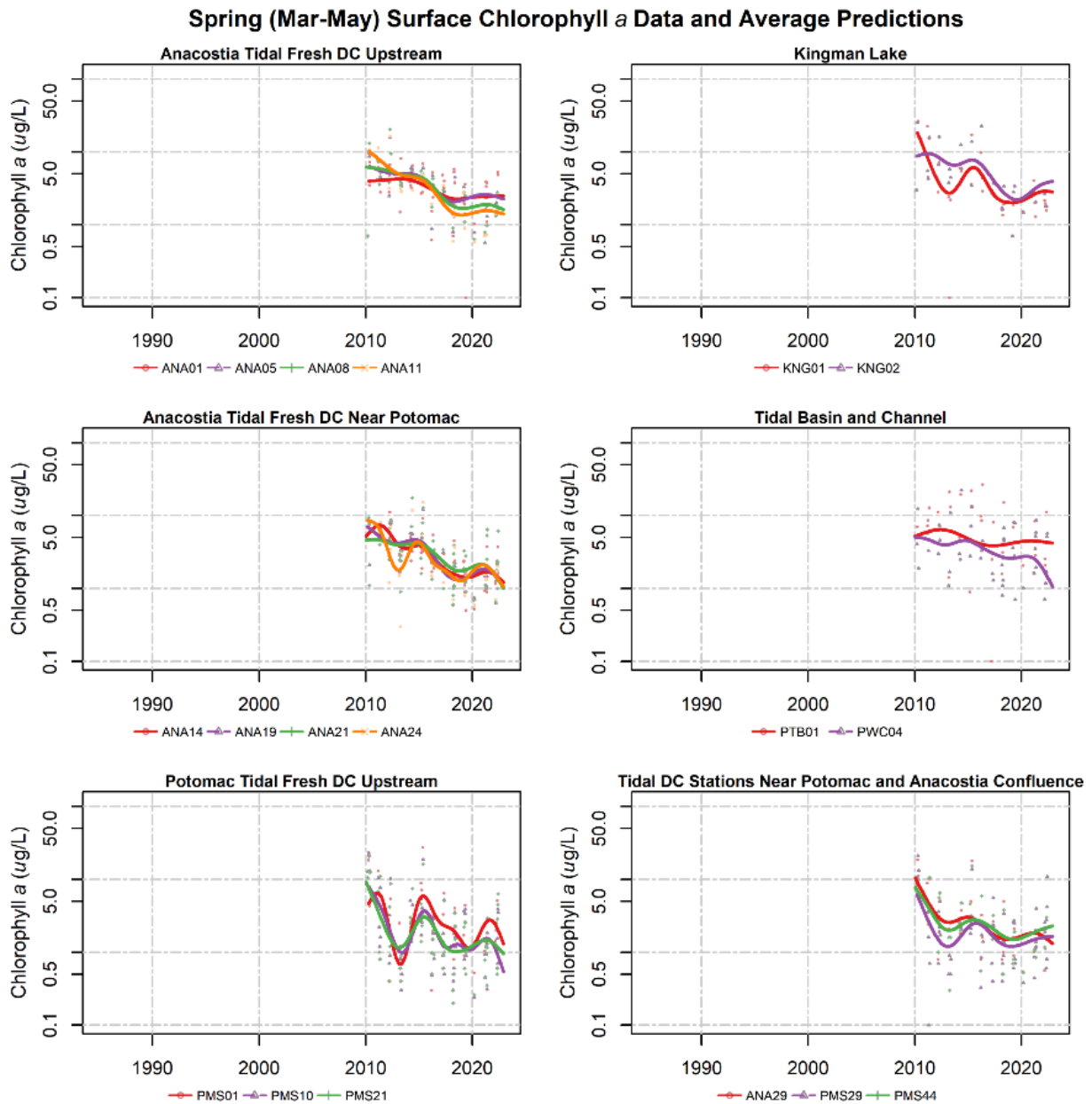


Figure 13b. Surface spring Chlorophyll *a* concentration data (dots) and average long-term pattern generated from non-flow adjusted Generalized Additive Models (GAMs). Colored dots represent March-May data corresponding to the monitoring station shown indicated in the legend; colored lines represent mean spring GAM estimates for the noted monitoring stations. For chlorophyll *a* at Washington D.C. tidal stations, the time series start in 2010 due to data availability.

#### 4.4 Surface Chlorophyll *a*: Summer (July-September)

Compared to the spring long-term trends in chlorophyll *a* concentration, the summer results show more stations with significantly degrading trends throughout the tributary. In the short-term, compared to the spring, there are less significantly improving stations except for the Washington D.C. stations. Overall, long-term patterns indicate more widespread degradation, while the short-term trends reveal localized improvements, especially in the upstream regions.

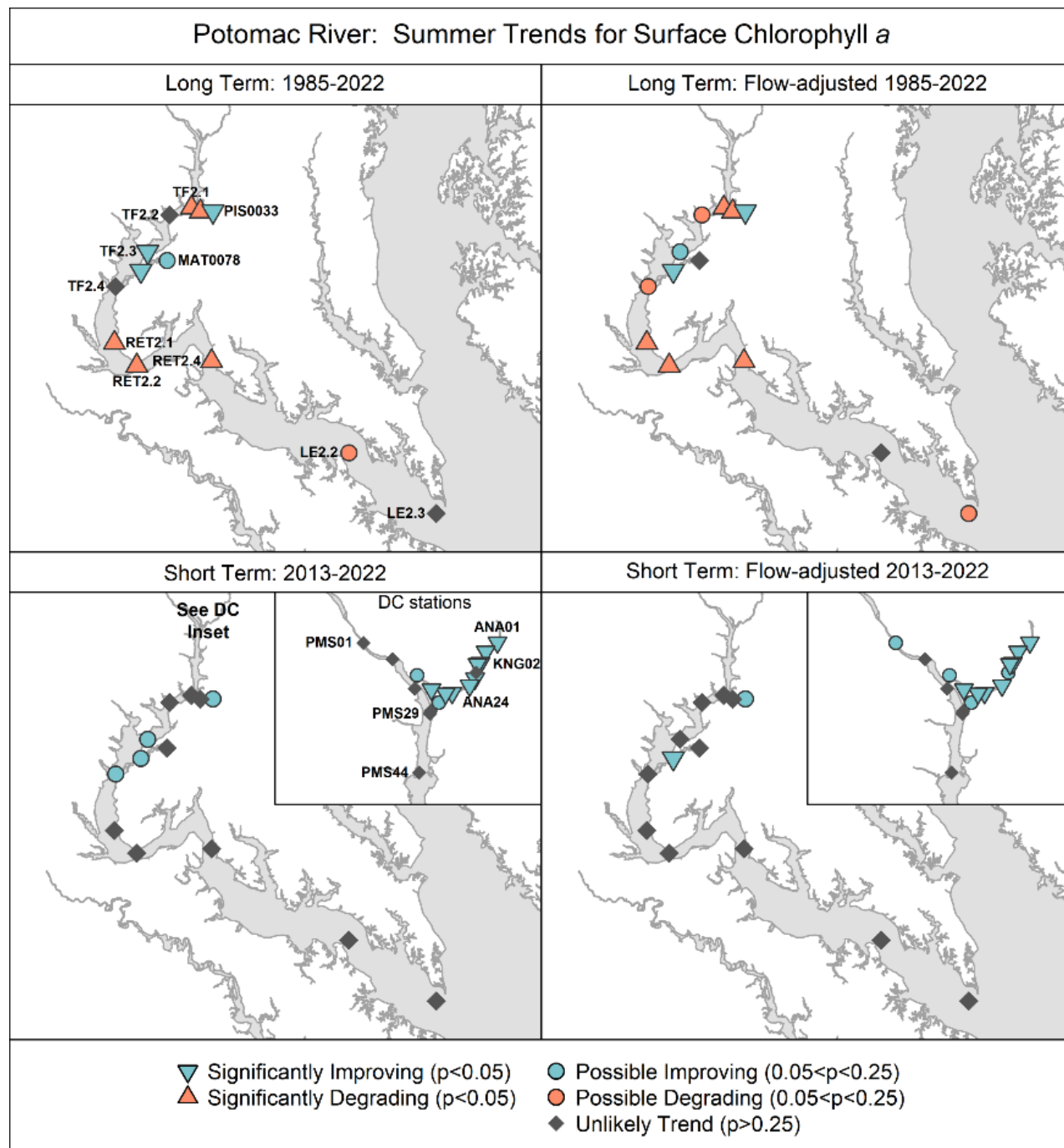


Figure 14. Trends in flow-adjusted surface summer (July-September) chlorophyll *a* concentrations as calculated using Generalized Additive Models (Murphy et al. 2019). Base map credit Chesapeake Bay Program, [www.chesapeakebay.net](http://www.chesapeakebay.net), North American Datum 1983. For more information on the tidal stations and Chesapeake Bay tidal water quality monitoring, refer to <https://www.chesapeakebay.net/what/programs/quality-assurance/tidal-water-quality-monitoring>.

Summer chlorophyll *a* concentrations are higher in the tidal fresh stations (Figure 15a) than in the spring (Figure 13a) and are also quite variable over time. The most dramatic decrease in concentrations is at MAT0016, but in recent years, the concentrations have increased. The degradations at the oligohaline (RET) stations appear slight but are clearer from these graphs. In the Anacostia River tidal fresh DC Upstream area, chlorophyll *a* concentrations exhibit a declining trend over time. Similar decreasing trends are observed in the Kingman Lake and Anacostia tidal fresh DC Near Potomac stations (Figure 15b).

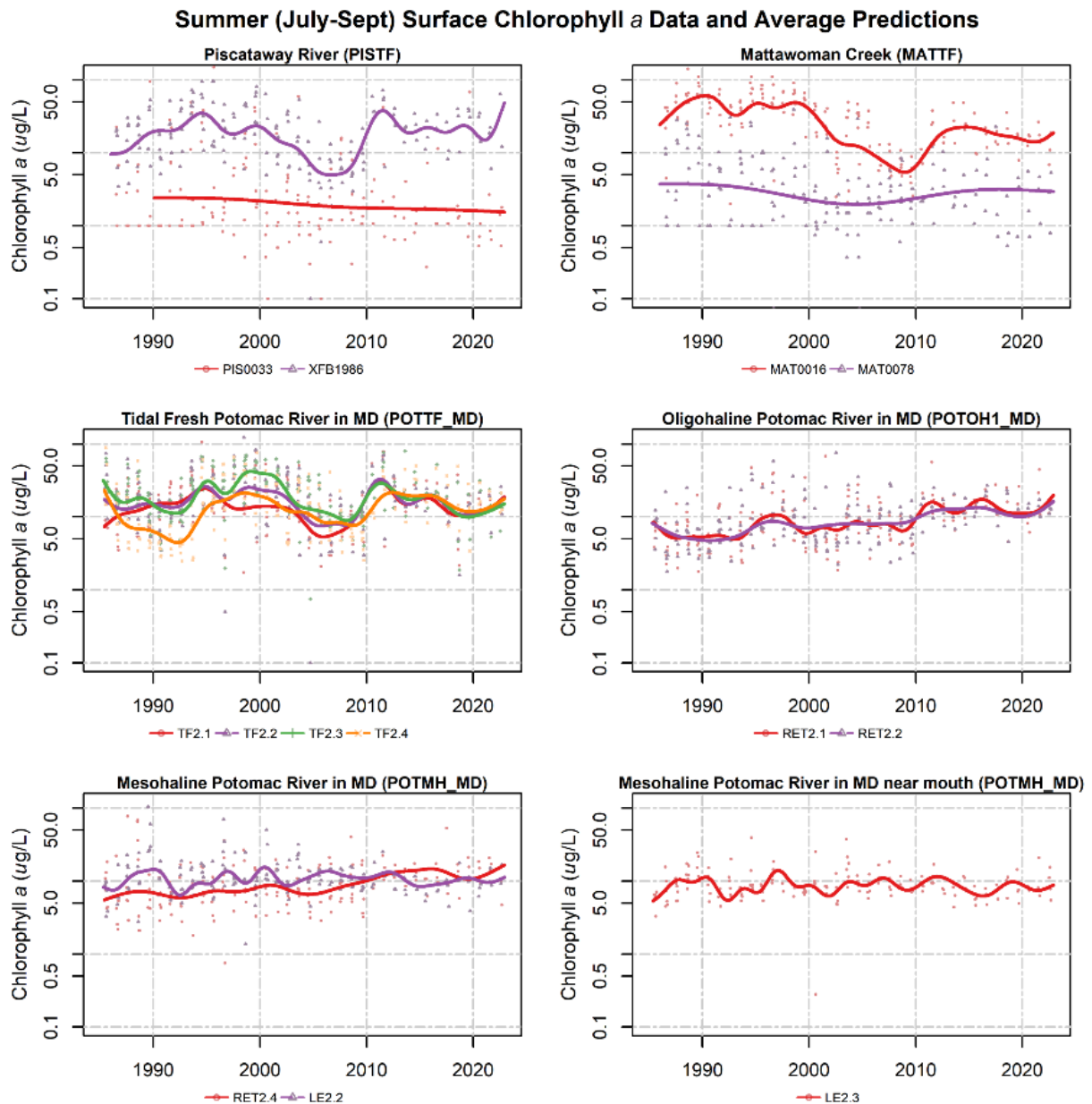


Figure 15a. Surface summer chlorophyll *a* concentration data (dots) and average long-term pattern generated from non-flow adjusted Generalized Additive Models (GAMs). Colored dots represent July-September data corresponding to the monitoring station shown indicated in the legend; colored lines represent mean summer GAM estimates for the noted monitoring stations.

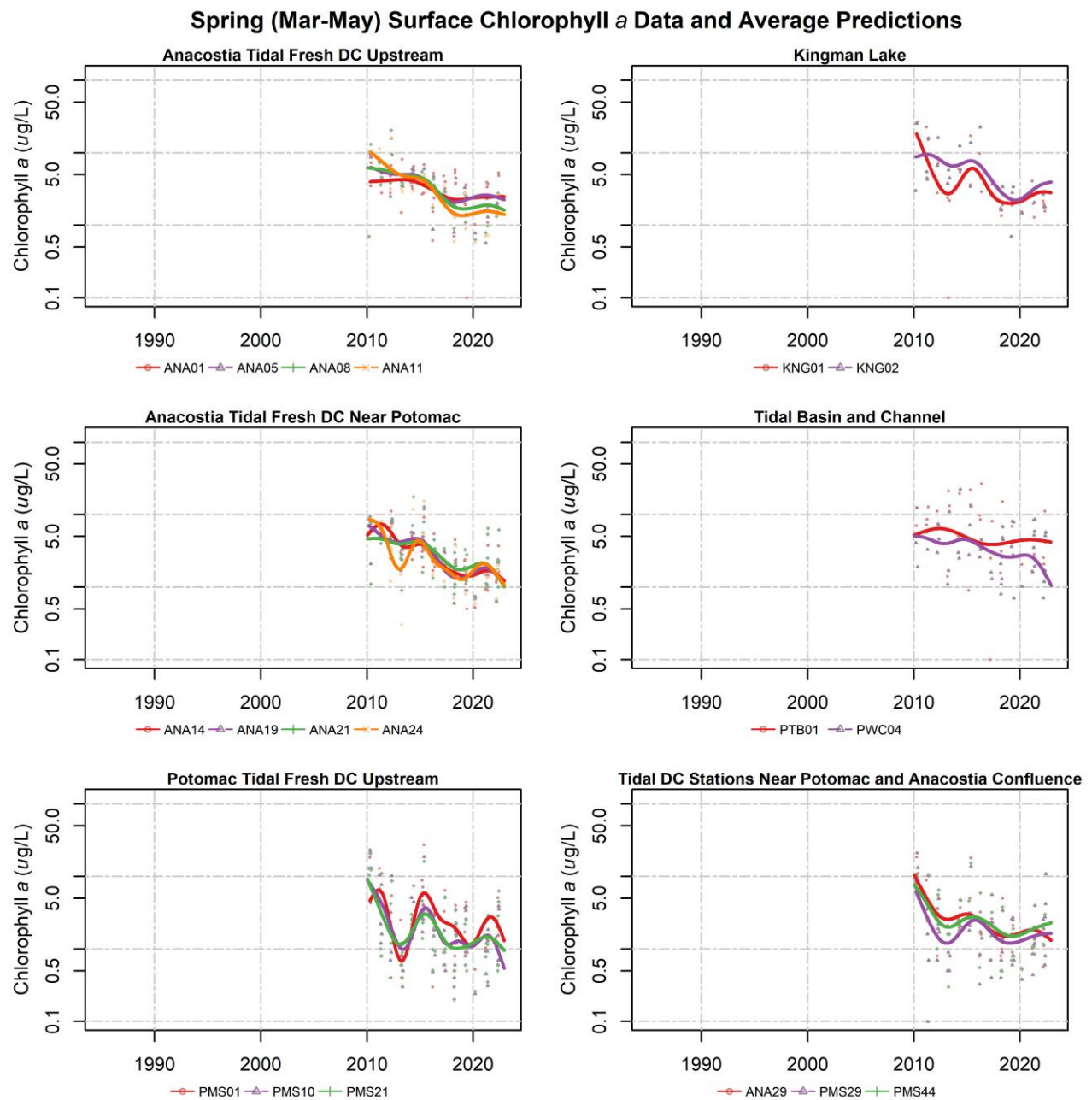


Figure 15b. Surface summer chlorophyll *a* concentration data (dots) and average long-term pattern generated from non-flow adjusted Generalized Additive Models (GAMs). Colored dots represent July-September data corresponding to the monitoring station shown indicated in the legend; colored lines represent mean summer GAM estimates for the noted monitoring stations. For chlorophyll *a* at Washington DC tidal stations, the time series start in 2010 due to data availability.



## 4.5 Secchi Disk Depth

Trends in Secchi disk depth, a measure of visibility through the water column, are varied along the tributary (Figure 16). In the long-term, Secchi depth shows degradation especially in the tidal fresh and oligohaline stations except for significantly improving trends for stations MAT0016 and TF2.4. In contrast, short-term trends reveal fewer degrading trends overall, with most stations showing unlikely trends. Stations MAT0016 and TF2.4 continue to show improving trends even in the short-term. The tidal Washington D.C. stations show mostly long-term improvements with mixed trends in the short-term (Figure 16).

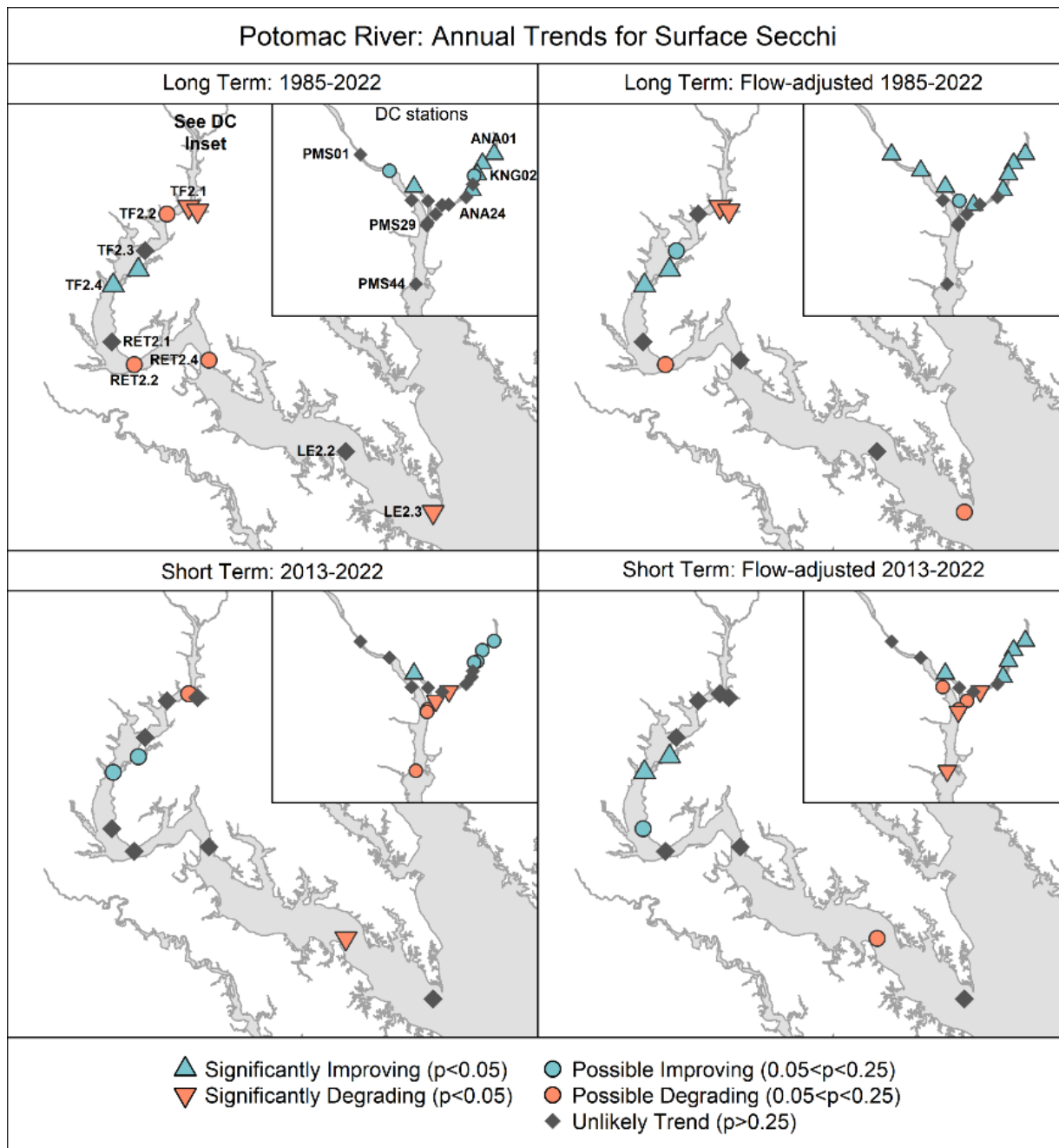


Figure 16. Annual flow-adjusted Secchi depth trends as calculated using Generalized Additive Models (Murphy et al. 2019). Base map credit Chesapeake Bay Program, [www.chesapeakebay.net](http://www.chesapeakebay.net), North American Datum 1983. For more information on the tidal stations and Chesapeake Bay tidal water quality monitoring, refer to <https://www.chesapeakebay.net/what/programs/quality-assurance/tidal-water-quality-monitoring>.

Secchi depth is generally less than 1 meter throughout the tidal Potomac, except for the lower Potomac stations where it is closer to 1.5-2 meters on average. Thus, the changes that appear in the trend map (Figure 14) are difficult to distinguish in some of the datasets (dots on the graphs) and average annual GAM estimates (lines on the graphs) (Figure 17a). The Mesohaline Potomac River in MD and near mouth stations show a noticeable increase in Secchi depth in recent years. Secchi depth in the tidal Washington D.C. stations is generally 1 meter or less, except for the Potomac River tidal fresh DC Upstream stations (Figure 17b).



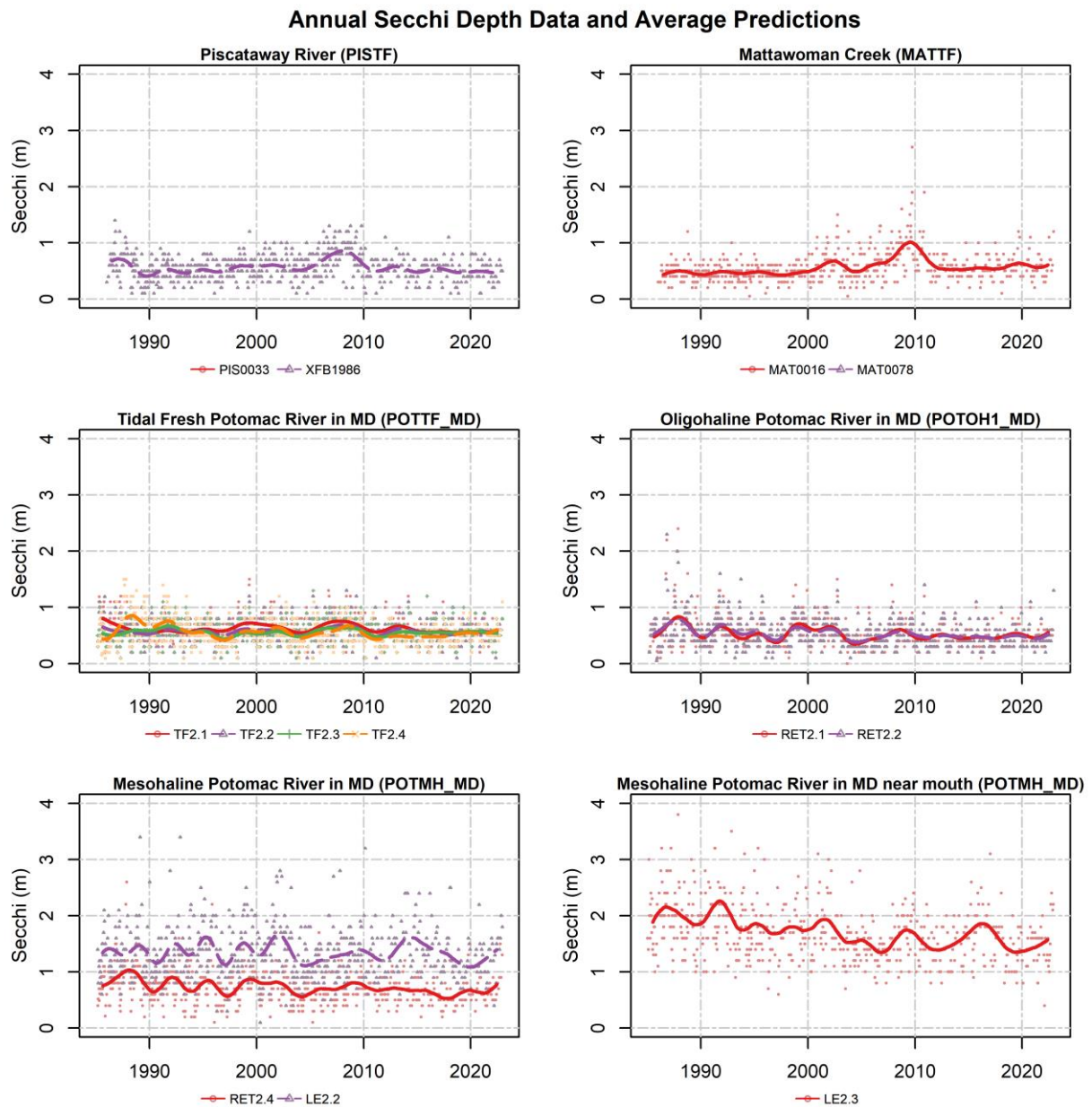


Figure 17a. Annual Secchi depth data (dots) and average long-term pattern generated from non-flow adjusted Generalized Additive Models (GAMs). Colored dots represent data corresponding to the monitoring station shown indicated in the legend; colored lines represent mean annual GAM estimates for the noted monitoring stations.

## Annual Secchi Depth Data and Average Predictions

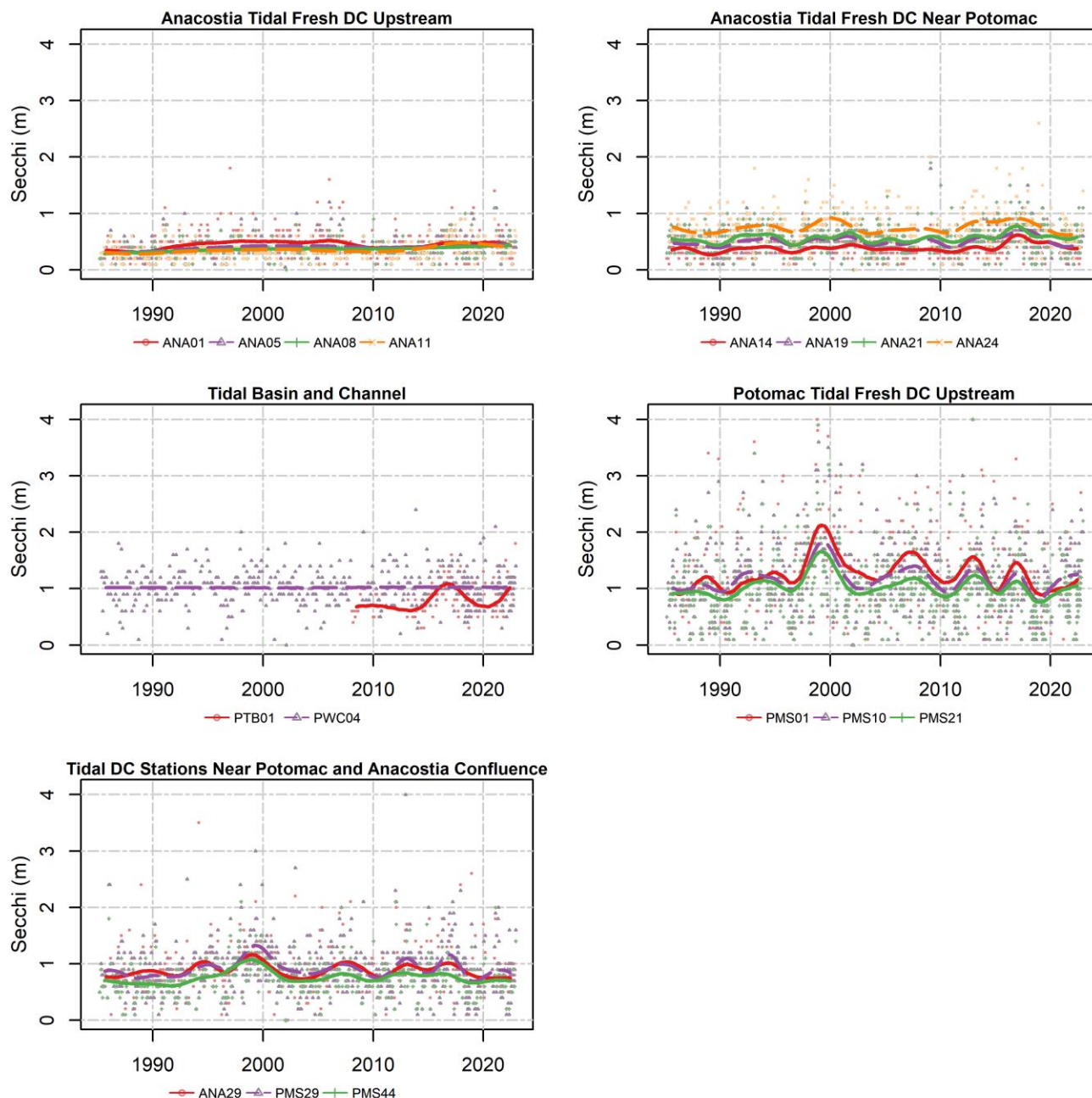


Figure 17b. Annual Secchi depth data (dots) and average long-term pattern generated from non-flow adjusted Generalized Additive Models (GAMs). Colored dots represent data corresponding to the monitoring station shown indicated in the legend; colored lines represent mean annual GAM estimates for the noted monitoring stations.

#### 4.6 Summer Bottom Dissolved Oxygen (June-September)

Long-term observed Potomac bottom DO concentrations are improving at all stations that show trends. Similarly, long-term flow-adjusted concentrations are improving at almost all stations, with the exception of significant degradation at RET2.2 and LE2.2 (top right, Figure 18). Over the short-term, the tidal fresh stations show degrading or unlikely trends. Short-term observed DO concentrations in the mesohaline show possibly improving trends (bottom left, Figure 18).

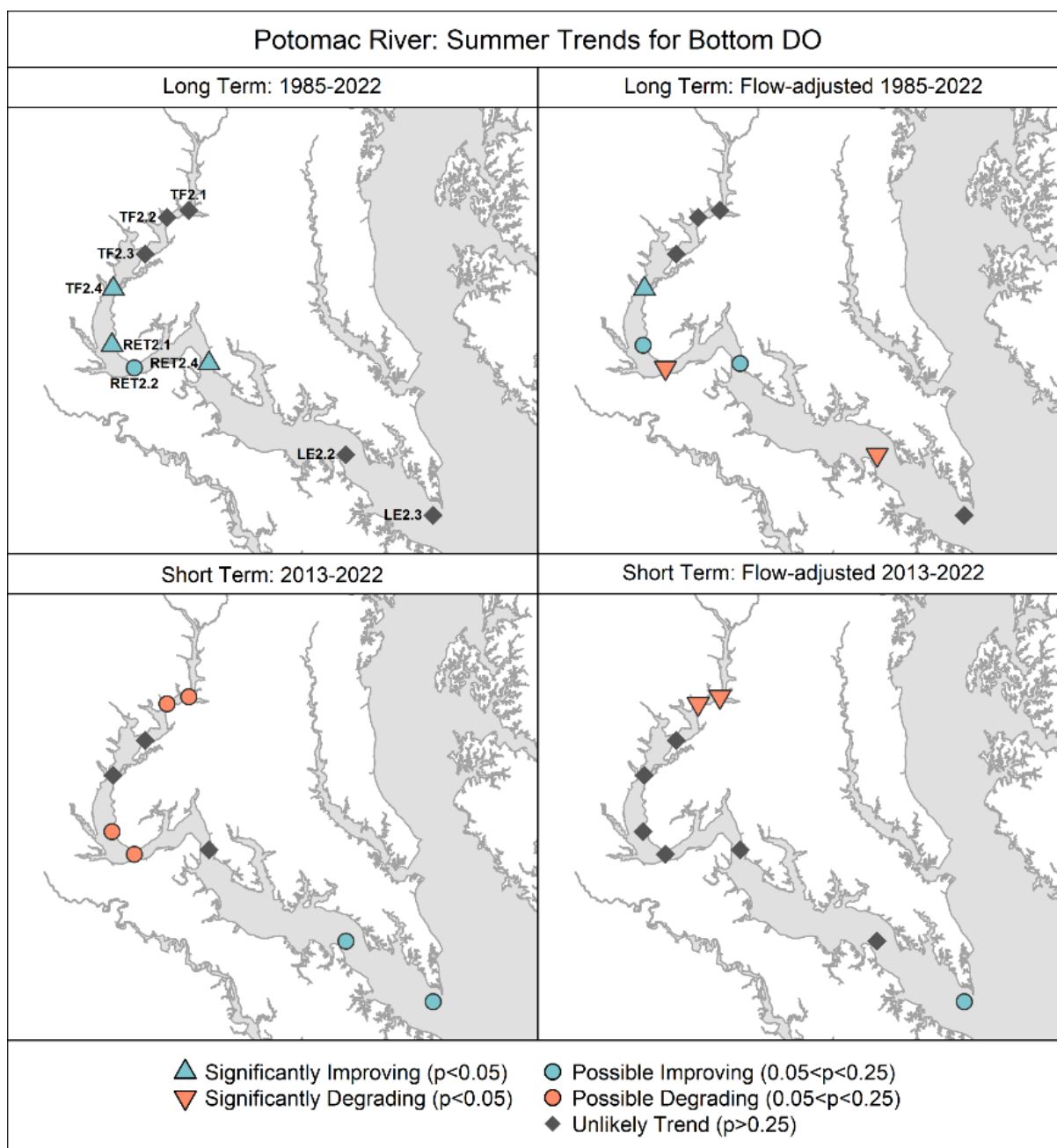


Figure 18. Flow-adjusted summer (June-September) bottom DO trends as calculated using Generalized Additive Models (Murphy et al. 2019). Base map credit Chesapeake Bay Program, [www.chesapeakebay.net](http://www.chesapeakebay.net), North American Datum 1983. For more information on the tidal stations and

Chesapeake Bay tidal water quality monitoring, refer to <https://www.chesapeakebay.net/what/programs/quality-assurance/tidal-water-quality-monitoring>.

Plots of the summer data and average summer GAM estimates demonstrate the spatial variability in bottom DO concentrations (Figure 19). Concentrations in the tidal fresh and oligohaline Potomac are much higher than in the mesohaline Potomac, although DO concentrations decline below the 5 mg/L summer Open Water 30-day mean DO criterion. Concentrations at LE2.2 and LE2.3 frequently are below the Deep Channel instantaneous criterion of 1 mg/L but both slightly improved in recent years. These slight changes result in the possibly improving trends shown in Figure 18.

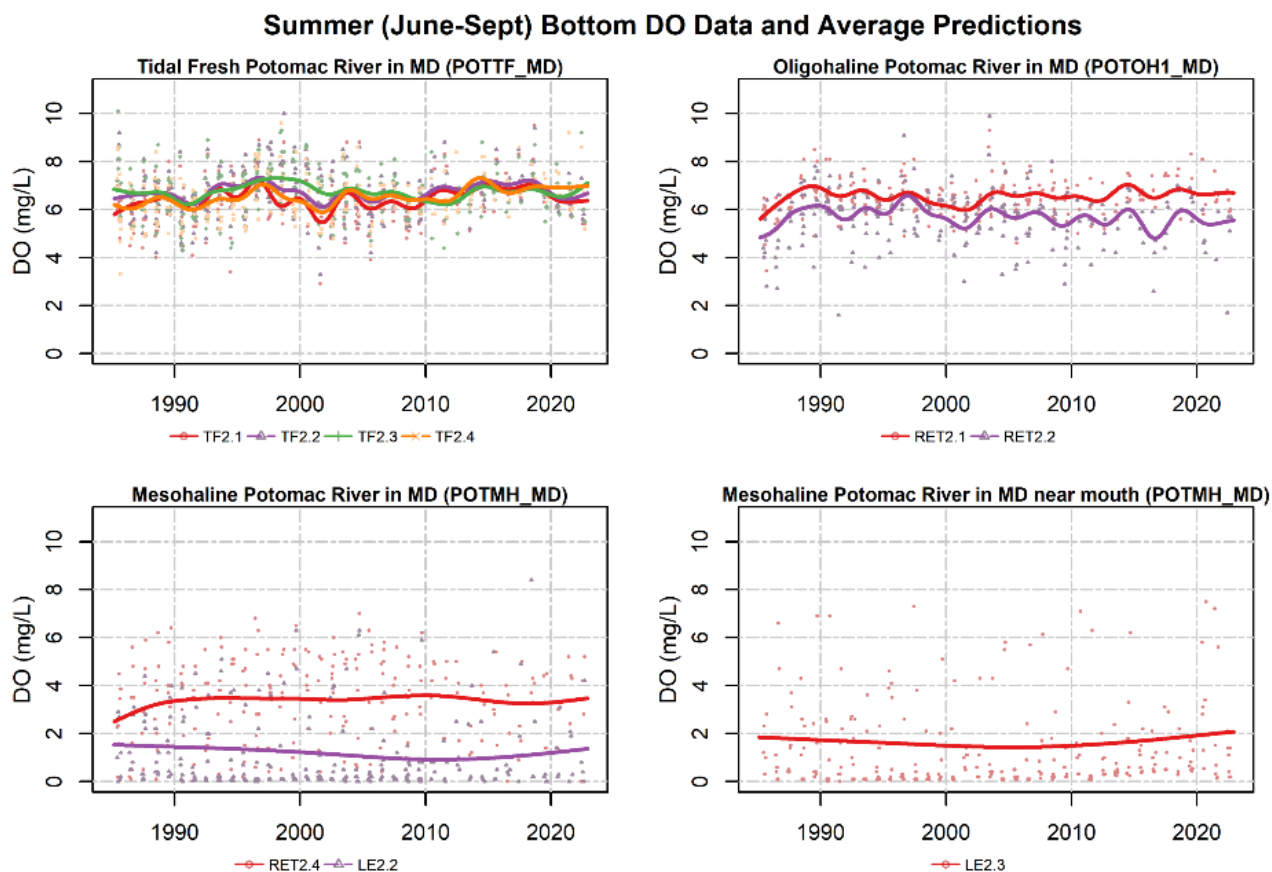


Figure 19. Summer (June-September) bottom DO concentration data (dots) and average long-term seasonal pattern generated from non-flow adjusted Generalized Additive Models (GAMs). Colored dots represent data corresponding to the monitoring station shown indicated in the legend; colored lines represent mean summer GAM estimates for the noted monitoring stations.

#### 4.7 Surface Water Temperature

Potomac River tributary surface water temperatures are increasing at most stations over the long- and short-term (Figure 20). This is consistent with other studies in Chesapeake Bay that document long-term increases in tidal water temperatures (Hinson et al., 2022; Ding and Elmore, 2015).



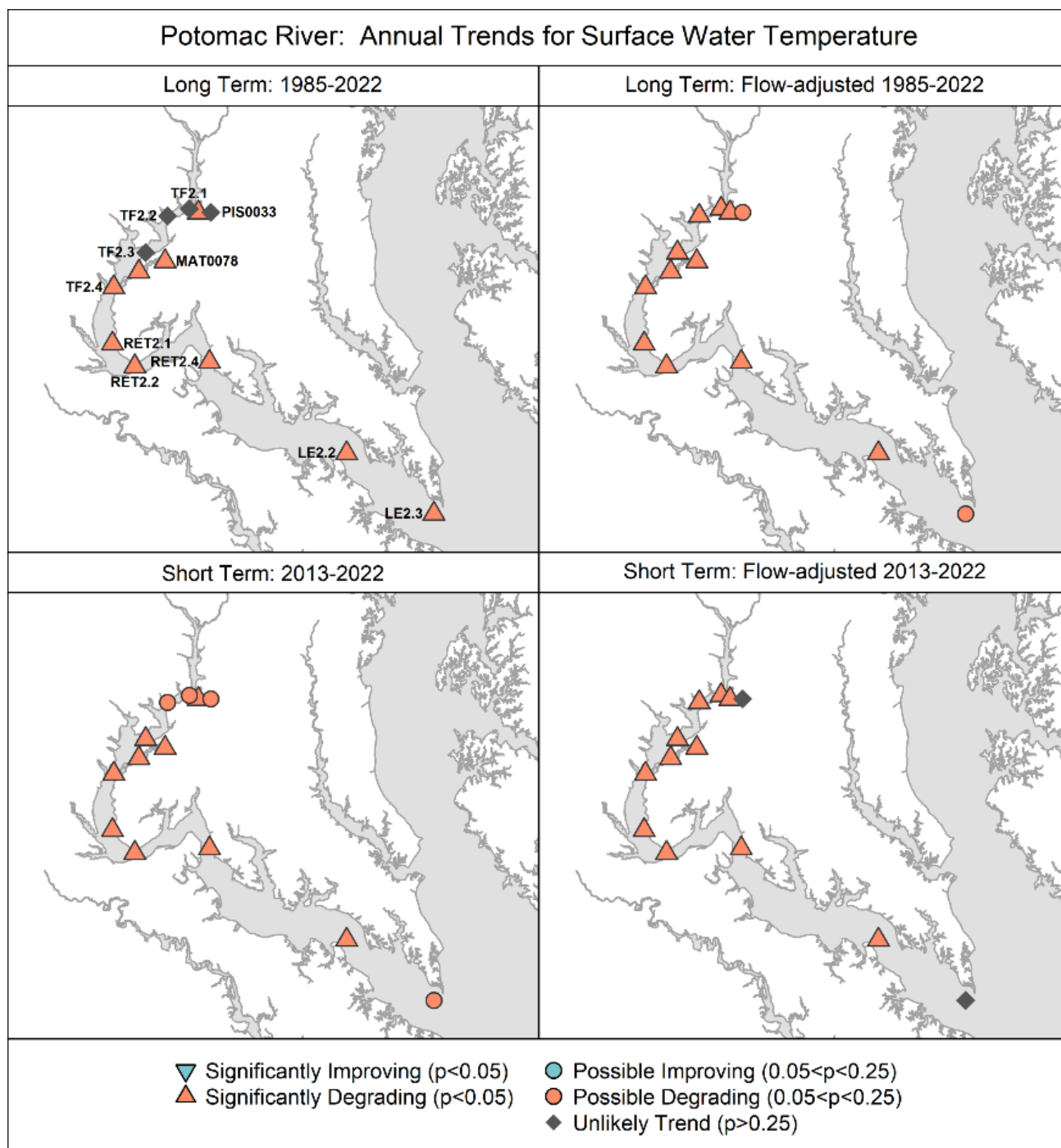


Figure 20. Annual flow-adjusted surface water temperature trends as calculated using Generalized Additive Models (Murphy et al. 2019). Base map credit Chesapeake Bay Program, [www.chesapeakebay.net](http://www.chesapeakebay.net), North American Datum 1983. For more information on the tidal stations and Chesapeake Bay tidal water quality monitoring, refer to <https://www.chesapeakebay.net/what/programs/quality-assurance/tidal-water-quality-monitoring>.

Water temperature varies seasonally in the tidal Chesapeake Bay waters, which is evident in the range of data values from almost 0 to 35 degrees Celsius ( $^{\circ}\text{C}$ ) (Figure 21). Long-term trends (Figure 20) are clear even with the large seasonal variability.

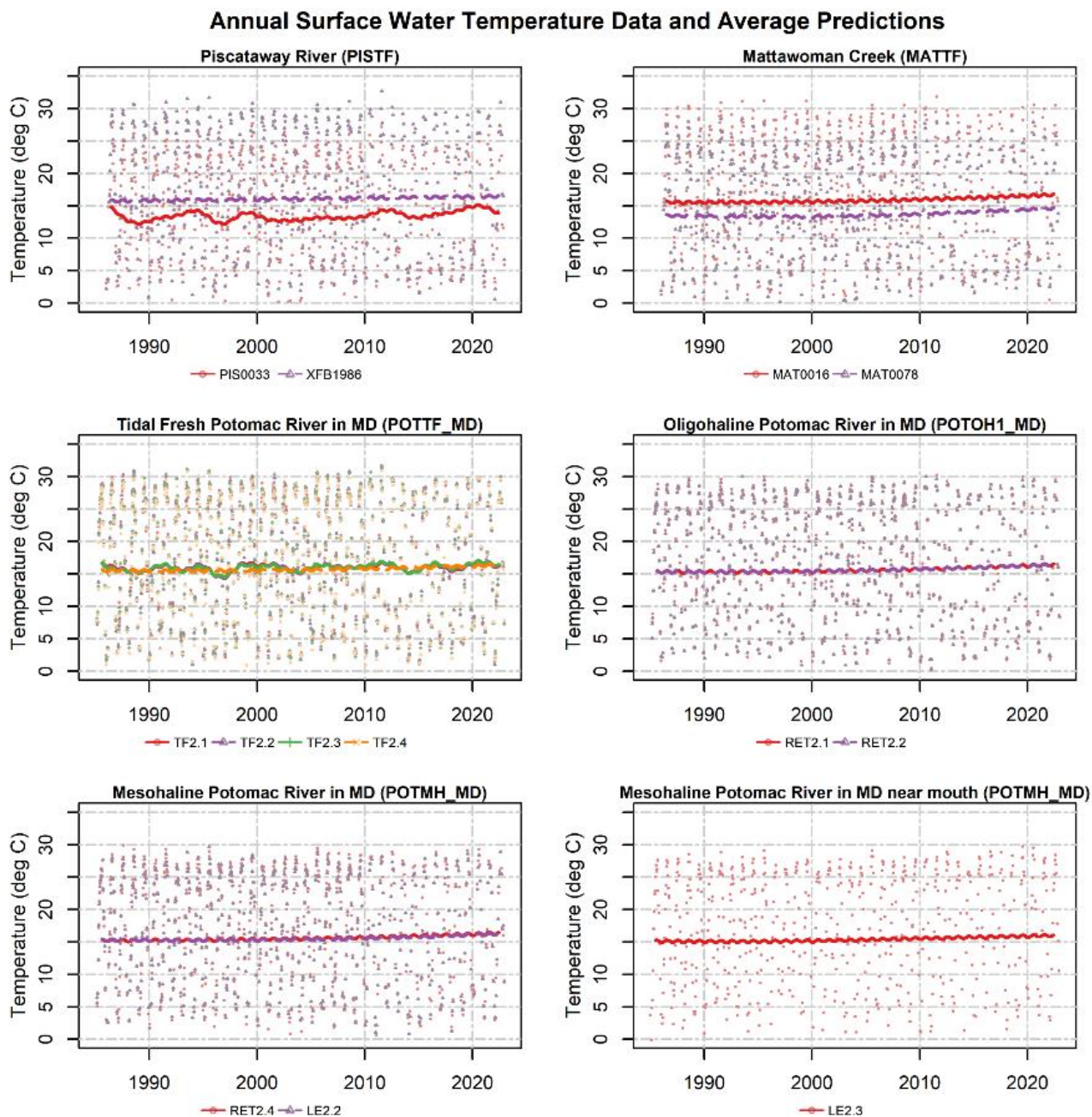


Figure 21. Annual surface water temperature data (dots) and average long-term pattern generated from non-flow adjusted Generalized Additive Models (GAMs). Colored dots represent data corresponding to

the monitoring station shown indicated in the legend; colored lines represent mean annual GAM estimates for the noted monitoring stations.

## 5. Factors Affecting Trends

### 5.1 Watershed Factors

#### 5.1.1. Effects of Physical Setting

The geology of the Potomac River watershed and its associated land use affects the quantity and transmission of nitrogen, phosphorus, and sediment delivered to non-tidal and tidal streams (Figure 22) (Brakebill et al., 2010; Ator et al., 2011; Ator et al., 2019; Ator et al., 2020; Noe et al., 2020). Flow-normalized load estimates remove most interannual variability associated with differences in streamflow, permitting a closer examination of responses to factors that change nutrient sources or transport (such as best management practices).



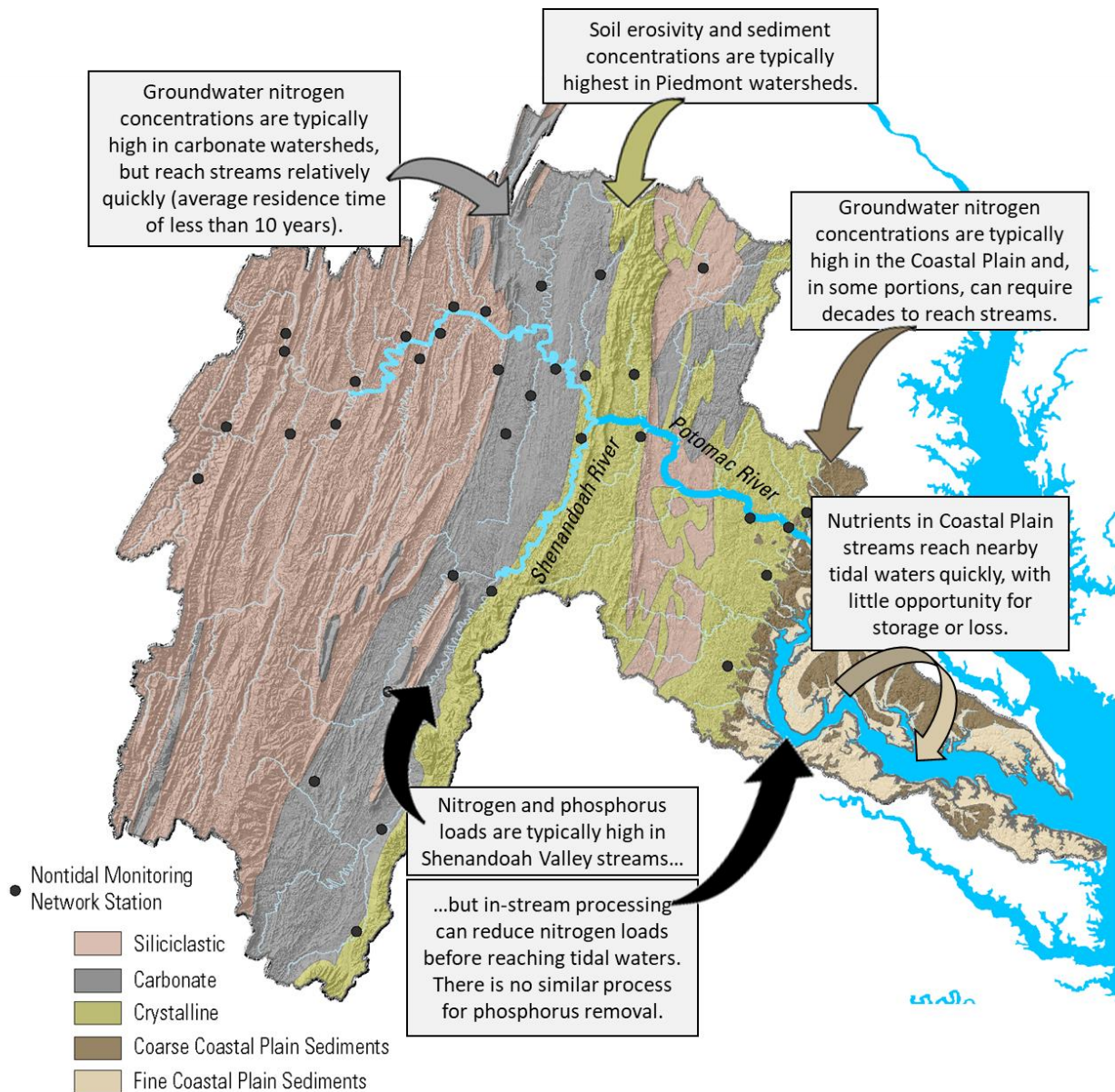


Figure 22: Effects of watershed hydrogeomorphology on nutrient transport to freshwater streams and tidal waters. Base map modified from (King *et al.*, 1974) and (Ator *et al.*, 2005), North American Datum 1983.

### Nitrogen

Groundwater is an important delivery pathway for nitrogen, as nitrate, to most streams in the Chesapeake Bay watershed (Ator and Denver, 2012; Lizarraga, 1997). The proportion of nitrogen in groundwater that reaches freshwater streams and/or tidal waters is heavily dependent on location in the watershed (Figure 22). Concentrations of groundwater nitrogen, primarily as nitrate, are typically highest in the Potomac River watershed in portions of the Valley and Ridge physiographic province underlain by carbonate rocks and in areas of the Coastal Plain with permeable, well-drained soils (Greene *et al.*, 2005; Terziotti *et al.*, 2017). The geology of these areas provides suitable land for agriculture but has little potential for denitrification (Böhlke and Denver, 1995; Lizarraga, 1997; Miller *et*



*al.*, 1997; Sanford and Pope, 2013), so nitrogen that is not removed by plants or exported in agricultural products can move relatively efficiently to groundwater and to streams. The typical residence time of groundwater delivered to streams in the Chesapeake Bay watershed is about 10 years, but ages vary from less than one year to greater than 50 years based on bedrock structure, groundwater flow paths, and aquifer depths (Lindsey and others, 2003). A similar range of water ages has been measured from Piedmont crystalline springs (0 – 34 years, Phillips and others, 2016). Groundwater represents about 50% of streamflow in most Chesapeake Bay streams, with the other half composed of soil moisture and runoff, which have residence times of months to days (Phillips, 2007).

### Phosphorus

Phosphorus binds to soil particles, and most phosphorus delivered to Chesapeake Bay is attached to sediment (Zhang and others, 2015); however, once fully phosphorus saturated, soils will not retain new applications, leading to increased export of dissolved phosphorus to streams from shallow soils and groundwater (Staver and Brinsfield, 2001). Phosphorus sorption capacity varies based on soil particle chemical composition and physical structure, with clays typically having the greatest number of sorption sites and highest average phosphorus concentrations (Sharpley, 1980). The highest soil phosphorus concentrations in the Potomac River watershed typically occur in agricultural areas (Ator *et al.*, 2011) where inputs of manure and fertilizer exceed crop needs. Some sedimentary rocks in the Potomac Piedmont province contain large phosphorus reservoirs (Terziotti, 2019). While these natural sources contribute to in-stream loads, most of this phosphorus is insoluble and only represents a dominant source in undeveloped watersheds. Reducing soil phosphorus concentrations can take a decade or more (Kleinman and others, 2011) and, until this occurs, watershed phosphorus loads may be unresponsive to management practices (Jarvie and others, 2013; Sharpley and others, 2013).

### Sediment

Factors affecting streambank erosion are highly variable throughout this watershed and include drainage area (Gellis and others, 2015; Gellis and Noe, 2013; Gillespie and others, 2018; Hopkins and others, 2018), bank sediment density (Wynn and Mostaghimi, 2006), vegetation (Wynn and Mostaghimi, 2006), stream valley geomorphology (Hopkins and others, 2018), and developed land uses (Brakebill and others, 2010). The delivery of sediment from upland soil erosion, streambank erosion, and tributary loading varies throughout the Potomac River watershed, but in-stream concentrations are typically highest in streams that drain Piedmont geology (Brakebill and others, 2010). The erosivity of Piedmont soils results from its unique topography and the prevalence of agricultural and urban land uses in these areas (Trimble 1975, Gellis et al. 2005, Brakebill et al. 2010).

### Delivery to tidal waters from the non-tidal watershed

The delivery of nitrogen, phosphorus, and sediment in non-tidal streams to tidal waters in the Potomac River watershed varies based on physical and chemical factors that affect in-stream retention, loss, or storage. In general, nutrient and sediment loads in tidal waters are most strongly influenced by conditions in proximal non-tidal streams that have less opportunity for denitrification and floodplain trapping of sediment sorbed phosphorus. In-stream denitrification rates vary spatially and temporally throughout the Potomac River watershed and typically increase with soil moisture and temperature

(Pilegaard, 2013). Differences in time of travel mean that more nitrogen load generated in the agricultural watersheds of Virginia's Shenandoah Valley can be removed through denitrification before reaching tidal waters than loads from urban areas surrounding Washington D.C., which are closer to the Potomac River (Ator *et al.*, 2011). There are no natural chemical processes that remove phosphorus from streams, but sediment and associated phosphorus can be trapped in floodplains before reaching tidal waters (Noe *et al.*, 2022). High rates of sediment trapping by Coastal Plain nontidal floodplains and head-of-tide tidal freshwater wetlands creates a "sediment shadow," or area with limited sediment availability for sediment accumulation and wetland accretion in many tidal rivers. This sediment shadow effect limits sediment delivery to Chesapeake Bay and reduces wetland resilience to the impacts of sea level rise (Ensign and others, 2013; Noe and Hupp, 2009). The average age of sediment stored in-channel is typically assumed to be less than one year (Gellis *et al.*, 2017). Delivery to tidal waters can be exponentially longer as sediment moves in and out of different storage zones during downstream transport and tidal cycles.

#### 5.1.2. Estimated Nutrient and Sediment Loads

Nutrient and sediment loads to the Potomac River are estimated from a combination of monitored loads from the U.S. Geological Survey (USGS) River Input Monitoring (RIM) station (USGS station number 01646580; USGS, 2022) located at the nontidal-tidal interface and below-RIM simulated loads from the Chesapeake Bay Program Watershed Model. Nitrogen, phosphorus, and suspended sediment loads to the tidal Potomac were primarily from the RIM basins, although contributions from the below-RIM areas were also substantial (Figure 23). Over the period of 1985-2022, 1.2, 0.075, and 75 million tons of nitrogen, phosphorus, and suspended sediment loads were exported through the Potomac River watershed, with 68%, 74%, and 56% of those loads from the RIM areas, respectively. Mann-Kendall trends and Sen's slope estimates are summarized for each loading source in Table 2.

Estimated TN loads showed a statistically significant ( $p < 0.01$ ) overall decline of 370 ton/yr in the period between 1985 and 2022. This reduction represents a combination of reductions in below-RIM loads (-290 ton/yr;  $p < 0.01$ ) and RIM loads (-85 ton/yr;  $p = 0.43$ ). Within the below-RIM loads, long-term statistically significant declines were observed with both point sources (-280 ton/yr;  $p < 0.01$ ) and atmospheric deposition to the tidal waters (-8.1 ton/yr;  $p < 0.01$ ). The significant below-RIM point source reductions in TN are a result of substantial efforts to reduce nitrogen loads from major wastewater treatment facilities by implementing biological nutrient removal (Lyerly *et al.*, 2014). The significant decline in atmospheric deposition of TN to the tidal waters is consistent with findings that atmospheric deposition of nitrogen has decreased due to benefits from the Clean Air Act implementation (Eshleman *et al.*, 2013; Lyerly *et al.*, 2014).

Estimated TP loads showed an overall decline of 7.9 ton/yr in the period between 1985 and 2022, although this decline is not statistically significant ( $p = 0.55$ ). This reduction is largely driven by the RIM loads (-6.1 ton/yr,  $p = 0.53$ ). Within the below-RIM loads, point sources showed a statistically significant decline in this period (-1.7 ton/yr;  $p < 0.01$ ), whereas nonpoint sources showed a long-term increase (1.1 ton/yr,  $p = 0.63$ ). The TP point source load reduction has also been attributed to significant efforts to reduce phosphorus in wastewater discharge through the phosphorus detergent ban in the early part of this record, as well as technology upgrades at wastewater treatment facilities (Lyerly *et al.*, 2014).

Estimated suspended sediment (SS) loads showed an overall decline of 11,000 ton/yr in the period between 1985 and 2022, although this decline is not statistically significant ( $p = 0.37$ ). Both the RIM and below-RIM loads showed long-term declines, but neither is statistically significant. Like TP and TN, SS loads from point sources below-RIM stations showed a statistically significant decline over this period ( $-140$  ton/yr;  $p < 0.01$ ).

## Potomac River

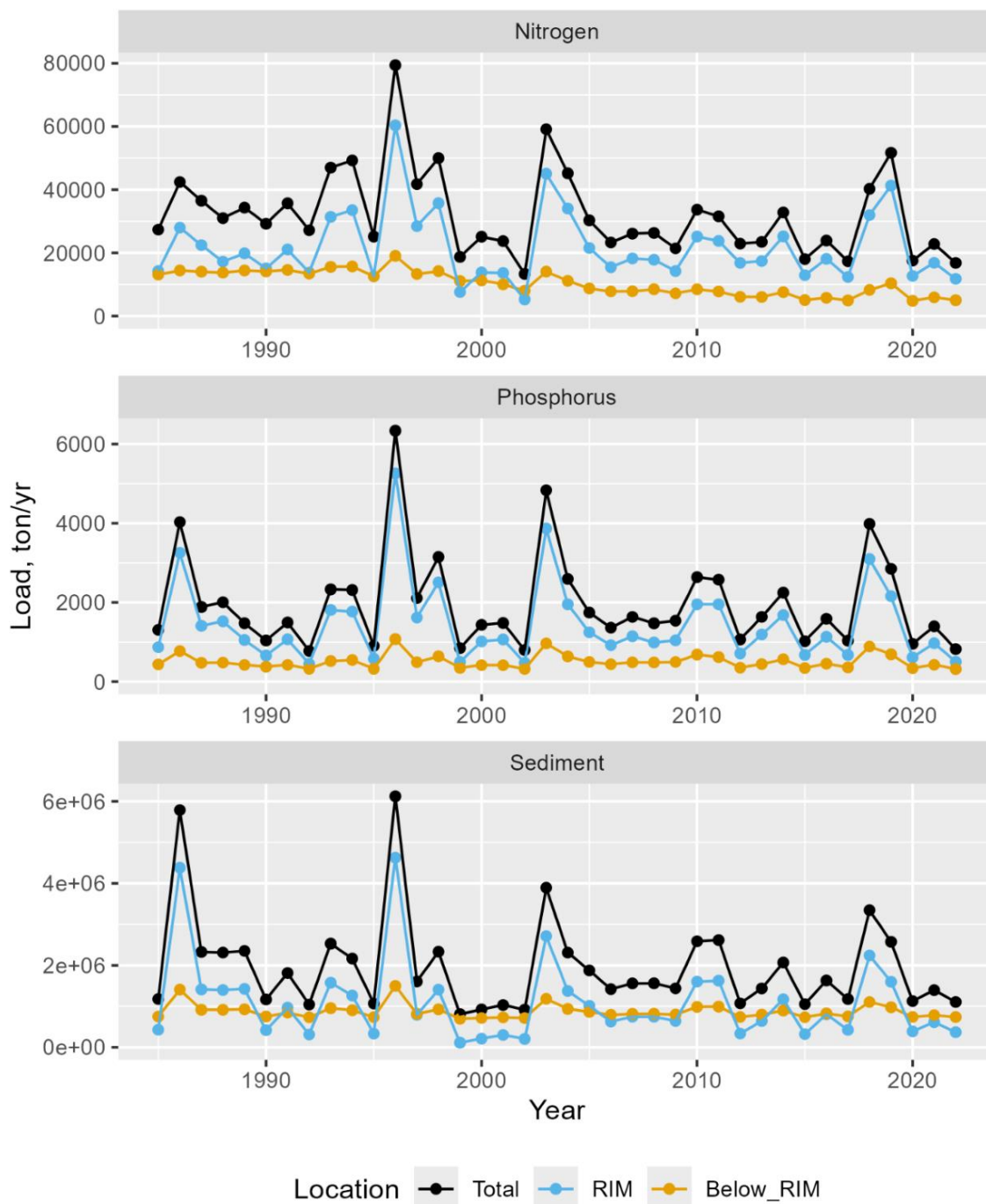


Figure 23. Estimated total loads (sum of RIM and Below-RIM) of nitrogen (TN), phosphorus (TP), and suspended sediment (SS) from the RIM and below-RIM areas of the Potomac River. RIM refers to the USGS River Input Monitoring site, station 01646580 (USGS, 2022) located just above the head of tide of this tributary, which includes upstream point source loads. Below-RIM estimates are a combination of simulated non-point and reported point-source loads.

Table 2. Summary of Mann-Kendall trends for the period of 1985-2022 for total nitrogen (TN), total phosphorus (TP), and suspended sediment (SS) loads to the Potomac River.

Categories	TN		TP		SS	
	Trend, metric ton/yr	p-value	Trend, metric ton/yr	p-value	Trend, metric ton/yr	p-value
Total watershed	-370	< 0.01	-7.9	0.55	-11,000	0.37
RIM watershed <sup>1</sup>	-85	0.43	-6.1	0.53	-9,600	0.35
Below-RIM watershed <sup>2</sup>	-290	< 0.01	-0.53	0.74	-1,400	0.45
<i>Below-RIM point source</i>	-280	< 0.01	-1.7	< 0.01	-140	< 0.01
<i>Below-RIM nonpoint source</i> <sup>3</sup>	-2.1	0.86	1.1	0.63	-1,300	0.53
<i>Below-RIM tidal deposition</i>	-8.1	< 0.01	-	-	-	-
<sup>1</sup> Loads for the RIM watershed were estimated loads at the USGS RIM station 01646580 (Potomac River at Chain Bridge, Washington, D.C.; USGS, 2022; <a href="https://cbrim.er.usgs.gov/loads_query.html">https://cbrim.er.usgs.gov/loads_query.html</a> ). <sup>2</sup> Loads for the below-RIM watershed were obtained from the Chesapeake Bay Program Watershed Model ( <a href="https://cast.chesapeakebay.net/">https://cast.chesapeakebay.net/</a> ). <sup>3</sup> Below-RIM nonpoint source loads were obtained from the Chesapeake Bay Program Watershed Model's progress runs specific to each year from 1985 and 2022, which were adjusted to represent actual hydrology using the method of the Chesapeake Bay Program's Loads to the Bay indicator (see <a href="https://www.chesapeakeprogress.com/clean-water/water-quality">https://www.chesapeakeprogress.com/clean-water/water-quality</a> ).						

### 5.1.3. Expected Effects of Changing Watershed Conditions

According to the Chesapeake Bay Program's Watershed Model known as the Chesapeake Assessment Scenario Tool (CAST; <https://cast.chesapeakebay.net/About/UpgradeHistory>, version Phase 6 - 7.6.0), changes in population size, land use, and pollution management controls between 1985 and 2022 would be expected to reduce long-term average nitrogen, phosphorus, and sediment loads to the tidal Potomac River by -32%, -37%, and -14%, respectively (Figure 24). In contrast to the annual loads analysis above, CAST loads are based on changes in management only and do not account for annual fluctuations in weather. CAST loads are calculated without lag times for delivery of pollutants or lags related to BMPs becoming fully effective after installation. In 1985, agriculture and wastewater were the two largest sources of nitrogen loads. By 2022, agriculture remained the largest nitrogen source; however, wastewater nitrogen loads had reduced by -75%, and the developed sector had taken its place as the second largest nitrogen source. Overall, decreasing nitrogen loads from agriculture (-25%), natural (-8%), stream bed and bank (-10%), and wastewater (-75%) sources were partially counteracted by increases from developed (+58%) and septic (+58%) sources.

The two largest sources of phosphorus loads as of 2022 were the agriculture and developed sectors. Overall, expected declines from agriculture (-40%), natural (-11%), stream bed and bank (-31%), and

wastewater (-78%) sources were partially counteracted by increases from developed (+56%) and septic (+391%) sources.

For sediment, the largest sources are stream bed and bank and shoreline areas: these two sources decreased by -15% and -1%, respectively between 1985 and 2022. Sediment loads from the agriculture sector decreased by -46%, while sediment load from developed areas increased by 28%.

Overall, changing watershed conditions are expected to result from the agriculture, natural, stream bed and bank, and wastewater sectors achieving reductions in nitrogen, phosphorus, and sediment loads between 1985 and 2022, whereas the developed and septic sectors are expected to increase in nitrogen, phosphorus, and sediment loads.

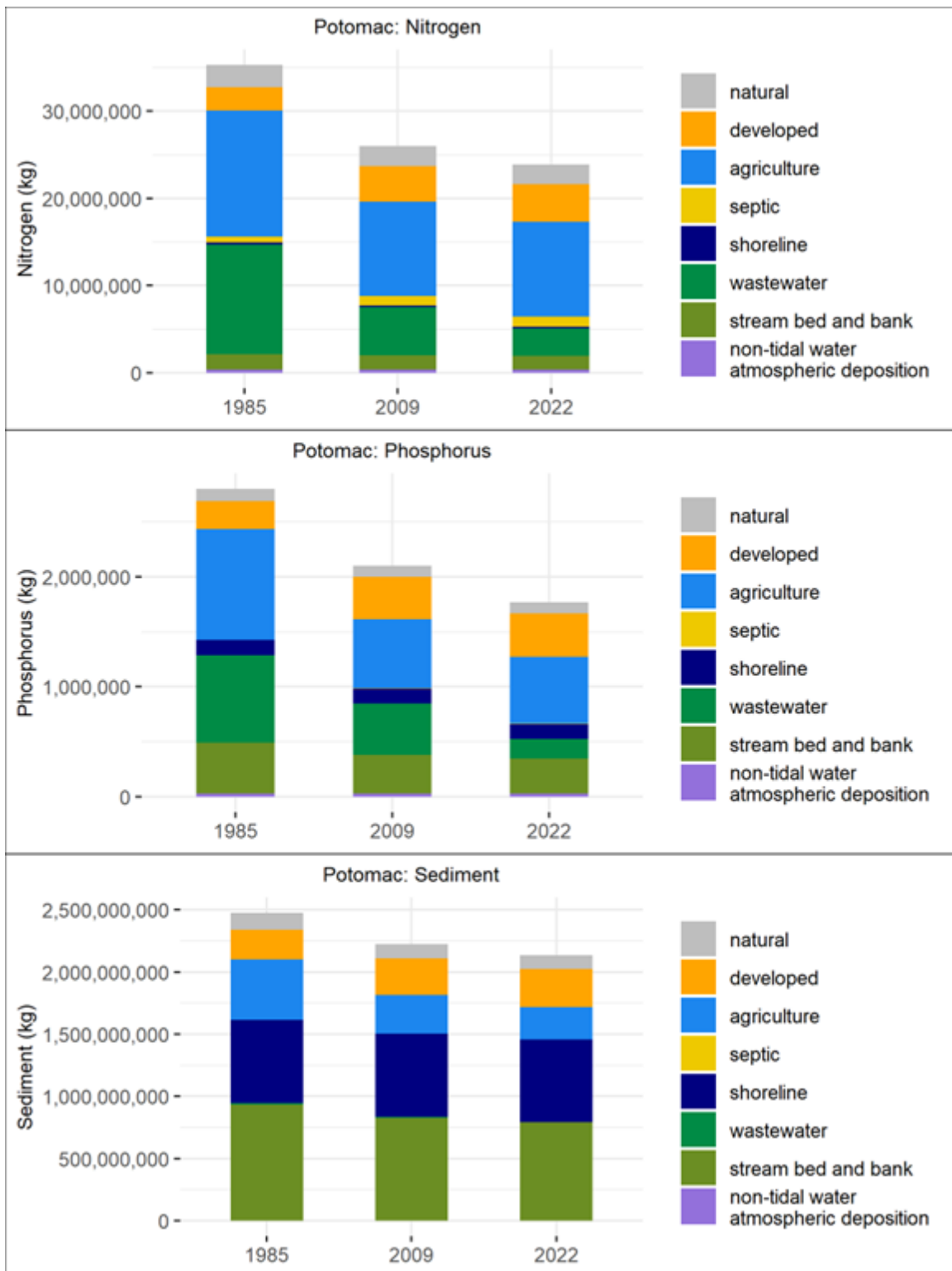


Figure 24. Expected long-term average loads of nitrogen, phosphorus, and sediment from different sources to the tidal Potomac, based on watershed conditions in 1985, 2009, and 2022

#### 5.1.4. Best Management Practices (BMPs) Implementation

Data on reported BMP implementation are available for download from CAST (<https://cast.chesapeakebay.net/About/UpgradeHistory>, version Phase 6 - 7.6.0). Reported BMP implementations on the ground as of 1985, 2009, and 2022 are compared to planned 2025 implementation levels in Figure 25 for a subset of major BMP groups measured in square kilometers. As of 2022, tillage, cover crops, pasture management, forest buffer and tree planting, stormwater management, agricultural nutrient management, and urban nutrient management were credited for 2,218; 785; 1,053; 24; 1,330; 5,639; and 1,309 square kilometers, respectively. Implementation levels for some practices are already close to achieving their planned 2025 levels: for example, 102% of planned acres for tillage had been achieved as of 2022. In contrast, about 67% of planned urban nutrient management implementation had been achieved as of 2022.

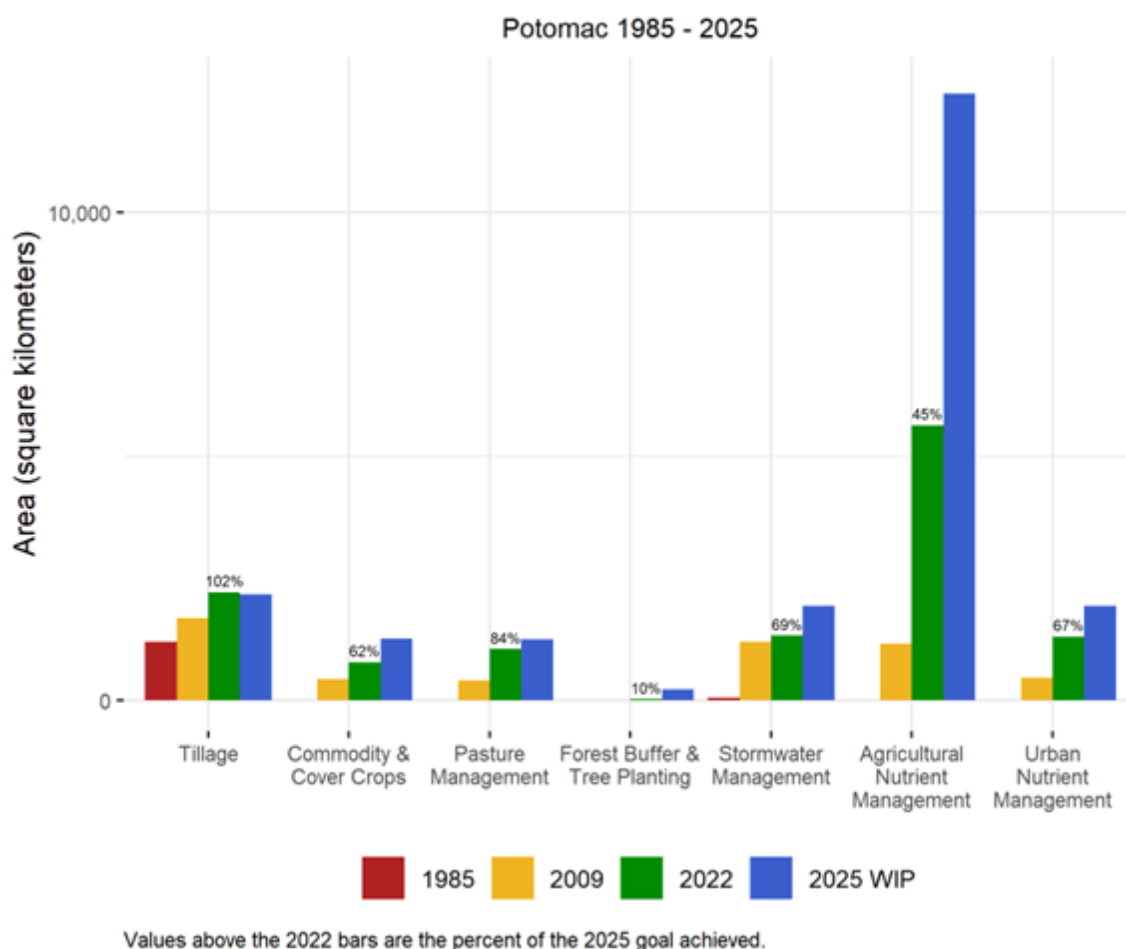


Figure 25. Best management practice (BMP) implementation and watershed implementation plan (WIP) goals in the Potomac watershed. Data are from the Chesapeake Assessment Scenario Tool (CAST; <https://cast.chesapeakebay.net/About/UpgradeHistory>, version Phase 6 - 7.6.0).

Stream restorations and animal waste management systems are two important BMPs that cannot be compared directly with those above because they are measured in different units. However, progress towards implementation goals can still be documented. Stream restoration (agricultural and urban) had



increased from 72 meters in 1985 to 148,533 meters in 2022. Over the same period, animal waste management systems treated 7,931 animal units in 1985 and 895,916 animal units in 2022 (one animal unit represents 1,000 pounds of live animal). These implementation levels represent 40% and 39% of their planned 2025 implementation levels, respectively.

#### 5.1.5. Flow-Normalized Watershed Nutrient and Sediment Loads

Flow normalization can better reveal temporal trends in river water quality by removing the effect of inter-annual variability in streamflow. Flow-normalized water quality trends help scientists evaluate changes in load resulting from changing sources, delays associated with storage or transport of historical inputs, and/or implemented management actions (Hirsch et al., 2010). Long-term (1985-2020) and short term (2011-2020) trends in flow-normalized nitrogen, phosphorus, and sediment trends have been reported for the nontidal network stations throughout the watershed (Mason et al., 2023) and can be found at the USGS National Water Information System (NWIS; USGS, 2022) (Table 3). These trends result from variability in nutrient applications, the delivery of nutrients and sediment from the landscape to streams, and from processes that affect in-stream loss or retention of nutrients and sediment.

Table 3. Long-term (1985-2020) and short-term (2011-2020) trends of flow-normalized total nitrogen (TN), total phosphorus (TP), and suspended-sediment (SS) loads for nontidal network monitoring locations in the Potomac River watershed (USGS, 2022). A more detailed summary of flow-normalized loads and trends measured at all USGS Chesapeake Bay Nontidal Network stations can be found at <https://www.usgs.gov/centers/chesapeake-bay-activities/science/chesapeake-bay-water-quality-loads-and-trends>. Degrading trends are highlighted in orange. Improving trends are highlighted in green, and no trends are not highlighted.

STAID	STNAM	Trend Start Water Year	Percent Change in Load		
			TN	TP	SS
01599000	GEORGES CREEK AT FRANKLIN, MD	2011	3.46	-23	-10.3
01601500	WILLS CREEK NEAR CUMBERLAND, MD	2011	24.5	4.03	33
01604500	PATTERSON CREEK NEAR HEADSVILLE, WV	2011	-5.39	-53.8	-16.4
01608500	SOUTH BRANCH POTOMAC RIVER NEAR SPRINGFIELD, WV	2011	8.52	-47.2	41.5
01609000	TOWN CREEK NEAR OLDTOWN, MD	2011	23	58.5	24.8
01610155	SIDELING HILL CREEK NEAR BELLEGROVE, MD	2011	7.94		
01611500	CACAPON RIVER NEAR GREAT CACAPON, WV	2011	-10.2	-33.1	4.36
01613095	TONOLOWAY CREEK NEAR HANCOCK, MD	2011	32	21.7	8.43
01613525	LICKING CREEK NEAR PECTONVILLE, MD	2011	20.6	-6.51	-55.7
01614500	CONOCOCHIEGUE CREEK AT FAIRVIEW, MD	2011	-3.56	34.4	15.6
01616500	OPEQUON CREEK NEAR MARTINSBURG, WV	2011	-9.42	-58.2	39.5
01619000	ANTIETAM CREEK NEAR WAYNESBORO, PA	2011	-11.6	-24.9	-5.16
01619500	ANTIETAM CREEK NEAR SHARPSBURG, MD	2011	-8.86	-10.5	67.4
01621050	MUDDY CREEK AT MOUNT CLINTON, VA	2011	-10.2		

01626000	SOUTH RIVER NEAR WAYNESBORO, VA	2011	14		
01628500	S F SHENANDOAH RIVER NEAR LYNNWOOD, VA	2011	-4.09		
01631000	S F SHENANDOAH RIVER AT FRONT ROYAL, VA	2011	-6.26	-26.2	-23.6
01632900	SMITH CREEK NEAR NEW MARKET, VA	2011	7.83	31.7	73.9
01634000	N F SHENANDOAH RIVER NEAR STRASBURG, VA	2011	-6.27	-43.5	-49.7
01637500	CATOCTIN CREEK NEAR MIDDLETOWN, MD	2011	15.6	1.33	29.6
01638480	CATOCTIN CREEK AT TAYLORSTOWN, VA	2011	2.49		
01639000	MONOCACY RIVER AT BRIDGEPORT, MD	2011	-5.49	-7.23	-9.79
01646000	DIFFICULT RUN NEAR GREAT FALLS, VA	2011	11.5	65	128
01646580	Potomac River at Chain Bridge, MD	2011	-4.14	-6.06	6
01651000	NORTHWEST BR ANACOSTIA RIVER NR HYATTSVILLE, MD	2011	-7.09	-15.4	19.1
01654000	ACCOTINK CREEK NEAR ANNANDALE, VA	2011	7.32	99.9	267
01658000	MATTAWOMAN CREEK NEAR POMONKEY, MD	2011	2.66		
01658500	S F QUANTICO CREEK NEAR INDEPENDENT HILL, VA	2011	-11.7	-10.7	-6.94
01599000	GEORGES CREEK AT FRANKLIN, MD	1985	-31.6		
01601500	WILLS CREEK NEAR CUMBERLAND, MD	1985	-21.9		
01614500	CONOCOCHIEGUE CREEK AT FAIRVIEW, MD	1985	-13.9	-29.9	21.3
01619500	ANTIETAM CREEK NEAR SHARPSBURG, MD	1985	-24.4		
01626000	SOUTH RIVER NEAR WAYNESBORO, VA	1985	-5.65		
01628500	S F SHENANDOAH RIVER NEAR LYNNWOOD, VA	1985	-21.1		
01631000	S F SHENANDOAH RIVER AT FRONT ROYAL, VA	1985	-11.5		
01632900	SMITH CREEK NEAR NEW MARKET, VA	1985	6.93		
01634000	N F SHENANDOAH RIVER NEAR STRASBURG, VA	1985	12.9		
01637500	CATOCTIN CREEK NEAR MIDDLETOWN, MD	1985	-2.34		
01638480	CATOCTIN CREEK AT TAYLORSTOWN, VA	1985	-24.7		
01639000	MONOCACY RIVER AT BRIDGEPORT, MD	1985	-40	-26.5	-22.4
01646000	DIFFICULT RUN NEAR GREAT FALLS, VA	1985	44.4		
01646580	Potomac River at Chain Bridge, MD	1985	-12.8	-26.8	-44.4

## 5.2 Tidal Factors

Once pollutants reach tidal waters, a complex set of environmental factors interact with them to affect key habitat indicators like algal biomass, DO concentrations, water clarity, submerged aquatic vegetation (SAV) abundance, and fish populations (Figure 26) (Kemp et al., 2005; Testa et al., 2017). For example, phytoplankton growth depends on nitrogen and phosphorus (Fisher et al., 1992; Kemp et al., 2005; Zhang et al., 2021) and on light and water temperature (Buchanan et al., 2005; Buchanan, 2020). In general, the saline waters of the lower Chesapeake Bay tend to be more transparent than tidal-fresh regions, and waters adjacent to nutrient input points are more affected by these inputs than more distant regions (Bukaveckas et al., 2011; Keisman et al., 2019; Testa et al., 2019). DO concentrations are affected by salinity- and temperature-driven stratification of the water column, wind-driven mixing, and phytoplankton respiration and decomposition (Scully, 2010; Murphy et al., 2011). When anoxia occurs at the water-sediment interface, nitrogen and phosphorus stored in the sediments can be released

through anaerobic chemical reactions (Testa and Kemp, 2012). When low-oxygen water and sediment burial suffocate benthic plant and animal communities, their nutrient consumption and water filtration services are lost. Conversely, when conditions improve enough to support abundant SAV and benthic communities, their functions can sustain and even advance progress towards a healthier ecosystem (Cloern, 1982; Phelps, 1994; Ruhl and Rybicki, 2010; Gurbisz and Kemp, 2014).

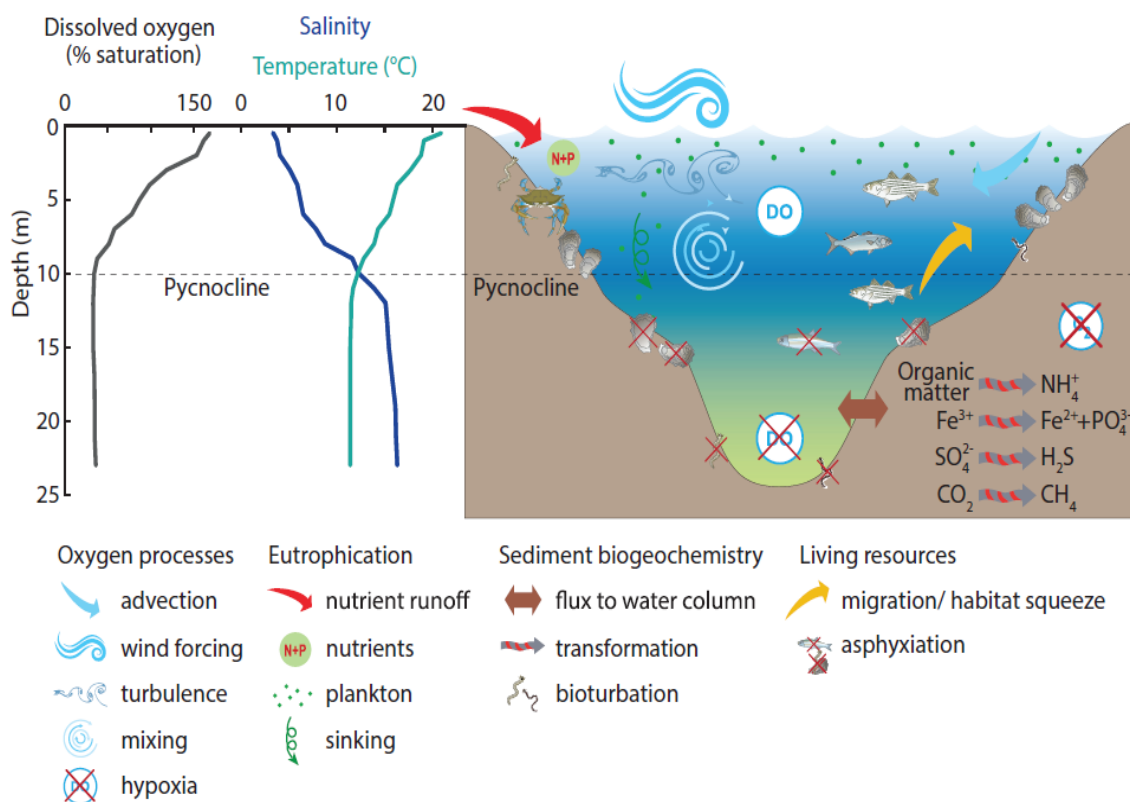


Figure 26. Conceptual diagram illustrating how hypoxia is driven by eutrophication and physical forcing, while affecting sediment biogeochemistry and living resources. From (Testa et al., 2017).

### 5.2.1. Watershed and Estuarine Volume

High nutrient loads relative to tidal river size are indicative of areas that are more susceptible to eutrophication (Bricker et al., 2003; Ferreira et al., 2007). The relationship between watershed area and tidal river size may also be an indicator of eutrophication potential; however, there are competing effects. A large watershed relative to the volume of receiving water would likely correlate with higher nutrient loads; however, a large watershed would also correlate with a higher flow rate and decreased flushing time (Bricker et al., 2008). Figure 27 is a comparison of watershed area, which includes tidal wetland area, versus estuarine volume for all estuaries and sub-estuaries identified in the CBP monitoring segment scheme. Larger estuaries will contain multiple monitoring segments and, in many cases, sub-estuaries. For example, the Potomac River contains monitoring segments in the tidal fresh, oligohaline, and mesohaline sections of the river as well as the entire Anacostia River and other sub-estuaries. Figures 28 and 29 are comparisons of estimated annual average nitrogen and phosphorus loads, respectively, for the 2021 progress scenario in CAST versus the estuarine volume for the same set

of estuaries and sub-estuaries. Table 4 shows the associated tributary name for the abbreviated name and group name represented in the watershed and estuarine volume figures.

The Potomac River estuary volume and watershed area contain approximately 9% of the total volume and 10% of the total watershed area of the Chesapeake Bay, respectively (Table 5). This ranks the Potomac mainstem as the Chesapeake Bay tributary with the 3<sup>rd</sup> largest volume and 3<sup>rd</sup> largest watershed area (Figure 27). The ratios of watershed area, nitrogen loading, and phosphorus loading to estuarine volume in the Potomac River watershed are generally consistent with other estuaries in the Chesapeake system. This agreement indicates a moderate level of susceptibility to eutrophication.

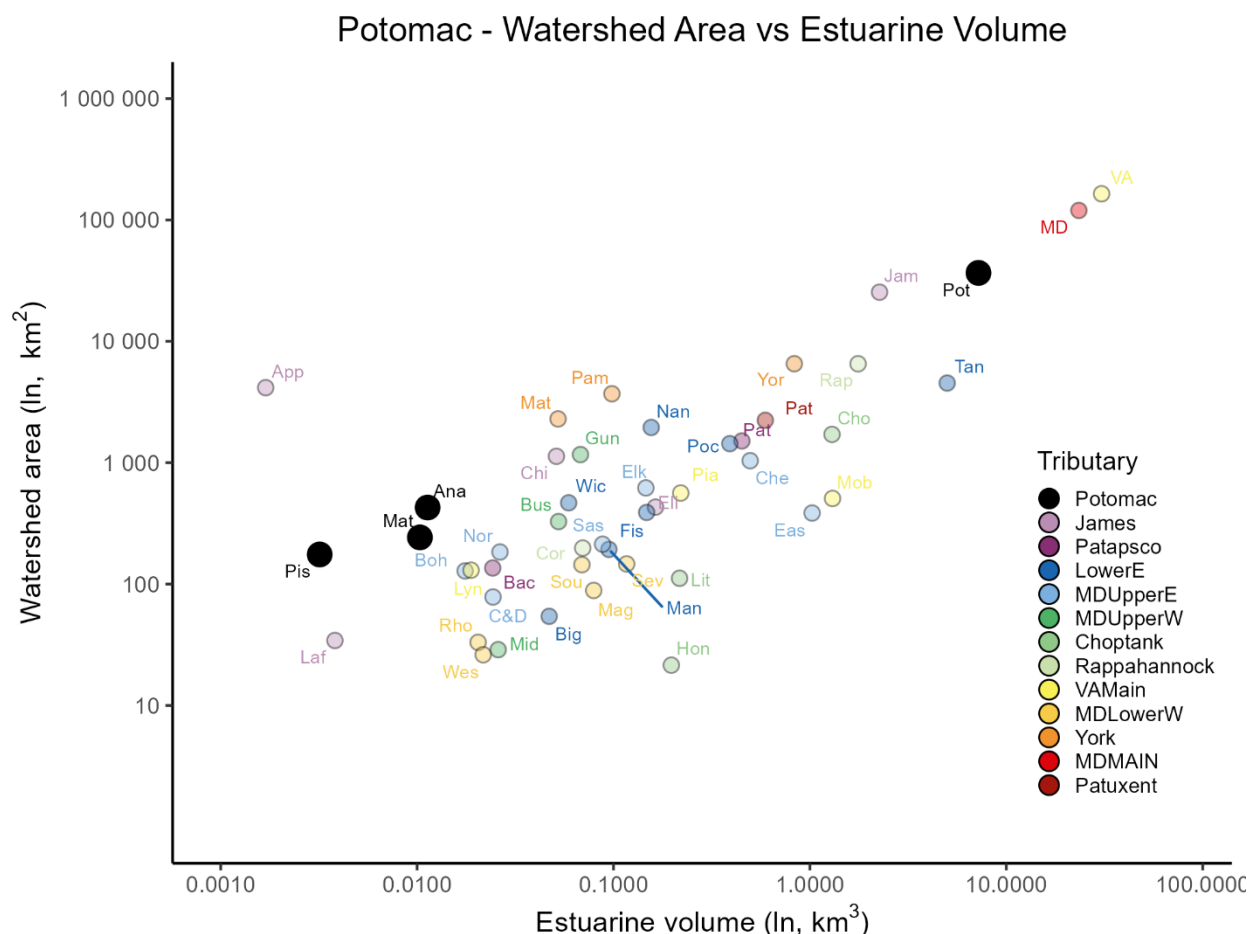


Figure 27. A comparison of watershed area (km<sup>2</sup>) vs estuarine volume (km<sup>3</sup>) for each Chesapeake Bay tributary. The table of tributary names and their abbreviations can be found below.

Table 4. Lists the associated full tributary name for the abbreviated name and group name represented in the watershed and estuarine volume figures. The names are from the Chesapeake Assessment Scenario Tool (CAST; <https://cast.chesapeakebay.net/Home/TMDLTracking#tributaryRptsSection>).

<u>Abbreviated tributary name</u>	<u>Full tributary name</u>	<u>Group name</u>
-----------------------------------	----------------------------	-------------------

Ana	Anacostia River	Potomac
App	Appomattox River	James
Bac	Back River	Patapsco
Big	Big Annemessex River	LowerE
Boh	Bohemia River	MDUpperE
Bus	Bush River	MDUpperW
C&D	Chesapeake & Delaware Canal	MDUpperE
Che	Chester River	MDUpperE
Chi	Chickahominy River	James
Cho	Choptank River	Choptank
Cor	Corrotoman River	Rappahannock
Eas	Eastern Bay	MDUpperE
Eli	Elizabeth River	James
Elk	Elk River	MDUpperE
Fis	Fishing Bay	LowerE
Gun	Gunpowder River	MDUpperW
Hon	Honga River	Choptank
Jam	James River	James
Laf	Lafayette River	James
Lit	Little Choptank River	Choptank
Lyn	Lynnhaven River	VAMain
Mag	Magothy River	MDLowerW
Man	Manokin River	LowerE
Mat	Mattawoman Creek	Potomac
Mat	Mattaponi River	York
MD	MD MAINSTEM	MD Main
Mid	Middle River	MDUpperW
Mob	Mobjack Bay	VAMain
Nan	Nanticoke River	LowerE
Nor	Northeast River	MDUpperE
Pam	Pamunkey River	York
Pat	Patapsco River	Patapsco
Pat	Patuxent River	Patuxent
Pia	Piankatank River	VAMain
Pis	Piscataway Creek	Potomac
Poc	Pocomoke River	LowerE
Pot	Potomac River	Potomac
Rap	Rappahannock River	Rappahannock
Rho	Rhode River	MDLowerW
Sas	Sassafras River	MDUpperE

Sev	Severn River	MDLowerW
Sou	South River	MDLowerW
Tan	Tangier Sound	LowerE
VA	VA MAINSTEM	VAMain
Wes	West River	MDLowerW
Wes	Western Branch (Patuxent River)	Patuxent
Wic	Wicomico River	LowerE
Yor	York River	York

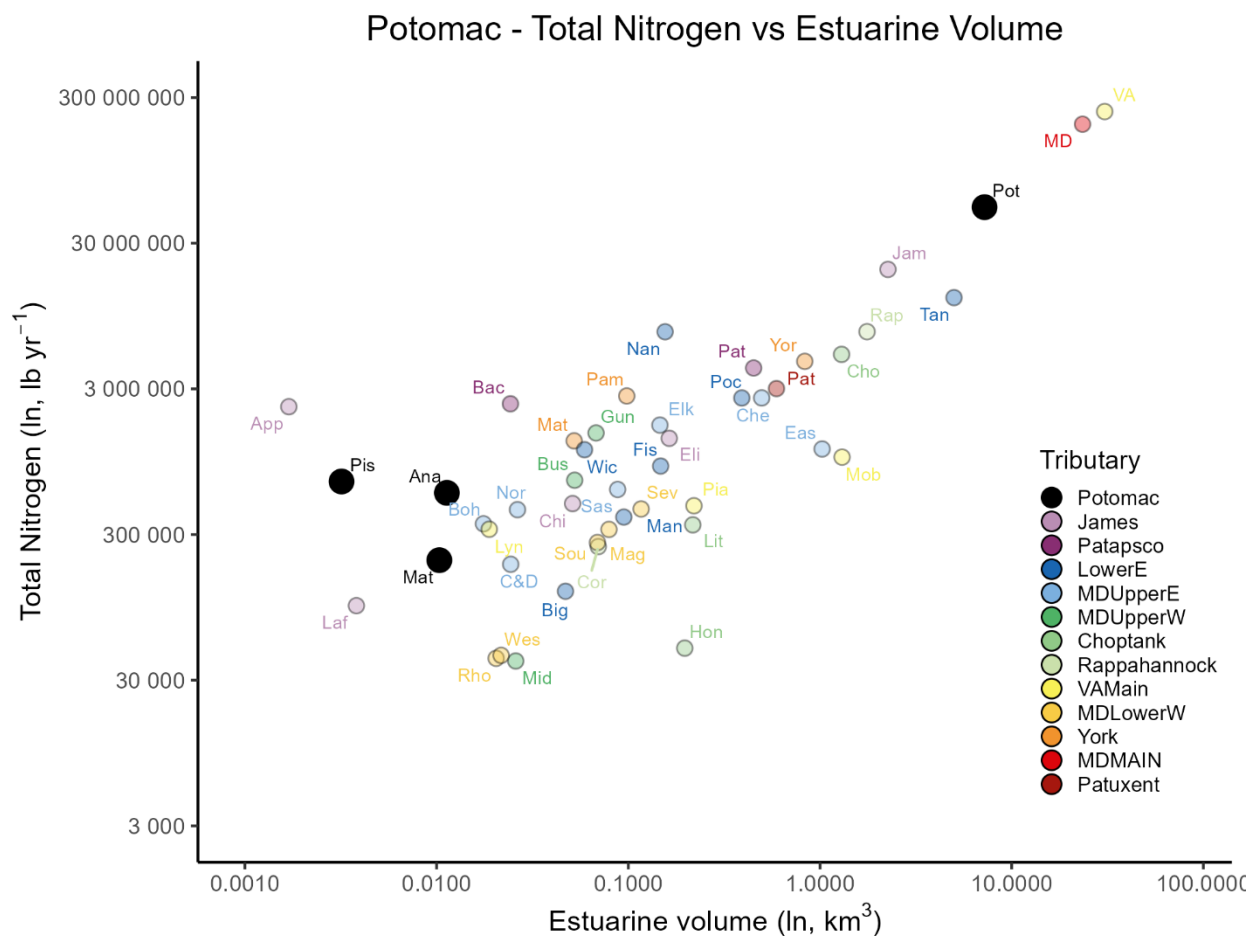


Figure 28. Average annual expected nitrogen loads versus estuarine volume. Nitrogen loads are from the 2021 progress scenarios in CAST (Chesapeake Bay Program, 2020), which is an estimate of nitrogen loads under long-term average hydrology given land use and reported management as of 2021.

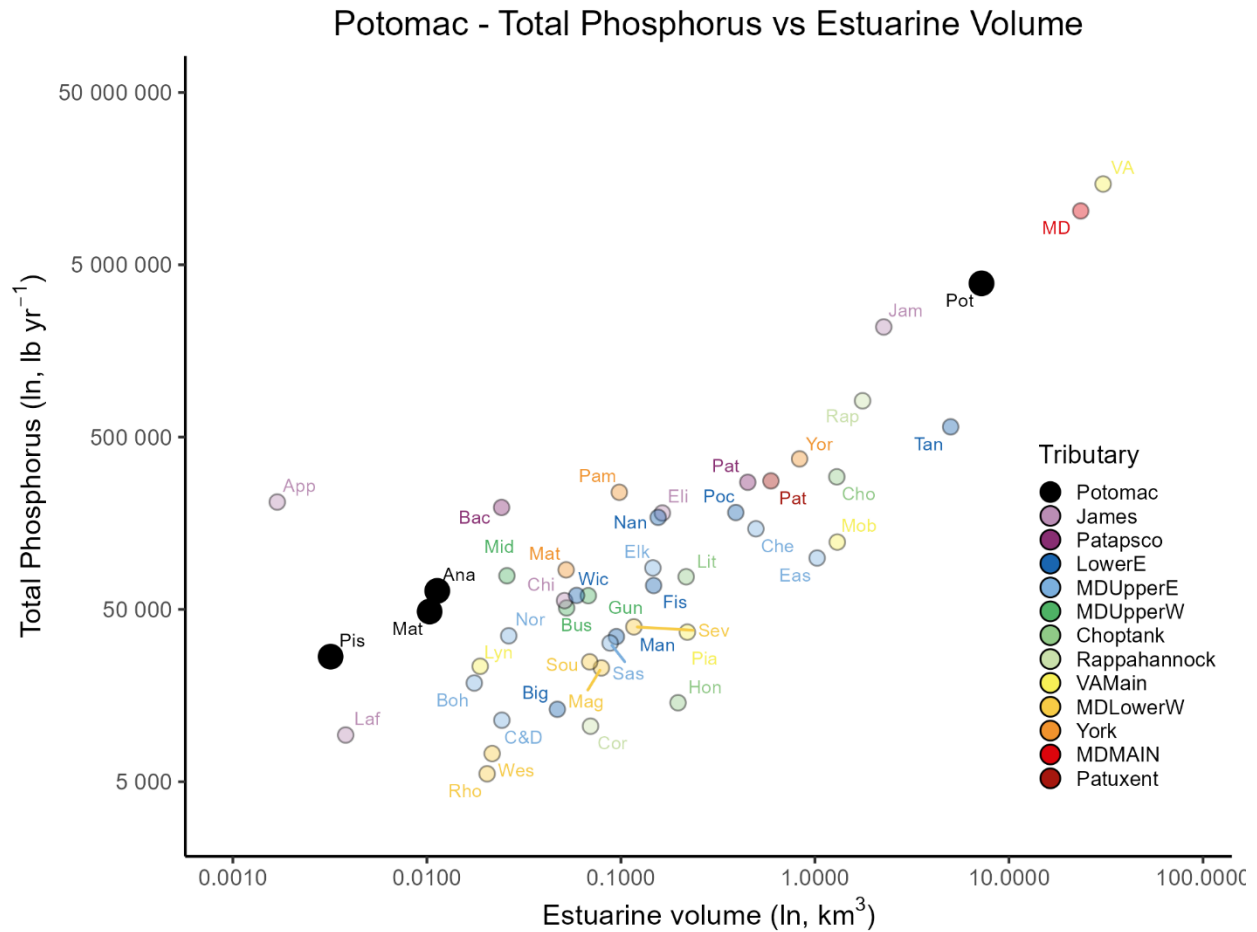


Figure 29. Average annual expected phosphorus loads versus estuarine volume. Phosphorus loads are from the 2021 progress scenarios in CAST (Chesapeake Bay Program, 2020), which is an estimate of phosphorus loads under long-term average hydrology given land use and reported management as of 2021.

Table 4. comparison of watershed area, which includes tidal wetland area, versus estuarine volume for all estuaries and sub-estuaries identified in the CBP monitoring segment scheme. Ratio of nitrogen and phosphorus loads to estuarine volumes. Data for watershed area and volume from CAST and nitrogen and phosphorous loads from 2021 progress scenarios in CAST.



Tributary	Area % Contribution <sup>1</sup>	Volume % Contribution <sup>2</sup>	N Ratio <sup>3</sup>	P Ratio <sup>4</sup>
MDLowerW	0.11	0.39	$3.67 \times 10^6$	$3.26 \times 10^5$
MDUpperW	0.39	0.19	$1.53 \times 10^7$	$1.30 \times 10^6$
Patapsco	0.42	0.60	$1.38 \times 10^7$	$9.87 \times 10^5$
Choptank	0.47	2.16	$3.26 \times 10^6$	$2.26 \times 10^5$
Patuxent	0.63	0.75	$5.34 \times 10^6$	$5.20 \times 10^5$
MDUpperE	0.67	2.31	$3.86 \times 10^6$	$2.36 \times 10^5$
Rappahannock	1.71	2.31	$4.19 \times 10^6$	$4.50 \times 10^5$
LowerE	2.30	7.46	$4.28 \times 10^6$	$1.87 \times 10^5$
York	3.19	1.24	$8.78 \times 10^6$	$7.10 \times 10^5$
James	7.93	3.14	$9.69 \times 10^6$	$1.06 \times 10^6$
Potomac	9.54	9.17	$7.53 \times 10^6$	$5.58 \times 10^5$
MDMAIN	30.50	29.64	$8.41 \times 10^6$	$4.38 \times 10^5$
VAMain	42.13	40.63	$7.55 \times 10^6$	$4.64 \times 10^5$

<sup>1</sup> Percent area contribution to the total Chesapeake Bay watershed area (km<sup>2</sup>).

<sup>2</sup> Percent volume contribution to the total Chesapeake Bay estuarine volume (km<sup>3</sup>).

<sup>3</sup> Ratio of Nitrogen loads to estuarine volume.

<sup>4</sup> Ratio of Phosphorus loads to estuarine volume.

### 5.2.2. Long-term Changes in Water Quality Longitudinal Profiles

This section presents a series of longitudinal profiles of five water quality parameters across all Potomac River tidal stations. The water quality parameters include TN, TP, chlorophyll *a*, water clarity as measured by Secchi depth (Secchi), and bottom DO. These profiles are generated from the results of GAM models estimated for each station. Cluster analysis is used to group years according to similarity of longitudinal profiles. The profiles of the same color represent years with similar upstream to downstream trends across all the stations in the Potomac River. Comparing these groups allows for assessment of both spatial and temporal patterns for a given parameter, and comparisons among parameters allows for assessment of associations of parameters.

In the Potomac River, TN shows a spatial pattern of decreasing TN from TF2.1 and TF2.2 to the estuary mouth, but the most drastic decrease occurs during a period of high flow years from 1994 - 1997 (red), at station LE2.2 to LE2.3. The periods 2008–2017 and 2020–2022 (purple), which includes the most recent years, shows lower TN than prior years over the Potomac River estuary (Figure 30).

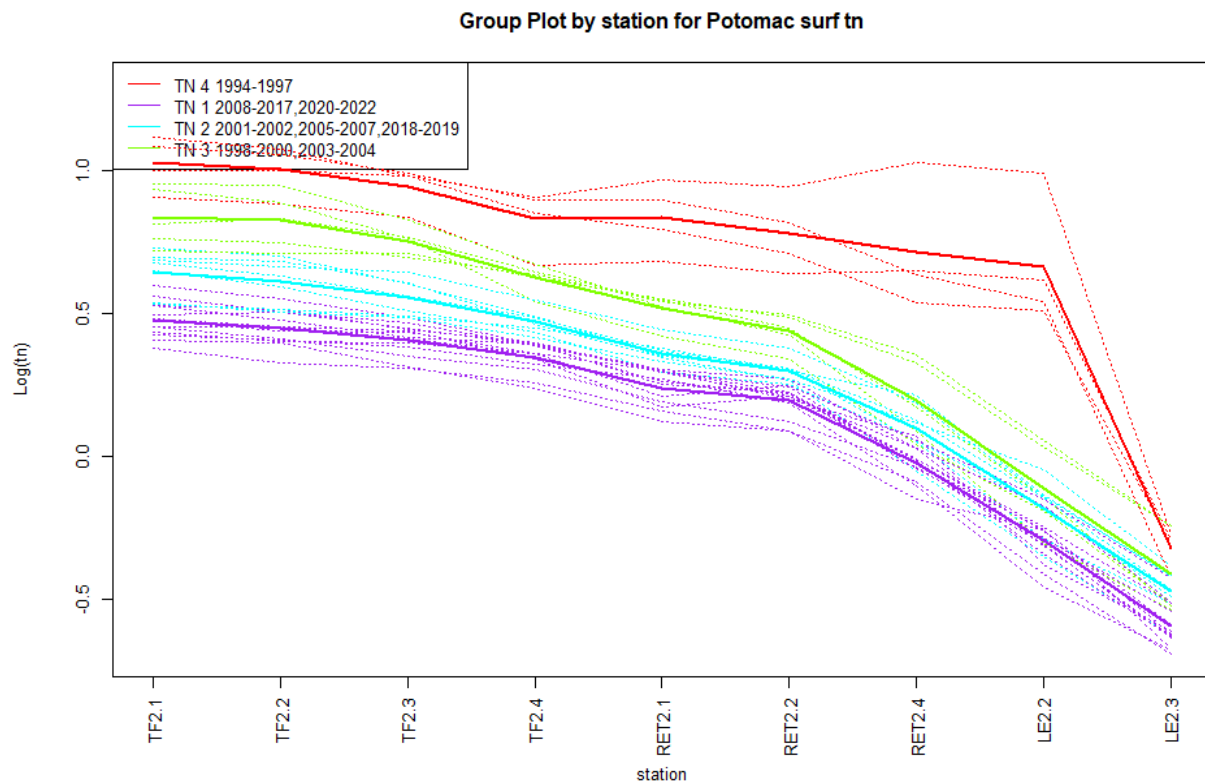


Figure 30: Station Total Nitrogen means from upstream to downstream plotted with year groups differentiated by color. Multiple dashed line traces within group show variability among group years.

In the Potomac River, TP shows a spatial pattern of slightly increasing TP from TF2.1 to RET2.2 and then decreasing toward the estuary mouth (Figure 31). The most recent years (2018–2022, purple) have lower TP than prior years over the entire Potomac River estuary, apart from the second most recent years (2005 – 2017, cyan) which have slightly lower TP at stations at the mouth of the tributary, LE2.2 and LE2.3. The earliest period (1994-1997, red) has consistently higher TP across stations, especially in

the upstream and mid-estuary regions (Figure 31).

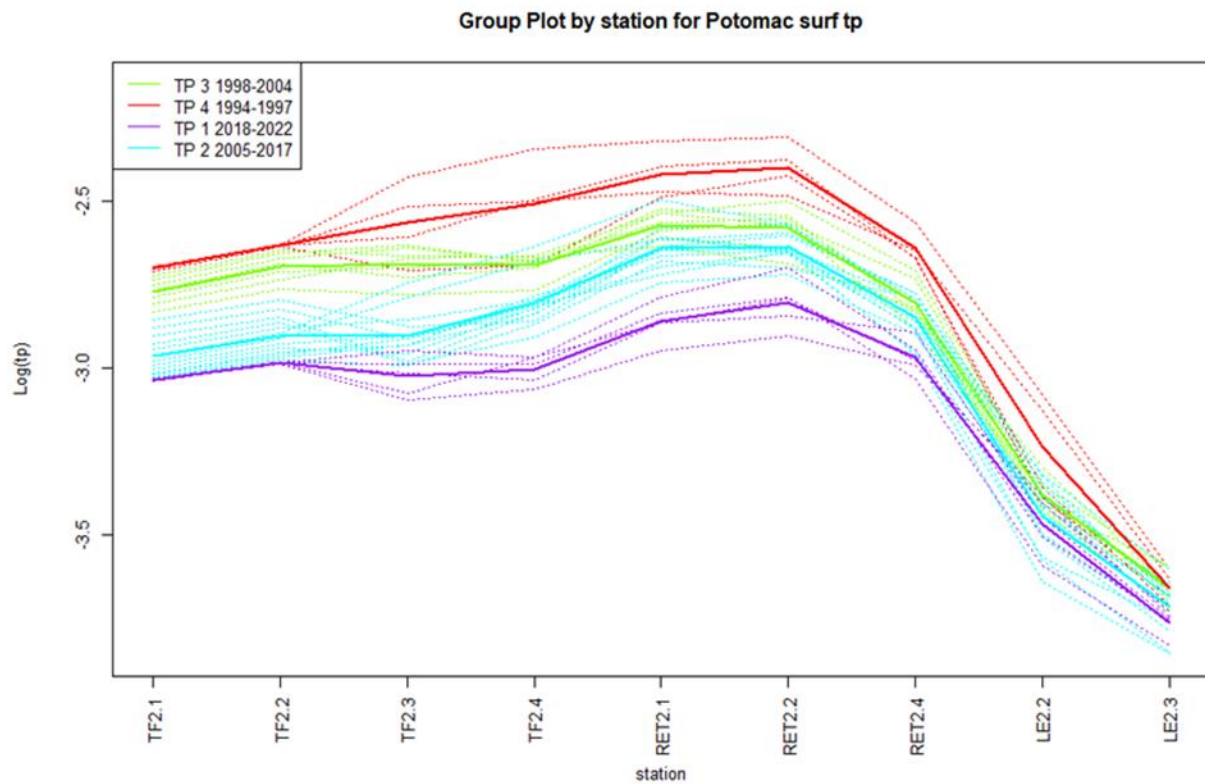


Figure 31: Station Total Phosphorus means from upstream to downstream plotted with year groups segregated by color. Multiple dashed line traces within group show variability among group years.

Surface chlorophyll *a* does not exhibit the consistent decrease over time that is exhibited by the nutrients TN and TP. Stations RET2.1 and RET2.2 have relatively lower levels of surface chlorophyll *a* compared to their neighboring upstream and downstream stations. In the tidal fresh, the highest levels of surface chlorophyll *a* occur in 1994–1997, 2010–2016, and 2022 (red) except for a peak in 1998–2001 (green) at TF2.3. The period 2004–2008 (purple), tends to have the lowest chlorophyll *a* compared to the other periods except at LE2.2. The years 1998–2001 (green) have a longitudinal profile that is least similar to other years: 1998 is a high flow year, 1999 and 2001 are below average flow years, and 2000 is an average flow year.

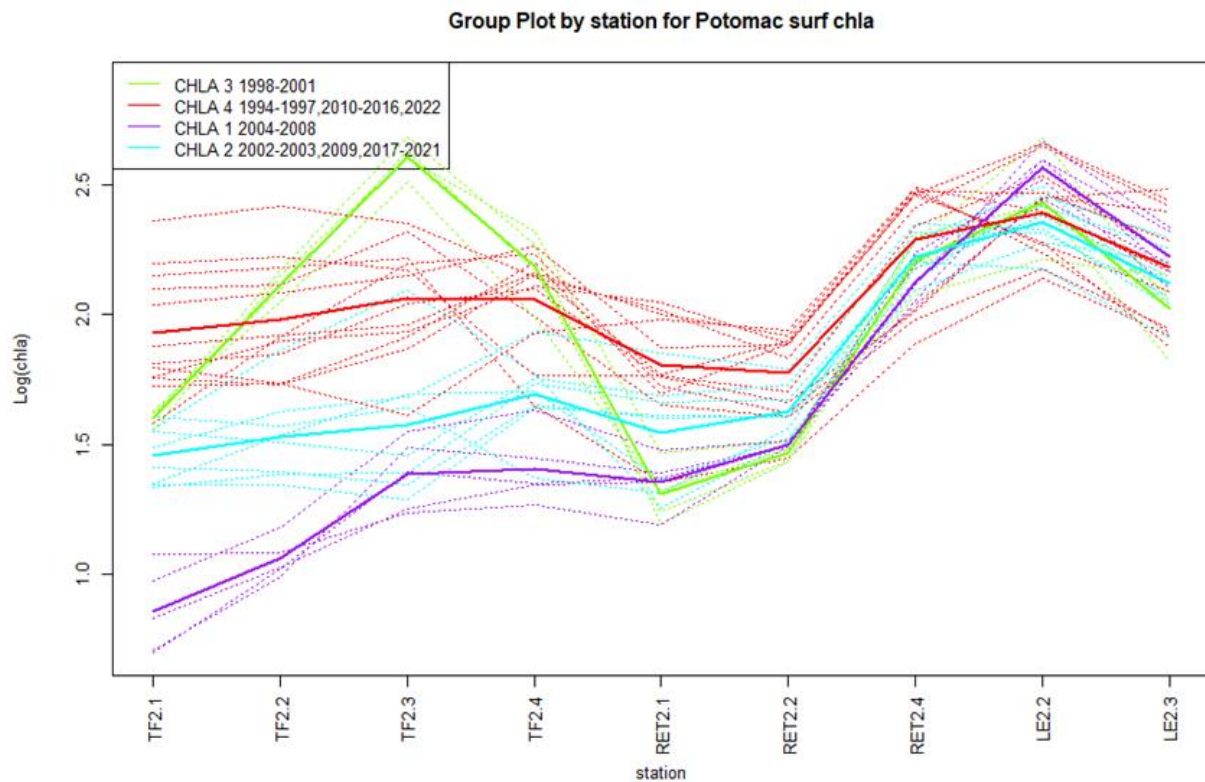


Figure 32: Station means of chlorophyll *a* plotted from upstream to downstream with year groups separated by color. Multiple dashed line traces within groups show variability among years within groups.

The longitudinal pattern for Secchi depth, as shown in Figure 33, is almost the inverse of the pattern exhibited by TP (Figure 31). Water clarity is relatively low in the tidal fresh through the RET stations (TF2.1 – RET2.2). However, in the lower estuary stations (LE2.2 to LE2.3), water clarity improves notably as indicated by higher Secchi depth values. This pattern is primarily due to estuarine mixing associated with riverine flows/inputs maintaining suspended particles in the water column, thus reducing water clarity in the lower tidal fresh and RET. Lower tidal fresh and RET water form a zone where phytoplankton are abundant, which also tends to reduce water clarity.

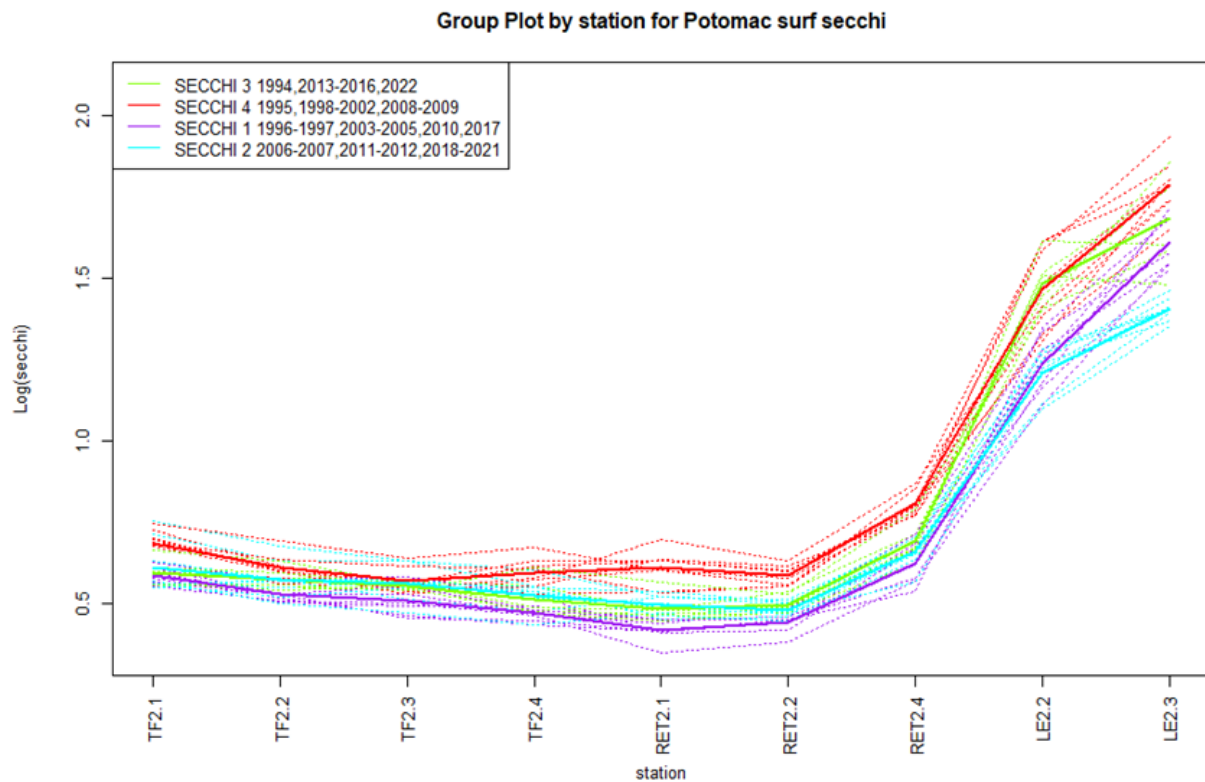


Figure 33: Station Secchi depth means plotted from upstream to downstream with year groups separated by color. Multiple dashed line traces within group show variability among group years. A larger log(secchi) represents improved water clarity.

Bottom dissolved oxygen (DO), as shown in Figure 34, is high in the upper tidal fresh regions (TF2.1–TF2.4) and decreases from the RET to the lower estuary (LE2.3). The RET stations (RET2.1–RET2.4) mark the start of this pronounced decrease. Low bottom DO trends in the lower estuary are largely influenced by the bathymetry at these stations because these are the deepest areas of the Potomac River estuary and are classified as the deep channel designated use (U.S. Environmental Protection Agency, 2003). Bottom DO trends improve slightly moving from the lower estuary to the main Bay.



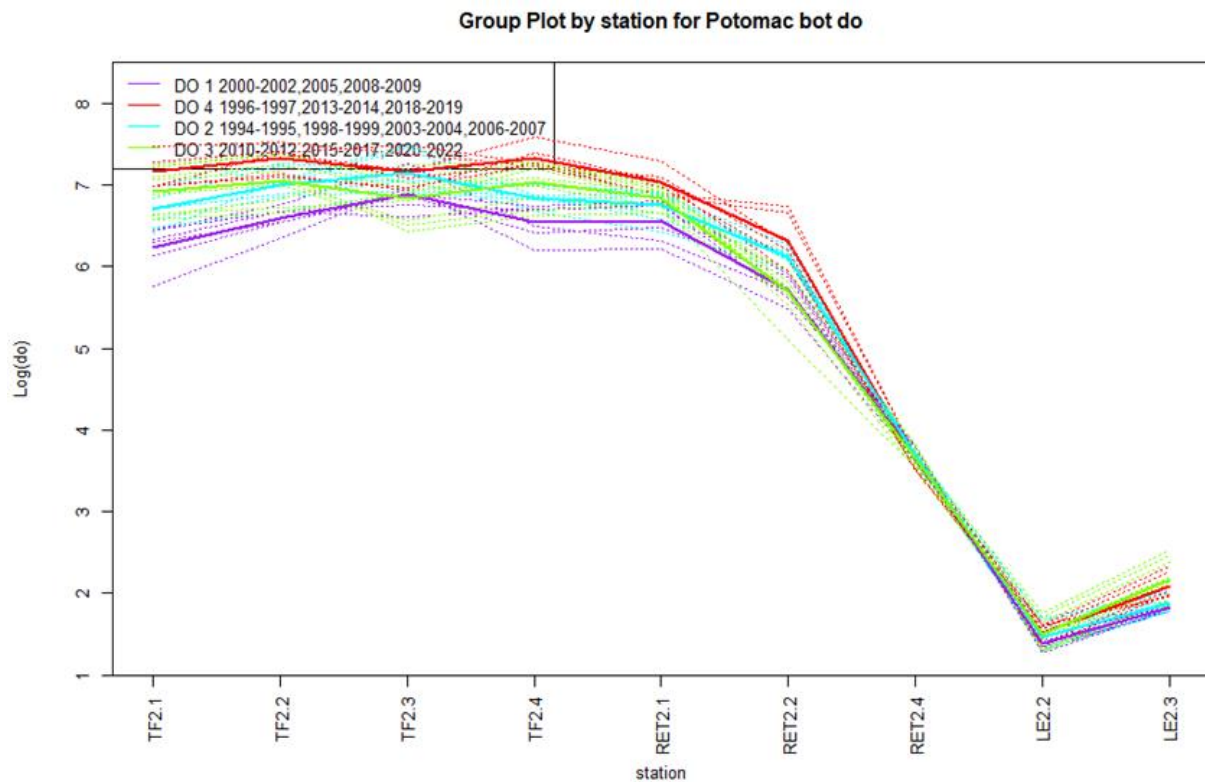


Figure 34: Station means of summer bottom Dissolved Oxygen plotted from upstream to downstream with year groups segregated by color. Multiple dashed line traces within group show variability among group years.

### 5.3 Changing Environmental Conditions

As one of the most environmentally vulnerable areas in the nation, all aspects of the Chesapeake Bay watershed and tributaries are experiencing changing environmental conditions, and the impacts are already being observed (Eggleston and Pope, 2013; Hinson et al., 2022). Overall, the watershed is experiencing increases in precipitation and temperatures which shape Chesapeake Bay tributary water quality trends (Najjar et al., 2010). These trends differ spatially and temporally throughout the watershed, and impacts are exacerbated by local stressors (e.g., land subsidence, land-use change, growth and development). Therefore, this section of the Tributary Summary is not an exhaustive discussion of how changing environmental conditions are influencing water quality in Chesapeake Bay tributaries but instead is an acknowledgement of the influence of some stressors on the trends discussed in this report. Efforts aimed to increase understanding of these changing environmental conditions on water quality patterns can help explain the progress gaps and transform monitoring findings into actionable information.

#### 5.3.1. Extreme Weather and Increased Precipitation

Under typical weather conditions, fresh water flowing from rivers and streams makes up about half of Chesapeake Bay's entire water volume. However, extremes in rainfall—whether too much or too little—

can have varying effects on the Bay ecosystem. During large rain events, river flow increases, delivering more fresh water into the Bay and decreasing Bay salinity (Murphy et al., 2019). During extreme rain events, sediment and nutrients may be scoured from behind river dams resulting in extraordinarily high nutrient and sediment loads to the bay (Langland, 2015). Stormwater runoff delivers nitrogen, phosphorus, and sediment into rivers and the Bay causing an increase in nutrient concentrations, which create dead zones and feed algal blooms. During periods with little rainfall or extended drought, the decrease in freshwater flows results in saltier conditions, affecting habitats and aquatic species.

The correlation of water quality with extreme weather events is observed through the Chesapeake Bay Water Quality Standards Attainment Indicator (Figure 35) (Chesapeake Bay Program, 2023). The attainment indicator uses a subset of the criteria otherwise necessary for a complete regulatory accounting of water quality standards attainment assessments of tidal water dissolved oxygen, water clarity and chlorophyll *a*. The indicator, therefore, is recognized as an estimate of true attainment of these water quality standards. Dips in the attainment of long-term water quality standards show the responsiveness of the Chesapeake Bay to extreme events such as Hurricane Ivan in 2004 and Hurricane Irene in 2011. When viewed in isolation, these extreme events would lead to non-attainment. However, the Indicator shown in Figure 35 also shows that estimated attainment recovers relatively quickly in the aftermath of extreme events, thus highlighting the resiliency of Chesapeake Bay.

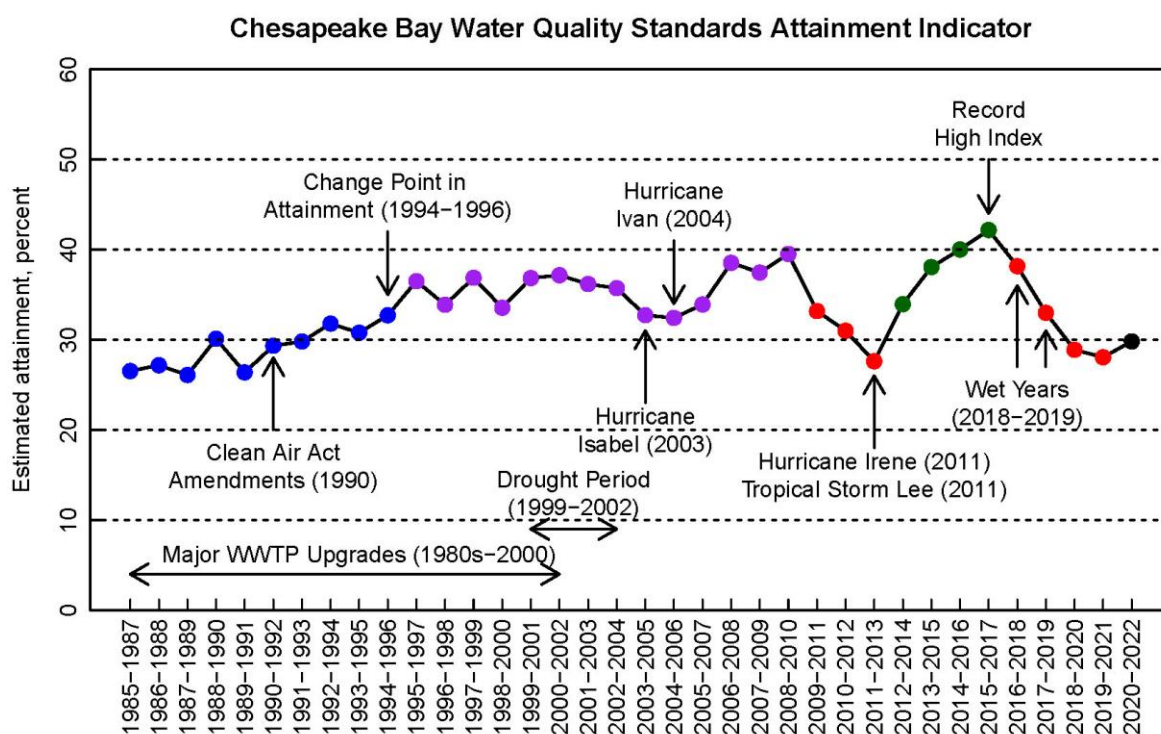


Figure 35. Chesapeake Bay Water Quality Standards Attainment Indicator valuated using three parameters from 1985–2022: dissolved oxygen, water clarity or submerged aquatic vegetation abundance, and chlorophyll *a*. Colors represent a different period: blue represents period before the change point, purple represents the period of steady attainment results, red represents the period of decreasing attainment after high flow years, and green represents the period of increasing attainment. Figure from (Zhang, Q. et al., 2018a; Updated 2024).

One-off events such as hurricanes are not the only measures influencing progress towards water quality attainment. Unusually prolonged wet weather in 2018 and 2019 caused higher than average river flows entering Chesapeake Bay that delivered high pollutant loads during that period (Figures 35, 36, 37, 38). Experts attribute the reduction in pollutant loads in 2020 to a combination of reduced river flow from less rainfall and to management actions controlling pollution in the Bay and watershed (Chesapeake Bay Program, 2023).

## Pollution Loads and River Flow to the Chesapeake Bay (1990-2022) 📊

River and Watershed Input of Pollution Loads. Years denote the water year measured between October 1 and September 30.

[VIEW CHART](#)

[VIEW TABLE](#)

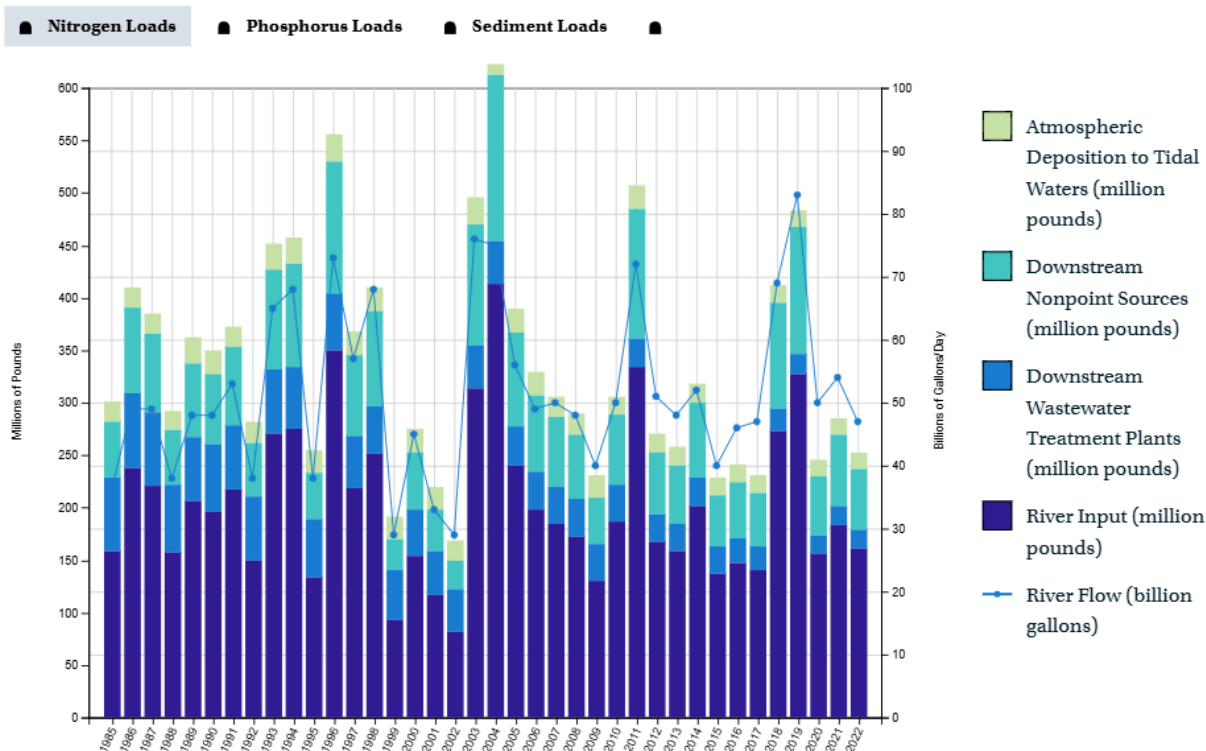


Figure 36: Nitrogen loads and River Flow to the Chesapeake Bay (1990-2022); River and Watershed Input of Nitrogen Loads. Years denote the water year measured between October 1 and September 30 and are named for the calendar years in which the periods end. Figure from Chesapeake Bay Program, 2025 (<https://www.chesapeakeprogress.com/clean-water/water-quality>).

## Pollution Loads and River Flow to the Chesapeake Bay (1990-2022)

River and Watershed Input of Pollution Loads. Years denote the water year measured between October 1 and September 30.

[VIEW CHART](#) [VIEW TABLE](#)

 Nitrogen Loads

 **Phosphorus Loads**

 Sediment Loads



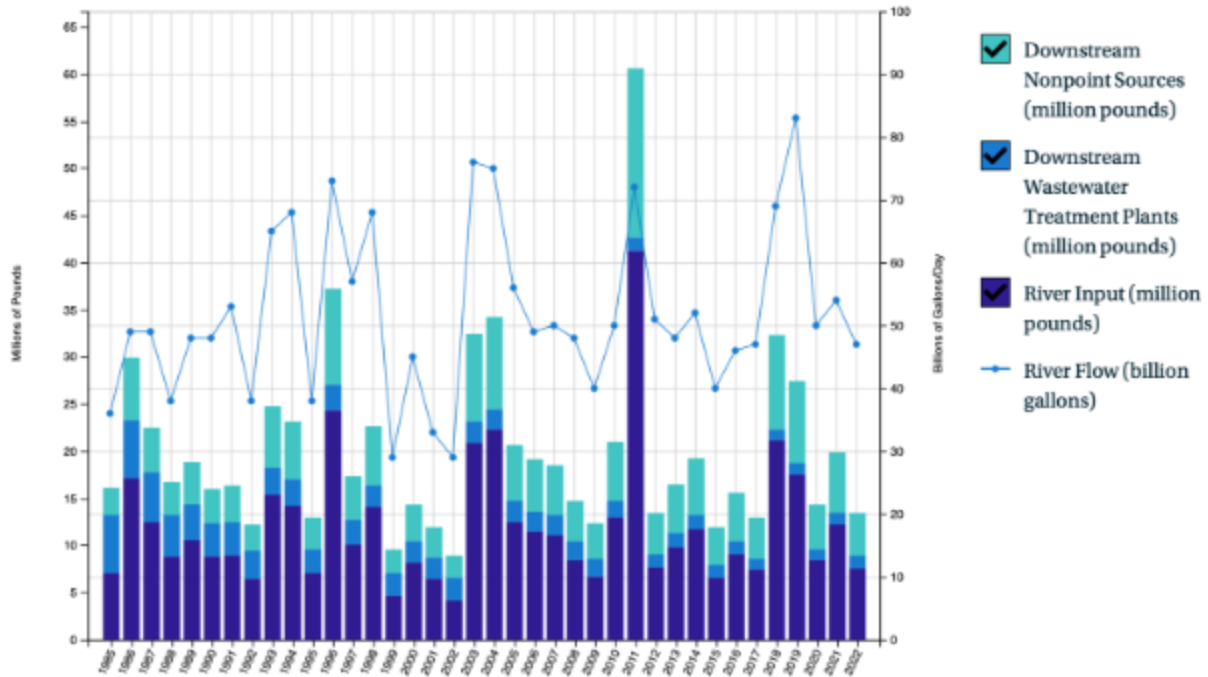


Figure 37: Phosphorus loads and River Flow to the Chesapeake Bay (1990-2022); River and Watershed Input of Phosphorus Loads. Years denote the water year measured between October 1 and September 30 and are named for the calendar years in which the periods end. Figure from Chesapeake Bay Program, 2025 (<https://www.chesapeakeprogress.com/clean-water/water-quality>).

## Pollution Loads and River Flow to the Chesapeake Bay (1990-2022)

River and Watershed Input of Pollution Loads. Years denote the water year measured between October 1 and September 30.

[VIEW CHART](#) [VIEW TABLE](#)

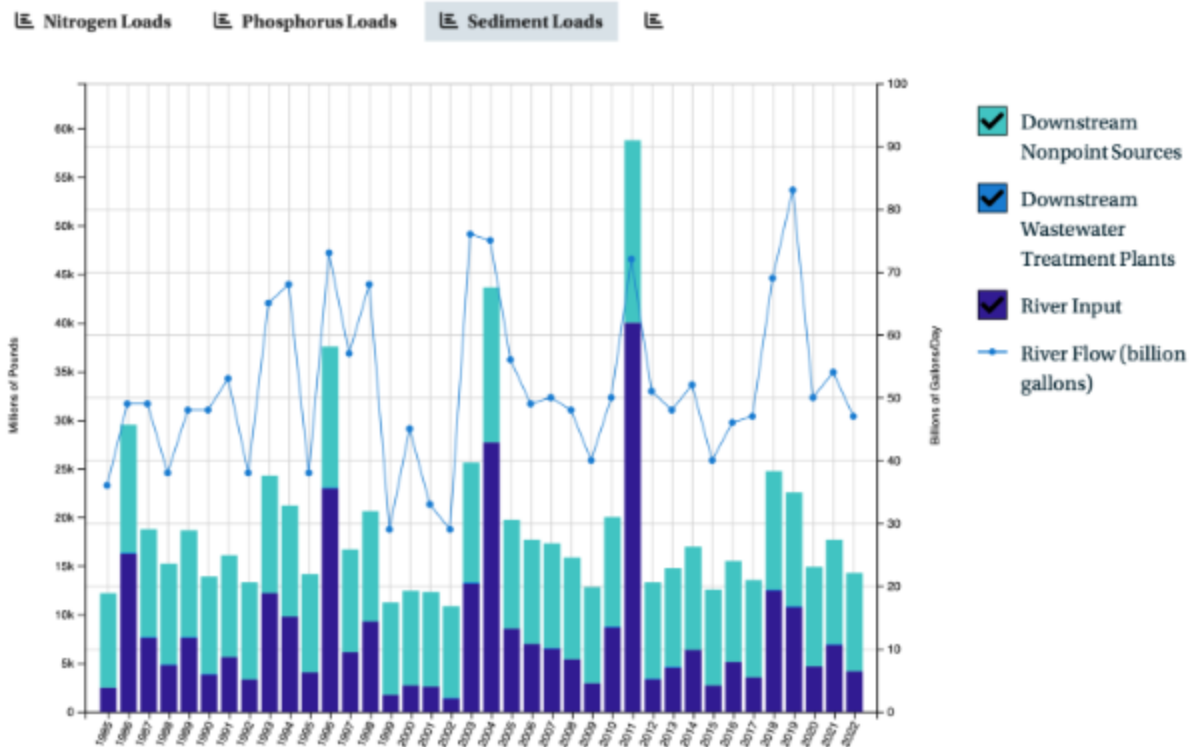


Figure 38: Sediment loads and River Flow to the Chesapeake Bay (1990-2022); River and Watershed Input of Sediment loads. Years denote the water year measured between October 1 and September 30 and are named for the calendar years in which the periods end. Figure from Chesapeake Bay Program, 2025 (<https://www.chesapeakeprogress.com/clean-water/water-quality>).

Many models predict increases in average annual precipitation for the Chesapeake Bay region, but studies have found greater seasonality in the projected precipitation change (Kunkel et al. 2013). Winter and spring projections show increased precipitation, followed by periods of drought in summer (Pyke et al. 2008; Najjar et al. 2010). These studies are supportive for understanding stream flow, but local assessments of changing environmental conditions and variability are still needed for determining vulnerability for Chesapeake Bay (St. Laurent et al., 2021). Figure 39 shows Parameter-elevation Relationship on Independent Slope Model (PRISM, 2020) precipitation data at the land-river scale spatially aggregated to the Potomac River watershed. Annual mean precipitation data for the Potomac River watershed from 1981 to 2022 show a gradual increase over the period of record.



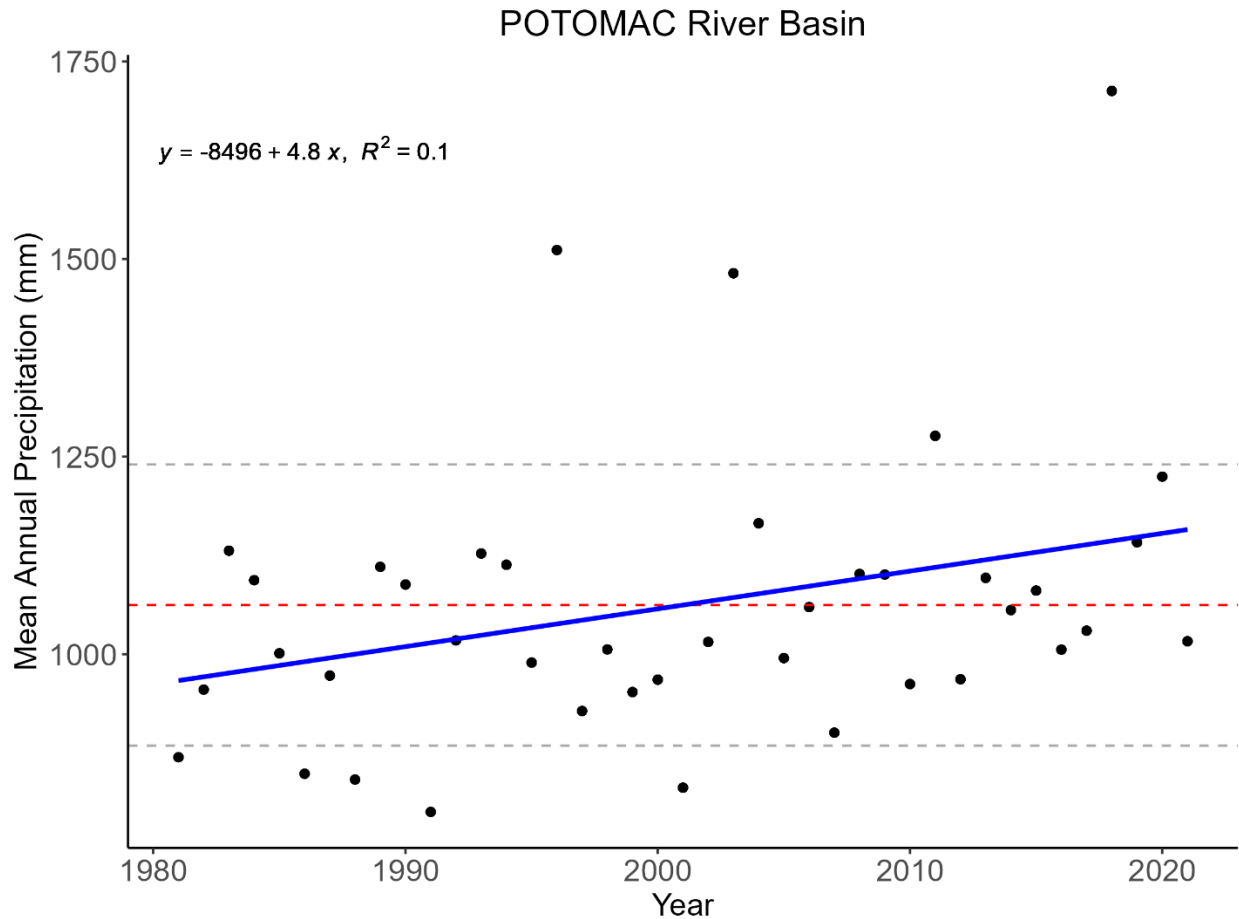


Figure 39. Potomac River mean annual precipitation from 1981 – 2022 from the Parameter-Elevation Relationship on Independent Slope Model (PRISM).

### 5.3.2. Warming Water Temperatures

The Chesapeake Bay is shallow, with a mean depth of 6.5 m; therefore, atmospheric variability has a large influence on water column temperatures (St. Laurent et al., 2021). As described in Section 4.7, both long-term and short-term surface water temperature trends across the tidal areas of the Potomac River are experiencing statistically significant warming (Figure 40). Increased atmospheric temperatures contribute to warmer water temperatures. Trend analyses of resulting marine heat waves, or prolonged anomalously warm events, indicate increases in marine heat wave frequency, duration, and cumulative yearly intensity (Mazzini and Pianca, 2022).

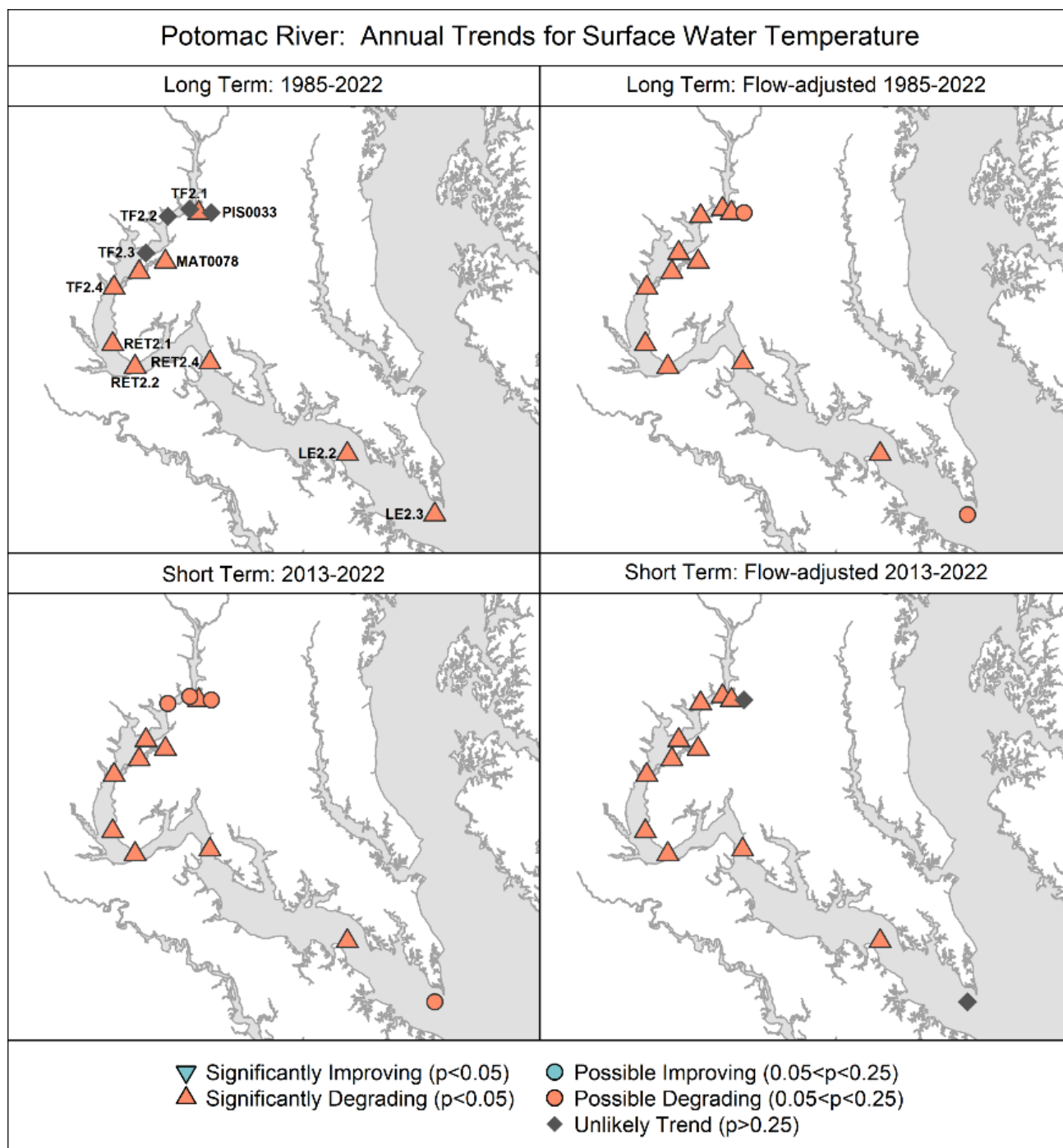


Figure 40. Annual flow-adjusted surface water temperature trends as calculated using Generalized Additive Models (Murphy et al. 2019). Base map credit Chesapeake Bay Program, [www.chesapeakebay.net](http://www.chesapeakebay.net), North American Datum 1983. For more information on the tidal stations and Chesapeake Bay tidal water quality monitoring, refer to <https://www.chesapeakebay.net/what/programs/quality-assurance/tidal-water-quality-monitoring>.

### 5.3.3. Sea-Level Rise

Sea level has risen due to the thermal expansion of ocean water and melting of glaciers and ice sheets (USGS, 2018). Over the past century, Chesapeake Bay waters have risen by about one foot, and according to a USGS study, Chesapeake Bay waters are predicted to rise another 1.3 to 5.2 feet over the next 100 years (Eggleston and Pope, 2013). This rate is higher than the global sea level rise average because the Chesapeake Bay region is also impacted by land subsidence, or sinking of land due to removal or displacement, half of which is estimated to be from groundwater removal (Eggleston and Pope, 2013).

NOAA Tides and Currents provides sea-level trends across the U.S. As an example, Lewisetta, VA is at the mouth of the Potomac tributary and shows an increasing sea level trend of 5.87 mm/year (Figure 41).

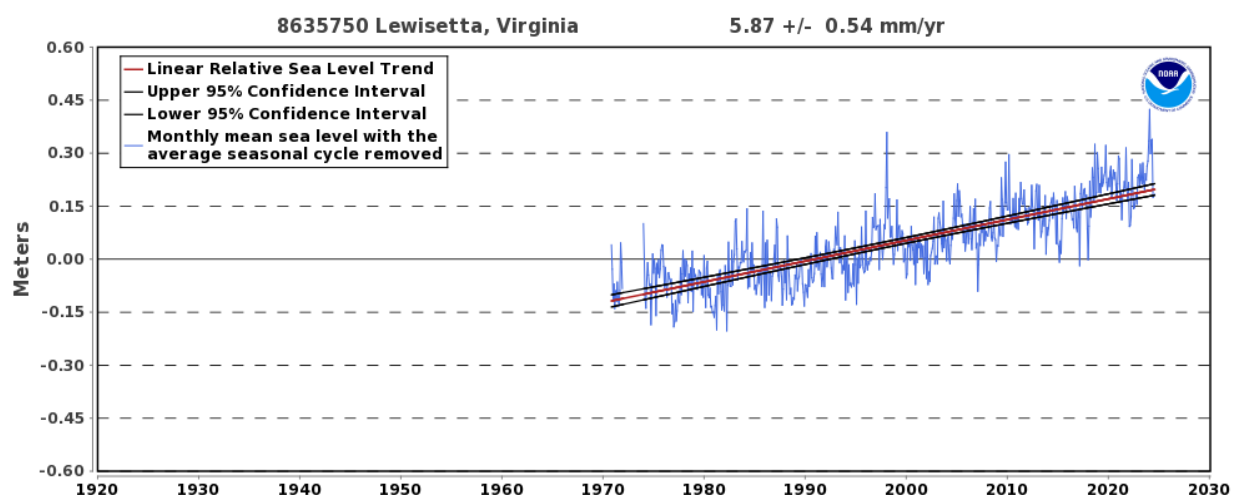


Figure 41. Lewisetta, Virginia monthly mean sea levels without the regular seasonal fluctuations from coastal ocean temperatures, salinity, wind, atmospheric pressure, and ocean currents. The relative sea level trend also shows the 95% confidence interval (NOAA, 2023b).

Higher water levels in Chesapeake Bay can result in loss of marshes and wetlands due to saltwater inundation. This is occurring due to erosion rates that are outpacing marsh accretion and/or marsh migration being blocked by development (Eggleston and Pope, 2013). Wetland habitat loss eliminates natural structures that trap pollution entering Chesapeake Bay, which is why integrating changing environmental conditions, such as sea-level rise, is critical when pursuing, designing, implementing, and maintaining restoration efforts (NOAA, 2023a).

#### 5.3.4. Connecting to Living Resources

Although measuring and discussing changing environmental conditions and their impacts on water quality is critical, it is also important to understand these influences in the context of the living resources water quality standards were designed to protect. Warming water temperatures reduce the solubility of oxygen in water (Tian et al., 2021). With both higher water temperature averages and extremes, habitats are limited by both low oxygen and high temperatures. Key aquatic species with economic and cultural value to the Chesapeake Bay, such as striped bass (*Morone saxatilis*), encounter a habitat squeeze as bottom hypoxia and warm surface temperatures compress suitable habitat space in the water column (Parham et al., 2023). Another consideration is that warming waters in Chesapeake Bay favor pathogenic bacteria like *Vibrio vulnificus*, which threaten human health directly and indirectly through key living resources that are valued for human consumption, such as oysters (Archer et al., 2023; Wright et al., 1996). Additionally, phenological shifts due to warmer water temperatures threaten decoupling of predator-prey relationships and the key fisheries they support (Batiuk et al., 2023). Increased precipitation also presents challenges for living resources by reducing suitable habitat. Heavier precipitation can yield increased hypoxia as the rate of phosphorus flushing from the landscape increases, and for oysters, heavy freshwater flows may lower salinity to a harmful level (Kimmel et al., 2014).

The NOAA Seasonal Summaries offer more information on how changing environmental conditions impacts living resources at finer spatial and temporal scales. These data describe salinity, DO, freshwater flow, and water temperature across Chesapeake Bay and provide critical insight into ecosystem conditions. Applications of the NOAA seasonal summaries include informing ecosystem-based management for fisheries at the state and regional level and comparing the recent seasonal data with long-term averages. The NOAA Seasonal Summaries can be accessed at NOAA Chesapeake Vot Interpretive Buoy System (National Oceanic and Atmosphere Association, 2023c).

## References

- Arnold, C. L., and Gibbons, C. J., 1996. Impervious Surface Coverage: The Emergence of a Key Environmental Indicator. *Journal of the American Planning Association* 62(2), pp. 243-258. <https://doi.org/10.1080/01944369608975688>.
- Archer, E. J., Baker-Austin, C., Osborn, T. J., Jones, N. R., Martínez-Urtaza, J., Trinanes, J., Oliver, J. D., Colón González, F. J., Lake, I. R., 2023. Climate warming and increasing *Vibrio vulnificus* infections in North America. *Scientific Reports* 13, 3893. <https://doi.org/10.1038/s41598-023-28247-2>.
- Ator, S. W., Blomquist, J. D., Webber, J. S., and Chanut, J. G., 2020. Factors driving nutrient trends in streams of the Chesapeake Bay watershed. *Journal of Environmental Quality* 49:812-834, DOI: 10.1002/jeq2.20101.
- Ator, S. W., Brakebill, J. W., and Blomquist, J. D., 2011. Sources, fate, and transport of nitrogen and phosphorus in the Chesapeake Bay watershed: An empirical model. U.S. Geological Survey Scientific Investigations Report 2011-5167, Reston, VA, p. 27. <http://pubs.usgs.gov/sir/2011/5167/>.
- Ator, S. W., Denver, J. M., Krantz, D. E., Newell, W. L., and Martucci, S. K., 2005. A Surficial Hydrogeologic Framework for the Mid-Atlantic Coastal Plain. U.S. Geological Survey U.S. Geological Survey Professional Paper 1680. <https://pubs.usgs.gov/pp/2005/pp1680/>.
- Ator, S.W. and Denver, J.M., 2012. Estimating contributions of nitrate and herbicides from groundwater to headwater streams, northern Atlantic coastal plain, United States. *Journal of the American Water Resources Association*, v. 48, no. 6., p. 1075 – 1090.
- Ator, S. W., García, A. M., Schwarz, G. E., Blomquist, J. D. and Sekellick, A. J., 2019. Toward explaining nitrogen and phosphorus trends in Chesapeake Bay tributaries, 1992–2012. *Journal of the American Water Resources Association* 55:1149-1168, DOI: 10.1111/1752-1688.12756.
- Bachman, L. J., Lindsey, B., Brakebill, J., and Powars, D. S., 1998. Ground-water discharge and base-flow nitrate loads of nontidal streams, and their relation to a hydrogeomorphic classification of the Chesapeake Bay Watershed, middle Atlantic coast. US Geological Survey Water-Resources Investigations Report 98-4059, Baltimore, MD, p. 71. <http://pubs.usgs.gov/wri/wri98-4059/>.
- Batiuk, R., Brownson, K., Dennison, W., Ehrhart, M., Hanson, J., Hanmer, R., Landry, B., Reichert-Nguyen, J., Soueidan, J., Tassone, S., Vogt, B 2023. Rising Watershed and Bay Water Temperatures: Ecological Implications and Management Responses – A STAC Workshop. STAC Publication Number 23-001. Edgewater, MD. (505 pages). [https://www.chesapeake.org/stac/wp-content/uploads/2023/01/FINAL\\_STAC-Report-Rising-Temps\\_April.pdf](https://www.chesapeake.org/stac/wp-content/uploads/2023/01/FINAL_STAC-Report-Rising-Temps_April.pdf).
- Böhlke, J. K. and J. M. Denver, 1995. Combined use of groundwater dating, chemical, and isotopic analyses to resolve the history and fate of nitrate contamination in two agricultural watersheds, Atlantic Coastal Plain, Maryland. *Water Resour. Res.* 31:2319-2339, DOI: 10.1029/95wr01584.
- Brakebill, J. W., Ator, S. W., and Schwarz, G. E., 2010. Sources of Suspended-Sediment Flux in Streams of the Chesapeake Bay Watershed: A Regional Application of the SPARROW Model1. *JAWRA Journal of the American Water Resources Association* 46:757-776, DOI: 10.1111/j.1752-1688.2010.00450.x.
- Bricker, S. B., Ferreira, J. G., and Simas, T., 2003. An integrated methodology for assessment of estuarine trophic status. *Ecological Modelling* 169:39-60, DOI: 10.1016/s0304-3800(03)00199-6.
- Bricker, S. B., Longstaff, B., Dennison, W., Jones, A., Boicourt, K., Wicks, C., and Woerner, J., 2008. Effects of nutrient enrichment in the nation's estuaries: A decade of change. *Harmful Algae* 8:21-32, DOI: 10.1016/j.hal.2008.08.028.
- Buchanan, C., 2020. A water quality binning method to infer phytoplankton community structure and function. *Estuaries and Coasts* 43:661-679, DOI: 10.1007/s12237-020-00714-3.

- Buchanan, C., Lacouture, R. V., Marshall, H. G., Olson, M., and Johnson, J. M., 2005. Phytoplankton reference communities for Chesapeake Bay and its tidal tributaries. *Estuaries* 28:138-159, DOI: 10.1007/bf02732760.
- Bukaveckas, P. A., Barry, L. E., Beckwith, M. J., David, V., Lederer, B., 2011. Factors Determining the Location of the Chlorophyll Maximum and the Fate of Algal Production within the Tidal Freshwater James River. *Estuaries and Coasts* 34, 569–582. DOI: 10.1007/s12237-010-9372-4
- Chesapeake Bay Program, 2018. Data Hub. <http://datahub.chesapeakebay.net/>.
- Chesapeake Bay Program, 2020. Chesapeake Assessment and Scenario Tool (CAST) Version 2019. <https://cast.chesapeakebay.net/Home/>.
- Chesapeake Bay Program, 2023. ChesapeakeProgress. <https://www.chesapeakeprogress.com/>.
- Chesapeake Bay Program, 2023. Tidal Water Quality Monitoring.
- Cloern, J. E., 1982. Does the Benthos Control Phytoplankton Biomass in South San Francisco Bay? *Marine Ecology Progress Series* 9:191-202, DOI: 10.3354/meps009191.
- Ding, H. and Elmore, A. J., 2015. Spatio-Temporal Patterns in Water Surface Temperature from Landsat Time Series Data in the Chesapeake Bay, U.S.A. *Remote Sensing of Environment* 168: 335–348. <https://doi.org/10.1016/j.rse.2015.07.009>.
- Eggleston, J., and Pope, J., 2013. Land subsidence and relative sea-level rise in the southern Chesapeake Bay region: U.S. Geological Survey Circular 1392, 30 p., <http://dx.doi.org/10.3133/cir1392>.
- Ensign, S. H., Hupp, C. R., Noe, G. B., Krauss, K. W., and Stagg, C. L., 2013. Sediment Accretion in Tidal Freshwater Forests and Oligohaline Marshes of the Waccamaw and Savannah Rivers, USA. *Estuaries and Coasts* 37:1107-1119, DOI: 10.1007/s12237-013-9744-7.
- Eshleman, K. N., Sabo, R. D., and Kline, K. M., 2013. Surface water quality is improving due to declining atmospheric N deposition. *Environ. Sci. Technol.* 47:12193-12200, DOI: 10.1021/es4028748.
- Ferreira, J. G., Bricker, S. B., and Simas, T. C., 2007. Application and sensitivity testing of a eutrophication assessment method on coastal systems in the United States and European Union. *J Environ Manage* 82:433-445, DOI: 10.1016/j.jenvman.2006.01.003.
- Fisher, T. R., Peele, E. R., Ammerman, J. W., and Harding, L. W., 1992. Nutrient limitation of phytoplankton in Chesapeake Bay. *Marine Ecology Progress Series* 82:51-63, DOI: 10.3354/meps082051.
- Gellis, A. C., Banks, W. S. L., Langland, M. J. and, Martucci, S. K., 2005. Summary of suspended-sediment data for streams draining the Chesapeake Bay Watershed, water years 1952-2002. US Geological Survey Scientific Investigations Report 2004-5056, Reston, VA, p. 59. <https://doi.org/10.3133/sir20045056>.
- Gellis, A. C., Myers, M. K., Noe, G. B., Hupp, C. R., Schenk, E. R., and Myers, L., 2017. Storms, channel changes, and a sediment budget for an urban-suburban stream, Difficult Run, Virginia, USA. *Geomorphology* 278:128-148, DOI: 10.1016/j.geomorph.2016.10.031.
- Gellis, A. C. and Noe, G. B., 2013. Sediment source analysis in the Linganore Creek watershed, Maryland, USA, using the sediment fingerprinting approach: 2008 to 2010. *Journal of Soils and Sediments* 13:1735-1753, DOI: 10.1007/s11368-013-0771-6.
- Gellis, A. C., Noe, G. B., Clune, J. W., Myers, M. K., Hupp, C. R., Schenk, E. R., and Schwarz, G. E., 2015. Sources of fine-grained sediment in the Linganore Creek watershed, Frederick and Carroll Counties, Maryland, 2008–10. U.S. Geological Survey Scientific Investigations Report 2014–5147, Reston, VA, p. 56. <http://dx.doi.org/10.3133/sir20145147>.
- Gillespie, J. L., Noe, G. B., Hupp, C. R., Gellis, A. C. and Schenk, E. R., 2018. Floodplain Trapping and Cycling Compared to Streambank Erosion of Sediment and Nutrients in an Agricultural Watershed. *JAWRA Journal of the American Water Resources Association* 54:565-582, DOI: 10.1111/1752-1688.12624.



- Greene, E. A., LaMotte, A. E., and Cullinan, K. A., 2005. Ground-water vulnerability to nitrate contamination at multiple thresholds in the mid-Atlantic region using spatial probability models. U.S. Geological Survey Scientific Investigations Report 2004-5118, Reston, VA, p. 32. <https://doi.org/10.3133/sir20045118>.
- Gurbisz, C. and Kemp, W. M., 2014. Unexpected resurgence of a large submersed plant bed in Chesapeake Bay: Analysis of time series data. *Limnology and Oceanography* 59:482-494, DOI: 10.4319/lo.2014.59.2.0482.
- Harding, L. W. and Perry, E. S., 1997. Long-term increase of phytoplankton biomass in Chesapeake Bay, 1950-1994. *Marine Ecology Progress Series* 157:39-52, DOI: 10.3354/meps157039.
- Hernandez Cordero, A. L., Tango, P. J., and Batiuk, R. A., 2020. Development of a multimetric water quality Indicator for tracking progress towards the achievement of Chesapeake Bay water quality standards. *Environmental Modeling & Assessment* 192:94, DOI: 10.1007/s10661-019-7969-z.
- Hinson, K. E., Friedrichs, M. A., St-Laurent, P., Da, F., & Najjar, R. G., 2022. Extent and causes of Chesapeake Bay warming. *Journal of the American Water Resources Association*. 58 (6): 805–825. <https://doi.org/10.1111/1752-1688.12916>.
- Hirsch, R. M., Moyer, D. L., and Archfield, S. A. 2010. Weighted Regressions on Time, Discharge, and Season (WRTDS), with an Application to Chesapeake Bay River Inputs. *JAWRA Journal of the American Water Resources Association* 46(5):857-880, DOI: <https://doi.org/10.1111/j.1752-1688.2010.00482.x>
- Hopkins, K. G., Noe, G. B., Franco, F., Pindilli, E. J., Gordon, S., Metes, M. J., Claggett, P. R., Gellis, A. C., Hupp, C. R., and Hogan, D. M., 2018. A method to quantify and value floodplain sediment and nutrient retention ecosystem services. *J Environ Manage* 220:65-76, DOI: 10.1016/j.jenvman.2018.05.013.
- Jarvie, H. P., Sharpley, A. N., Spears, B., Buda, A. R., May L., and Kleinman, P. J., 2013. Water quality remediation faces unprecedented challenges from "legacy phosphorus". *Environ. Sci. Technol.* 47:8997-8998, DOI: 10.1021/es403160a.
- Keisman, J., Friedrichs, C., Batiuk, R., Blomquist, J., Cornwell, J., Gallegos, C., Lyubchich, S., Moore, K., Murphy, R., Orth, R., Sanford, L., Tango, P., Testa, J., Trice, M. and Zhang, Q., 2019. Understanding and explaining 30 years of water clarity trends in the Chesapeake Bay's tidal waters. Chesapeake Bay Program Scientific and Technical Advisory Committee STAC Publication Number 19-004, Edgewater, MD, p. 25. [http://www.chesapeake.org/pubs/411\\_Keisman2019.pdf](http://www.chesapeake.org/pubs/411_Keisman2019.pdf).
- Kemp, W. M., Boynton, W. R., Adolf, J. E., Boesch, D. F., Boicourt, W. C., Brush, G., Cornwell, J. C., Fisher, T. R., Glibert, P. M., Hagy, J. D., Harding, L. W., Houde, E. D., Kimmel, D. G., Miller, W. D., Newell, R. I. E., Roman, M. R., Smith, E. M., and Stevenson, J. C., 2005. Eutrophication of Chesapeake Bay: Historical trends and ecological interactions. *Marine Ecology Progress Series* 303:1-29, DOI: 10.3354/meps303001.
- Kimmel, D., Tarnowski, M., Newell, R., 2014. The Relationship between Interannual Climate Variability and Juvenile Eastern Oyster Abundance at a Regional Scale in Chesapeake Bay. *North American Journal of Fisheries Management*. 34. DOI: 10.1080/02755947.2013.830999.
- King, P. B., Beikman, H. M., and Edmonston, G. J., 1974. Geologic map of the United States (exclusive of Alaska and Hawaii). U.S. Geological Survey. <https://doi.org/10.3133/70136641>.
- Kleinman, P., Sharpley, A., Buda, A., McDowell, R., and Allen, A., 2011. Soil controls of phosphorus in runoff: Management barriers and opportunities. *Canadian Journal of Soil Science* 91:329-338, DOI: 10.4141/cjss09106.

- Kunkel, K.E., Karl, T. R., Easterling, D. R., Redmond, K. R., Young, J., Yin, X.Y., and Hennon, P., 2013. Probable maximum precipitation and climate change. *Geophysical Research Letters* 40:1402 - 1408, doi:10.1002/grl.50334, 2013.
- Lacouture, R.V., Johnson, J.M., Buchanan, C. *et al.* Phytoplankton index of biotic integrity for Chesapeake Bay and its tidal tributaries. *Estuaries and Coasts: J ERF* **29**, 598–616 (2006).  
<https://doi.org/10.1007/BF02784285>
- Langland, M.J., 2015, Sediment transport and capacity change in three reservoirs, Lower Susquehanna River Basin, Pennsylvania and Maryland, 1900–2012: U.S. Geological Survey Open-File Report 2014–1235, 18 p., <https://dx.doi.org/10.3133/ofr20141235>
- Lindsey, B. D., Phillips, S. W. , Donnelly, C. A., Speiran, G. K., Plummer, L. N., Böhlke, J. K., Focazio, M. J., and Burton, W. C., 2003. Residence times and nitrate transport in ground water discharging to streams in the Chesapeake Bay watershed. U.S. Geological Survey Water-Resources Investigations Report 03-4035, New Cumberland, PA, p. 201.  
<https://pubs.usgs.gov/publication/wri034035>.
- Lizarraga, J. S., 1997. Estimation and analysis of nutrient and suspended-sediment loads at selected sites in the Potomac River Basin, 1993-95. US Geological Survey Water-Resources Investigations Report 97-4154, Baltimore, MD, p. 23. <https://doi.org/10.3133/wri974154>.
- Lyerly, C. M., Cordero, A. L. H., Foreman, K. L., Phillips, S. W., and Dennison, W. C., 2014. New insights: Science-based evidence of water quality improvements, challenges, and opportunities in the Chesapeake. Annapolis, MD, p. 47. [http://ian.umces.edu/pdfs/ian\\_report\\_438.pdf](http://ian.umces.edu/pdfs/ian_report_438.pdf).
- Maryland Department of Natural Resources (DNR). 2022. Eyes on the Bay.  
<https://eyesonthebay.dnr.maryland.gov/>
- Mason, C.A., Colgin, J.E., and Moyer, D.L., 2023, Nitrogen, phosphorus, and suspended-sediment loads and trends measured at the Chesapeake Bay Nontidal Network stations: Water years 1985-2020 (ver. 2.0, January 2023): U.S. Geological Survey data release,  
<https://doi.org/10.5066/P96H2BDO>
- Mazzini, P.L.F. and Pianca, C., 2022. Marine Heatwaves in the Chesapeake Bay. *Frontiers in Marine Science* 8:750265. doi: 10.3389/fmars.2021.750265
- Miller, C. V., J. M. Denis, S. W. Ator and J. W. Brakebill, 1997. Nutrients in streams during baseflow in selected environmental settings of the Potomac River Basin. *J. Am. Water Resour. Assoc.* 33:1155-1171, DOI: 10.1111/j.1752-1688.1997.tb03543.x.
- Murphy, R. R., Kemp, W. M., and Ball, W. P., 2011. Long-term trends in Chesapeake Bay seasonal hypoxia, stratification, and nutrient loading. *Estuaries and Coasts* 34:1293-1309, DOI: 10.1007/s12237-011-9413-7.
- Murphy, R. R., Perry, E., Harcum, J., and Keisman, J., 2019. A Generalized Additive Model approach to evaluating water quality: Chesapeake Bay case study. *Environmental Modelling & Software* 118:1-13, DOI: 10.1016/j.envsoft.2019.03.027.
- Najjar, R.G., Pyke, C.R., Adams, M.B., Breitburg, D.L., Kemp, M., Hershner, C., Howarth, R., Mulholland, M., Paolisso, M., and Secor, D., 2010. Potential climate-change impacts on the Chesapeake Bay. *Estuarine, Coastal and Shelf Science*, 86, 1-20. DOI: 10.1016/j.ecss.2009.09.026
- National Oceanic and Atmospheric Administration. 2023a. Sea Level Rise Viewer.  
<https://coast.noaa.gov/digitalcoast/tools/slr.html>.
- National Oceanic and Atmospheric Administration. 2023b. Tides and Currents: Relative Sea Level Trends.  
<https://tidesandcurrents.noaa.gov/sltrends/>.
- National Oceanic and Atmospheric Administration. 2023c. Chesapeake Bay Interpretive Buoy System.  
<https://buoybay.noaa.gov/explore/seasonal-summaries>.

- Noe, G. B., M. J. Cashman, K. Skalak, A. Gellis, K. G. Hopkins, D. Moyer, J. Webber, A. Benthem, K. Maloney, J. Brakebill, A. Sekellick, M. Langland, Q. Zhang, G. Shenk, J. Keisman and C. Hupp, 45 2020. Sediment dynamics and implications for management: State of the science from longterm research in the Chesapeake Bay watershed, USA. *WIREs Water* 7:e1454, DOI: 10.1002/wat2.1454.
- Noe, G. B., Hopkins, K. G., Claggett, P. R., Schenk, E. R., Metes, M. J., Ahmed, L., Doody, T. R., Hupp, C. R., 2022. Streambank and floodplain geomorphic change and contribution to watershed and material budgets. *Environmental Research Letters*, 17, 064015. DOI: 10.1088/1748-9326/ac6e47.
- Noe, G. B. and Hupp, C. R., 2009. Retention of riverine sediment and nutrient loads by coastal plain floodplains. *Ecosystems* 12:728-746, DOI: 10.1007/s10021-009-9253-5.
- Parham, T., Uphoff, J., Keppel, A., Karrh, R., 2023. Climate Change and Resident Chesapeake Bay Striped Bass Habitat. Presentation to the Chesapeake Bay Program Modeling Workgroup Quarterly Review – January 2023.  
<https://d18lev1ok5leia.cloudfront.net/chesapeakebay/documents/Climate-Change-and-Striped-Bass-Chesapeake-Habitat-Tom-Parham-Andrew.pdf>.
- Phelps, H. L., 1994. The Asiatic Clam (*Corbicula fluminea*) Invasion and System-Level Ecological Change in the Potomac River Estuary near Washington, D. C. *Estuaries* 17:614-621, DOI: 10.2307/1352409.
- Phillips, S. W., 2007. Synthesis of U.S. Geological Survey science for the Chesapeake Bay ecosystem and implications for environmental management. U.S. Geological Survey Circular 1316, Reston, VA, p. 76. <https://doi.org/10.3133/cir1316>.
- Phillips, S.W., Focazio, M.J., Bachman L.J., 2016. Discharge, Nitrate Load, and Residence Time for Ground Water in the Chesapeake Bay Watershed. USGS Fact Sheet FS-150-99.  
<http://pubsdata.usgs.gov/pubs/fs/fs15099/>
- Pilegaard, K., 2013. Processes regulating nitric oxide emissions from soils. *Philos Trans R Soc Lond B Biol Sci* 368:20130126, DOI: 10.1098/rstb.2013.0126.
- PRISM, Oregon State University, <https://prism.oregonstate.edu>, data created 4 Feb 2014, accessed 16 Dec 2020.
- Pyke, C.R., Najjar, R.G., Adams, M.B., Breitburg, D.L., Kemp, M., Hershner, C., Howarth, R., Mulholland, M., Paolisso, M., and Secor, D., 2008. Climate Change and the Chesapeake Bay: State-of-the-Science Review and Recommendations. A Report from the Chesapeake Bay Program Science and Technical Advisory Committee (STAC), Annapolis, MD, 59: 29– 40.
- Ruhl, H.A., Rybicki, N.B., 2010. Long-term reductions in anthropogenic nutrients link to improvements in Chesapeake Bay habitat. *Proceedings of the National Academy of Sciences* 107(38) 16566.
- Scully, M. E., 2010. Wind Modulation of Dissolved Oxygen in Chesapeake Bay. *Estuaries and Coasts*
- Sanford, W. E. and J. P. Pope, 2013. Quantifying groundwater's role in delaying improvements to Chesapeake Bay water quality. *Environ. Sci. Technol.* 47:13330-13338, DOI: 10.1021/es401334k. 33:1164-1175, DOI: 10.1007/s12237-010-9319-9.
- Sharpley, A.N., 1980, The Enrichment of Soil Phosphorus in Runoff Sediments: *Journal of Environmental Quality*, v. 9, no. 3, p. 521–526.
- Sharpley, A., Jarvie, H.P., Buda, A., May, L., Spears, B., and Kleinman, P., 2013, Phosphorus legacy: overcoming the effects of past management practices to mitigate future water quality impairment: *Journal of Environmental Quality*, v. 42, no. 5, p. 1308–1326.
- Smith, E. M. and Kemp, W. M., 1995. Seasonal and regional variations in plankton community production and respiration for Chesapeake Bay. *Marine ecology progress series* 116:217-231, DOI.

- St. Laurent, K. A., Coles, V. J., and Hood, R. R., 2021. Climate Extremes and Variability Surrounding Chesapeake Bay: Past, Present, and Future. *Journal of the American Water Resources Association* 58 ( 6): 826– 854. <https://doi.org/10.1111/1752-1688.12945>.
- Staver, K.W., and Brinsfield, R.B., 2001, Agriculture and Water Quality on the Maryland Eastern Shore: Where Do We Go from Here? Long-term solutions to accelerated eutrophication must provide mechanisms for redistributing nutrients flowing into concentrated animal-producing regions: *BioScience*, v. 51, no. 10, p. 859–868.
- Tango, P.J. and Batiuk R.A., 2013. Deriving Chesapeake Bay Water Quality Standards. *Journal of the American Water Resources Association*, v. 49, no. 5, p. 1007 – 1024. <https://doi.org/10.1111/jawr.12108>
- Terziotti, S., 2019. Distribution of phosphorus in soils and aggregated within geologic mapping units, conterminous United States: U.S. Geological Survey data release. Accessed <https://doi.org/10.5066/P918DF1E>.
- Terziotti, S., Capel, P. D., Tesoriero, A. J., Hopple, J. A., and Kronholm, S. C., 2017. Estimates of nitrate loads and yields from groundwater to streams in the Chesapeake Bay watershed based on land use and geology. U.S. Geological Survey Scientific Investigations Report 2017-5160, Reston, VA, p. 20. <https://doi.org/10.3133/sir20175160>.
- Testa, J. M., Clark, J. B., Dennison, W. C., Donovan, E. C., Fisher, A. W., Ni, W., Parker, M., Scavia, D., Spitzer, S. E., Waldrop, A. M., Vargas, V. M. D., and Ziegler, G., 2017. Ecological Forecasting and the Science of Hypoxia in Chesapeake Bay. *BioScience* 67:614-626, DOI: 10.1093/biosci/bix048.
- Testa, J. M. and Kemp, W. M., 2012. Hypoxia-induced shifts in nitrogen and phosphorus cycling in Chesapeake Bay. *Limnology and Oceanography* 57:835-850, DOI: 10.4319/lo.2012.57.3.0835.
- Testa, J. M., Lyubchich, V., and Zhang, Q., 2019. Patterns and trends in Secchi disk depth over three decades in the Chesapeake Bay estuarine complex. *Estuaries and Coasts* 42:927-943, DOI: 10.1007/s12237-019-00547-9.
- Tian R., Cerco, C. F., Bhatt, G., Linker, L. C., and Shenk, G. W. 2021. Mechanisms Controlling Climate Warming Impact on the Occurrence of Hypoxia in Chesapeake Bay. *Journal of the American Water Resources Association* 6:855 - 875, <https://doi.org/10.1111/1752-1688.12907>
- Trimble, S. W., 1975. A volumetric estimate of man-induced soil erosion on the southern Piedmont Plateau. Agricultural Research Service, U.S. Department of Agriculture Agricultural Research Service Publication ARS-S-40, pp. 142-154. Accession: 000279944.
- U.S. Environmental Protection Agency, 2003. Ambient Water Quality Criteria for Dissolved Oxygen, Water Clarity and Chlorophyll a for the Chesapeake Bay and Its Tidal Tributaries. EPA 903-R-03-002. U.S. Environmental Protection Agency, Region 3, Chesapeake Bay Program Office, Annapolis, Maryland. [Permanent Link](#).
- U.S. Environmental Protection Agency, 2004. Chesapeake Bay Program Analytical Segmentation Scheme: Revisions, Decisions and Rationales 1983-2003. USEPA Region III Chesapeake Bay Program Office EPA 903-R-04-008, Annapolis, Maryland, p. 64.
- U.S. Geological Survey, 2022. Chesapeake Bay Water-Quality Loads and Trends, accessed August 20, 2022 at <https://www.usgs.gov/centers/chesapeake-bay-activities/science/chesapeake-bay-water-quality-loads-and-trends>.
- U.S. Geological Survey, 2018. Water Science School: Sea Level and Climate. <https://www.usgs.gov/special-topics/water-science-school/science/sea-level-and-climate>
- U.S. Geological Survey, 2022, USGS water data for the Nation: U.S. Geological Survey National Water Information System database, accessed August 20, 2022, at <https://doi.org/10.5066/F7P55KJN>.

- Virginia Institute of Marine Science (VIMS). 2022. Virginia Estuarine & Coastal Observing System. <https://vecos.vims.edu/home>
- Weisberg, S.B., Ranasinghe, J.A., Dauer, D.M. et al. An estuarine benthic index of biotic integrity (B-IBI) for Chesapeake Bay. *Estuaries* 20, 149–158 (1997). <https://doi.org/10.2307/1352728>
- Wright, A. C., Hill, R. T., Johnson, J. A., Roshan, M. C., Colwell, R. R., & Morris, J. G., Jr, 1996. Distribution of *Vibrio vulnificus* in the Chesapeake Bay. *Applied and environmental microbiology*, 62(2), 717–724. <https://doi.org/10.1128/aem.62.2.717-724.1996>
- Wynn, T. and Mostaghimi, S., 2006. The Effects of Vegetation and Soil Type on Streambank Erosion, Southwestern Virginia, USA. *Journal of the American Water Resources Association* 42:69-82, DOI: 10.1111/j.1752-1688.2006.tb03824.x.
- Zhang, Q., Brady, D. C., Boynton, W. R., and Ball, W. P., 2015. Long-term trends of nutrients and sediment from the nontidal Chesapeake watershed: An assessment of progress by river and season. *Journal of the American Water Resources Association* 51:1534-1555, DOI: 10.1111/1752-1688.12327.
- Zhang, Q., Fisher, T. R., Trentacoste, E. M., Buchanan, C., Gustafson, A. B., Karrh, R., Murphy, R. R., Keisman, J., Wu, C., Tian, R., Testa, J. M., and Tango, P. J., 2021. Nutrient limitation of phytoplankton in Chesapeake Bay: Development of an empirical approach for water-quality management. *Water Research* 188:116407, DOI: 10.1016/j.watres.2020.116407.
- Zhang, Q., Murphy, R. R., Tian, R., Forsyth, M. K., Trentacoste, E. M., Keisman, J., and Tango, P. J., 2018a. Chesapeake Bay's water quality condition has been recovering: Insights from a multimetric indicator assessment of thirty years of tidal monitoring data. *Science of the Total Environment* 637-638:1617-1625, DOI: 10.1016/j.scitotenv.2018.05.025.
- Zhang, Q., Murphy, R. R., Tian, R., Forsyth, M. K., Trentacoste, E. M., Keisman, J., and Tango, P. J., 2018b. Chesapeake Bay's water quality condition has been recovering: Insights from a multimetric indicator assessment of thirty years of tidal monitoring data. *Science of the Total Environment* 637-638:1617-1625, DOI: 10.1016/j.scitotenv.2018.05.025.
- Zhang, Q., Tango, P. J., Murphy, R. R., Forsyth, M. K., Tian, R., Keisman, J., and Trentacoste, E. M., 2018c. Chesapeake Bay dissolved oxygen criterion attainment deficit: Three decades of temporal and spatial patterns. *Frontiers in Marine Science* 5:422, DOI: 10.3389/fmars.2018.00422.

## Appendix A: Glossary of Terms

**Anoxic** - condition in which the water column is characterized by a complete absence of oxygen. Anoxic conditions typically result from excessive decomposition of organic material by bacteria, high respiration by phytoplankton, stratification of the water column due to salinity or temperature effects or a combination of these factors. Anoxic conditions can result in fish kills or localized extinction of benthic communities.

**Anthropogenic** - resulting from or generated by human activities.

**Benthos** - refers to organisms that dwell on or within the bottom of a waterway or waterbody. Includes both hard substratum habitats (e.g., oyster reefs) and sedimentary habitats (sand and mud bottoms).

**B-IBI** - the benthic index of biotic integrity of Weisberg et al. (1997). The B-IBI is a multi-metric index that compares the condition of a benthic community to reference conditions.

**Biological Nutrient Removal (BNR)** - A temperature dependent process in which the ammonia nitrogen present in wastewater is converted by bacteria first to nitrate nitrogen and then to nitrogen gas. This technique is used to reduce the concentration of nitrogen in sewage treatment plant effluents.

**Chlorophyll *a*** - a green pigment found in plant cells that functions as the receptor for energy in the form of sunlight. This energy is used in the production of cellular materials for growth and reproduction in plants. Chlorophyll *a* concentrations are measured in micrograms per liter (µg/L) and are used as an estimate of the total biomass of phytoplankton cells in the water column. In general, high levels of chlorophyll *a* are believed to be indicative of excessive growth of phytoplankton resulting from excess nutrients such as nitrogen and phosphorus in the water column.

**Chlorophytes** - algae belonging to the division Chlorophyta often referred to as true “green algae.” Chlorophytes occur in unicellular, colonial, and filamentous forms and are generally more common in tidal freshwater and oligohaline portions of estuaries.

**Cryptomonads** - algae belonging to the division Cryptophyta that have accessory pigments in addition to chlorophyll *a* which give these small, flagellated cells a red, brown, or yellow color.

**Cyanophytes** (or Cyanobacteria) - algae-like bacteria belonging to the division Cyanophyceae that are procaryotic and that occur in single-celled, filamentous, and colonial forms. In general, high concentrations of cyanophytes are considered indicative of poor water quality.

**Diatoms** - algae belonging to the division Bacillariophyta that have a cell wall that is composed primarily of silica and that consists of two separate halves. Most diatoms are single celled, but some are colonial and filamentous forms. Diatoms are generally considered to be indicative of good water quality and are appropriate food for many zooplankton.

**Dinoflagellates** - biflagellated, predominately unicellular protists that are capable of photosynthesizing. Many dinoflagellates are covered with cellulose plates or with a series of membranes. Some dinoflagellates periodically reproduce in large numbers causing blooms that are often referred to as “red tides.” Certain species produce toxins and blooms of these forms have been implicated in fish kills. High concentrations of dinoflagellates are generally considered indicative of poor water quality.



**Dissolved oxygen (DO)** - the concentration of oxygen in solution in the water column, measured in milligrams per liter (mg/L). Most aquatic organisms rely on oxygen for cellular metabolism, and as a result, low levels of dissolved oxygen adversely affect important living resources such as fish and the benthos. In general, dissolved oxygen levels decrease with increasing pollution.

**Dissolved inorganic nitrogen (DIN)** - the concentration of inorganic nitrogen compounds including ammonia ( $\text{NH}_4$ ), nitrates ( $\text{NO}_3$ ) and nitrites ( $\text{NO}_2$ ) in the water column measured in milligrams per liter (mg/L). These dissolved inorganic forms of nitrogen are directly available for uptake by phytoplankton by diffusion without first undergoing the process of decomposition. High concentrations of dissolved inorganic nitrogen can result in excessive growth of phytoplankton which in turn can adversely affect other living resources.

**Dissolved inorganic phosphorus ( $\text{PO}_4$ )** - the concentration of inorganic phosphorus compounds consisting primarily of orthophosphates ( $\text{PO}_4$ ). The dissolved inorganic forms of phosphorus are directly available for uptake by phytoplankton by diffusion without first undergoing the process of decomposition. High concentrations of dissolved inorganic phosphorus can result in excessive growth of phytoplankton which in turn can adversely affect other living resources.

**Estuary** - A semi-enclosed body of water that has a free connection with the open sea and within which seawater is diluted measurably with freshwater derived from land drainage.

**Eucaryote** - organisms made of cells containing discrete organelles and a nucleus separated from the cytoplasm by a membrane.

**Fall line** - location of the maximum upstream extent of tidal influence in an estuary typically characterized by a waterfall.

**Fixed Point Stations** - stations for long-term trend analysis whose location is unchanged over time.

**Flow adjusted concentration (FAC)** - concentration which has been recalculated to remove the variation caused by freshwater flow into a stream. By removing variation caused by flow, the effects of other factors such as nutrient management strategies can be assessed.

**Habitat** - a local environment that has a community distinct from other such habitat types. For the B-IBI of Chesapeake Bay, seven habitat types were defined as combinations of salinity and sedimentary types - tidal freshwater, oligohaline, low mesohaline, high mesohaline sand, high mesohaline mud, polyhaline sand and polyhaline mud.

**Hypoxic** - condition in which the water column is characterized by dissolved oxygen concentrations less than 2 milligrams per liter (mg/L) but greater than 0 mg/L. Hypoxic conditions typically result from excessive decomposition of organic material by bacteria, high respiration by phytoplankton, stratification of the water column due to salinity or temperature effects or a combination of these factors. Hypoxic conditions can result in fish kills or localized extinction of benthic communities.

**Light attenuation (KD)** - Absorption, scattering, or reflection of light by dissolved or suspended material in the water column expressed as the change in light extinction per meter of depth. Light attenuation reduces the amount of light available to submerged aquatic vegetation.

**Loading** - the total mass of contaminant or nutrient added to a stream or river generally expressed in kilograms per year (kg/yr) or pounds per year (lbs/yr).

**Macrobenthos** - a size category of benthic organisms that are retained on a mesh of 0.5 millimeters (mm).

**Mesohaline** - refers to waters with salinity values ranging between 0.5 and 18.0 parts per thousand (ppt).

**Metric** - a parameter or measurement of ecological community structure (e.g., abundance, biomass, species diversity).

**Non-point source** - a source of pollution that is distributed widely across the landscape surrounding a water body (e.g., run-off from residential and agricultural land) instead of being at a fixed location (e.g., wastewater treatment plant outlet).

**Oligohaline** - refers to waters with salinity values ranging between 0.5 and 5.0 parts per thousand (ppt).

**Percent of light at the leaf surface (PLL)** - the percentage of light at the surface of the water column that reaches the surface of the leaves of submerged aquatic vegetation generally estimated for depths of 0.5 and 1.0 meter (m). Without sufficient light at the leaf surface, submerged aquatic plants cannot perform photosynthesis and hence cannot grow or reproduce.

**Phytoplankton** - that portion of the plankton capable of producing its own food by photosynthesis. Typical members of the phytoplankton include diatoms, dinoflagellates, and chlorophytes.

**P-IBI** - the phytoplankton index of biotic integrity (Buchanan et al., 2005; Lacouture et al., 2006). The P-IBI is a multi-metric index that compares the condition of a phytoplankton community to reference conditions.

**Plankton** - aquatic organisms that drift within and that are incapable of movement against water currents. Some plankton have limited locomotor ability that allows them to change their vertical position in the water column.

**Point source** - a source of pollution that is concentrated at a specific location such as the outfall from a sewage treatment plant or factory.

**Polyhaline** - refers to waters with salinity values ranging between 18.0 and 30 parts per thousand (ppt).

**Primary productivity** - the rate of production of living material through the process of photosynthesis that for phytoplankton is typically expressed in grams of carbon per liter of water per hour. High rates of primary productivity are generally considered to be related to excessive concentrations of nutrients such as nitrogen and phosphorus in the water column.

**Probability based sampling** - all locations within a stratum have an equal chance of being sampled. Allows estimation of the percent of the stratum meeting or failing the benthic restoration goals.

**Prokaryote** - organisms the cells of which do not have discrete organelles or a nucleus (e.g., Cyanobacteria).

**Pycnocline** - a rapid change in salinity in the water column indicating stratification of water with depth, resulting from changes in either salinity or water temperature.

**Random Station** - a station selected randomly within a stratum. In every successive sampling event, new random locations are selected.

**Recruitment** - The successful dispersal, settlement, and development of larval forms of plants or animal to a reproducing adult.

**Reference condition** - the structure of benthic communities at reference sites.

**Reference sites** - sites determined to be minimally impacted by anthropogenic stress. Conditions at these sites are considered to represent goals for restoration of impacted benthic communities. Reference sites were selected by Weisberg et al. (1997) as those outside highly developed watersheds, distant from any point-source discharge, with no sediment contaminant effect, with no low dissolved oxygen effect, and with a low level of organic matter in the sediment.

**Restoration Goal** - refers to obtaining an average B-IBI value of 3.0 for a benthic community indicating that values for metrics approximate the reference condition.

**Riparian Buffer** - An area of trees and shrubs with a minimum width of 100 feet located up gradient, adjacent, and parallel to the edge of a water feature which 1) reduces excess amounts of sediment, organic matter, nutrients, and other pollutants in surface runoff, 2) reduces soluble pollutants in shallow ground water flow, 3) creates shade along water bodies to lower aquatic temperatures, 4) provides a source of detritus and large woody debris for aquatic organisms, 5) provides riparian habitat and corridors for wildlife, and 6) reduces erosion of streambanks and shorelines.

**Salinity** - the concentration of dissolved salts in the water column measured in milligrams per liter (mg/L), parts per thousand (ppt) or practical salinity units (psu). The composition and distribution of plant and animal communities is directly affected by salinity in estuarine systems. The effects of salinity on living resources must be taken into consideration when interpreting the potential effects of human activities on living resources.

**Secchi depth** - the depth of light penetration expressed in meters as measured using a Secchi disk. Light penetration depth directly affects the growth and recruitment of submerge aquatic vegetation.

**Stratum** - a geographic region of unique ecological condition or managerial interest.

**Submerged aquatic vegetation (SAV)** - rooted vascular plants (e.g., *Zostera marina* (eelgrass), *Ruppia maritima* (widgeon grass), *Stuckenia pectinata* (sago pondweed)) that grow in shallow water areas. SAV is important in marine environments because it is a major food source, provides refuge for juvenile crabs and fish, stabilizes sediments preventing shoreline erosion and excessive suspended materials in the water column, and produces oxygen in the water column.

**Threshold** - a value of a metric that determines the B-IBI scoring. For all metrics except abundance and biomass, two thresholds are used - the lower 5<sup>th</sup> percentile and the 50<sup>th</sup> percentile (median) of the distribution of values at reference sites. Samples with metric values less than the lower 5<sup>th</sup> percentile are scored as a 1. Samples with values between the 5<sup>th</sup> and 50<sup>th</sup> metrics are scored as 3, and values greater than the 50<sup>th</sup> percentile are scored as 5. For abundance and biomass, values below the 5<sup>th</sup> and above the 95<sup>th</sup> percentile are scored as 1, values between the 5<sup>th</sup> and 25<sup>th</sup> and the 75<sup>th</sup> and 95<sup>th</sup> percentiles are scored as 3 and values between the 25<sup>th</sup> and 75<sup>th</sup> percentiles are scored as 5.

**Tidal freshwater** - refers to waters with salinity values ranging between 0 and 0.5 parts per thousand (ppt) which are located in the upper reaches of the estuary at or just below the maximum upstream extent of tidal influence.

**Total nitrogen (TN)** - the concentration of both inorganic and organic compounds in the water column which contain nitrogen measured in milligrams per liter (mg/L). Nitrogen is a required nutrient for protein synthesis. Inorganic forms of nitrogen are directly available for uptake by phytoplankton while organic compounds must first be decomposed by bacteria prior to being available for use for other organisms. High levels of total nitrogen can be detrimental to living resources either as a source of nutrients for excessive phytoplankton growth or as a source of excessive bacterial decomposition that can increase the incidence and extent of anoxic or hypoxic events.

**Total phosphorus (TP)** - the concentration of both inorganic and organic compounds in the water column which contain phosphorus measured in milligrams per liter (mg/L). Phosphorus is a required nutrient for cellular metabolism and the production of cell membranes. Inorganic forms of phosphorus are directly available for uptake by phytoplankton while organic compounds must first be decomposed by bacteria prior to being available for use for other organisms. High levels of total phosphorus can be detrimental to living resources either as a source of nutrients for excessive phytoplankton growth or as a source of excessive bacterial decomposition that can increase the incidence and extent of anoxic or hypoxic events.

**Total suspended solids (TSS)** - the concentration of suspended particles in the water column, measured in milligrams per liter (mg/L). The composition of total suspended solids includes both inorganic (fixed) and organic (volatile) compounds. The fixed suspended solids component is composed of sediment particles, while the volatile suspended solids component is composed of detrital particles and planktonic organisms. The concentration of total suspended solids directly affects water clarity, which in turn affects the development and growth of submerged aquatic vegetation.

## Appendix B: Additional Plots

Appendix B contains additional tidal trend maps and plots for:

- Bottom Total Nitrogen

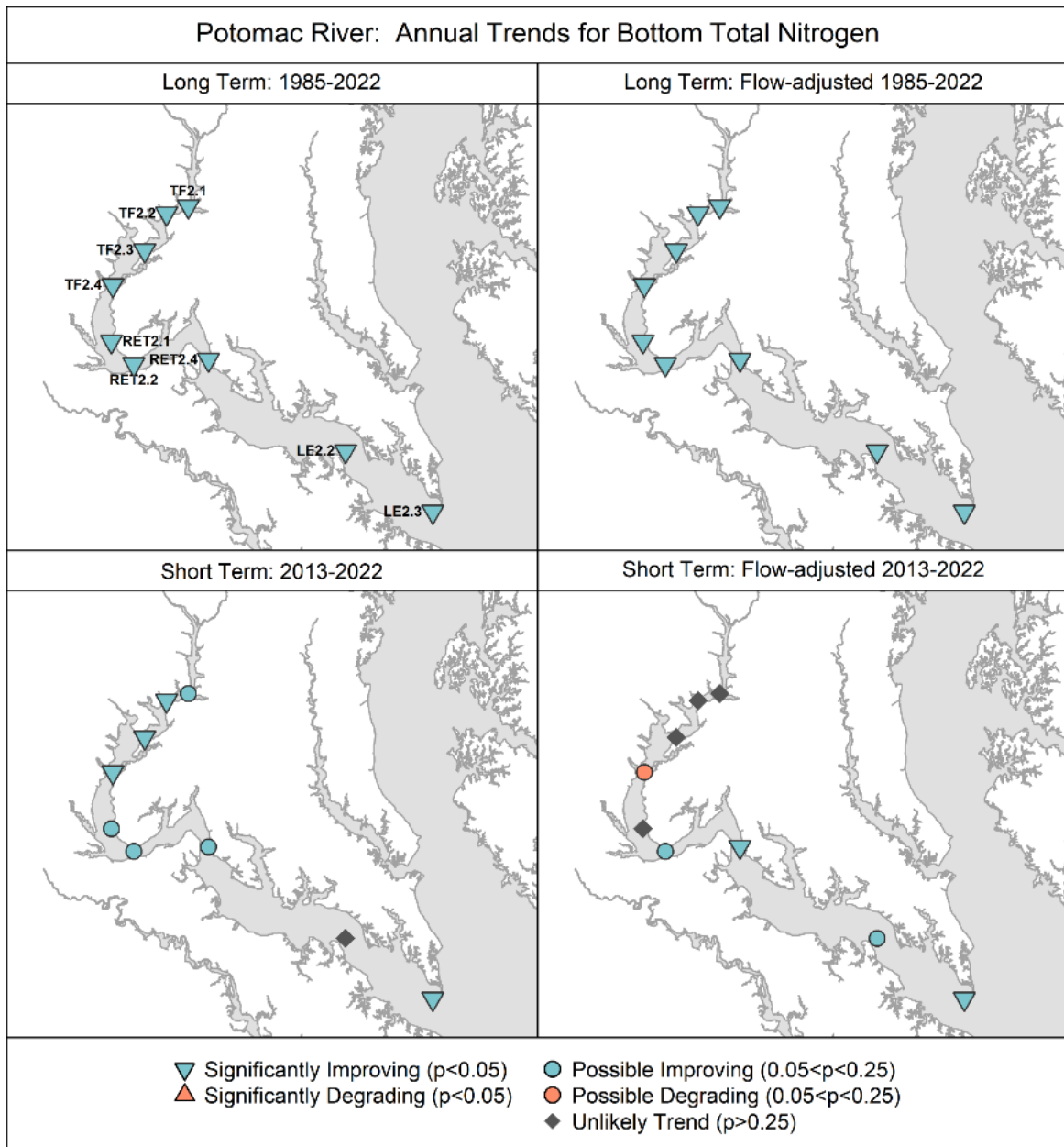


Figure A1. Annual flow-adjusted surface total nitrogen concentration trends as calculated using Generalized Additive Models (Murphy et al. 2019). Base map credit Chesapeake Bay Program, [www.chesapeakebay.net](http://www.chesapeakebay.net), North American Datum 1983. For more information on the tidal stations and Chesapeake Bay tidal water quality monitoring, refer to <https://www.chesapeakebay.net/what/programs/quality-assurance/tidal-water-quality-monitoring>.

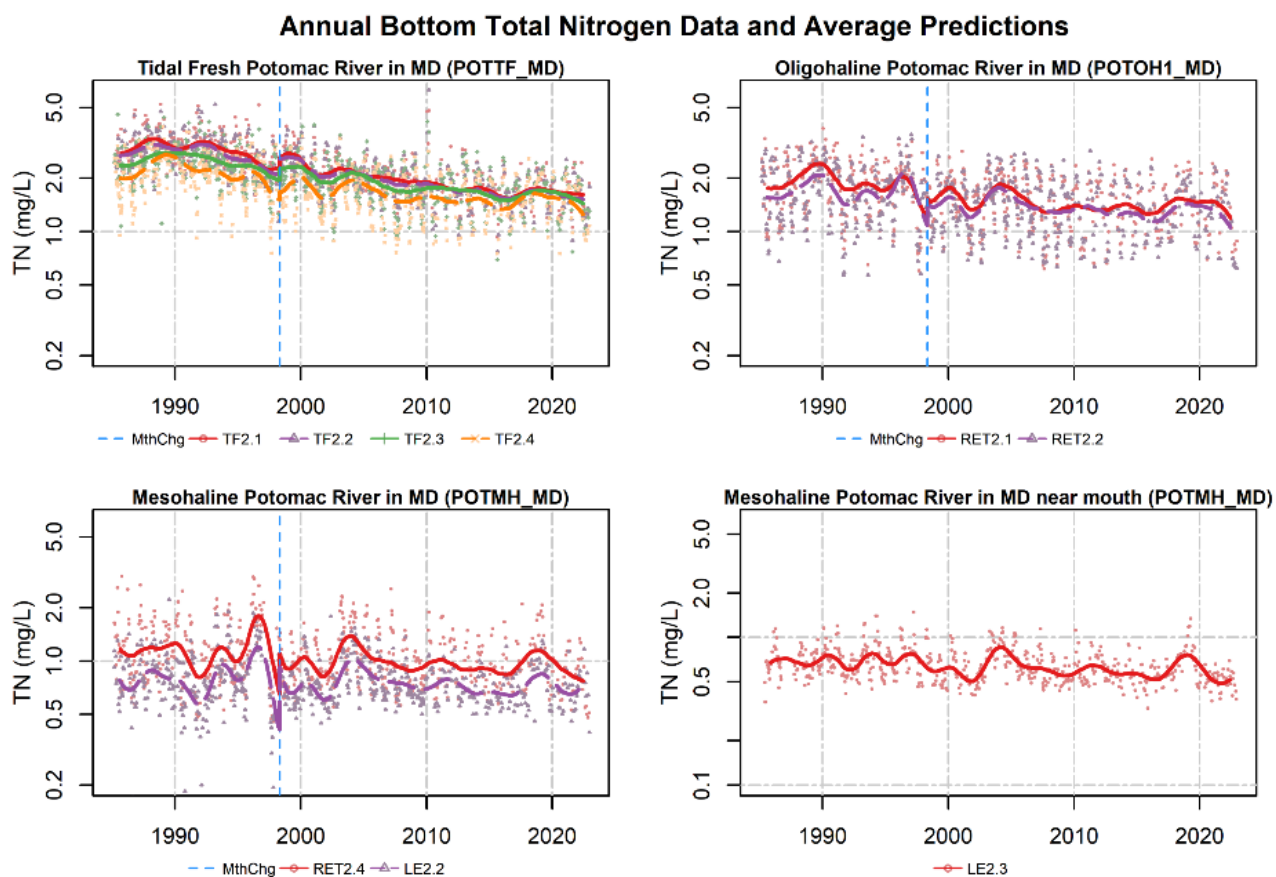


Figure A2. Annual bottom total nitrogen concentration data (dots) and average long-term pattern generated from non-flow adjusted Generalized Additive Models (GAMs). Colored dots represent data corresponding to the monitoring station shown indicated in the legend; colored lines represent mean annual GAM estimates for the noted monitoring stations.



- Bottom Total Phosphorus

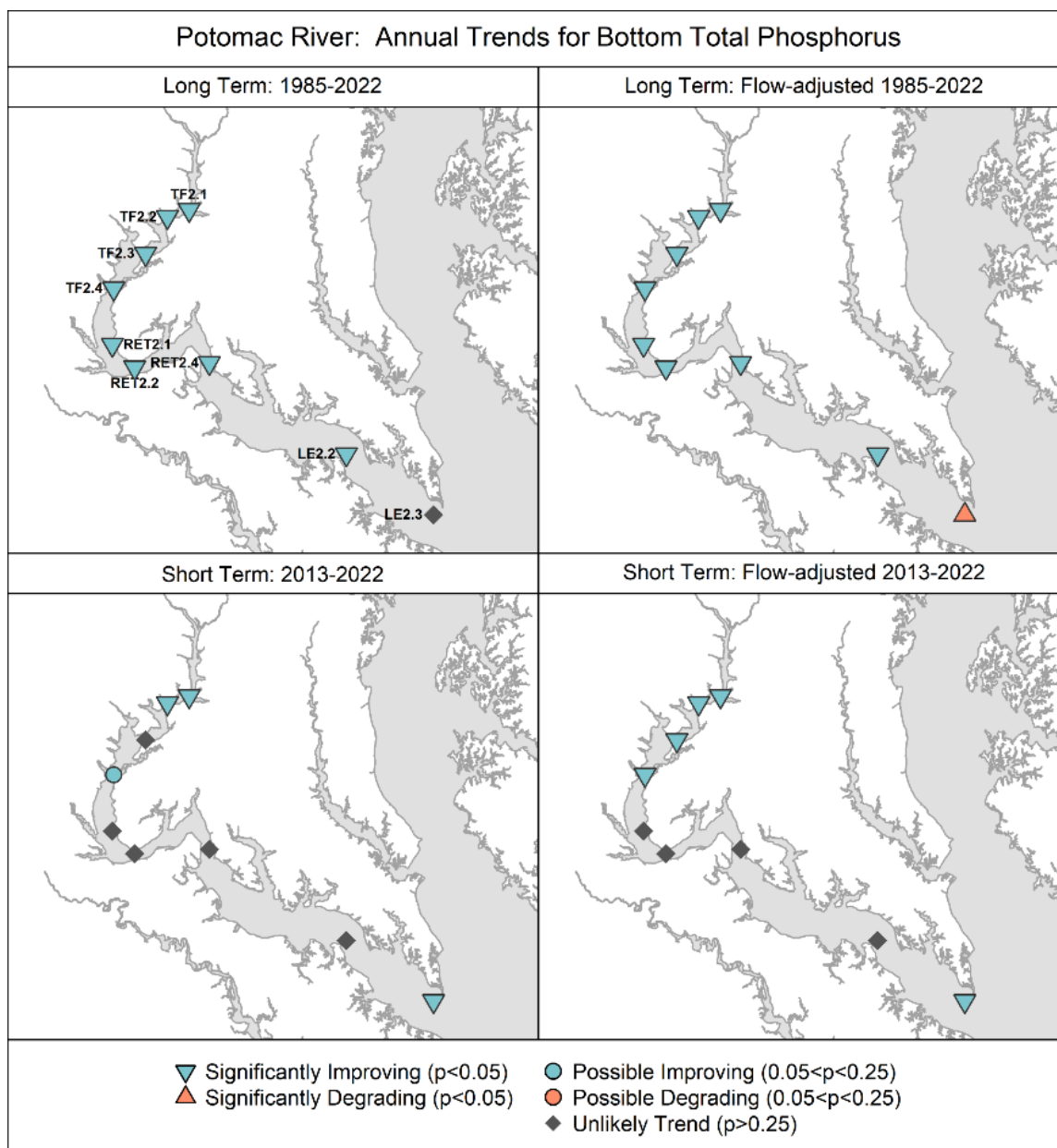


Figure A3. Annual flow-adjusted surface total phosphorus concentration trends as calculated using Generalized Additive Models (Murphy et al. 2019). Base map credit Chesapeake Bay Program, [www.chesapeakebay.net](http://www.chesapeakebay.net), North American Datum 1983. For more information on the tidal stations and Chesapeake Bay tidal water quality monitoring, refer to <https://www.chesapeakebay.net/what/programs/quality-assurance/tidal-water-quality-monitoring>.

### Annual Bottom Total Phosphorus Data and Average Predictions

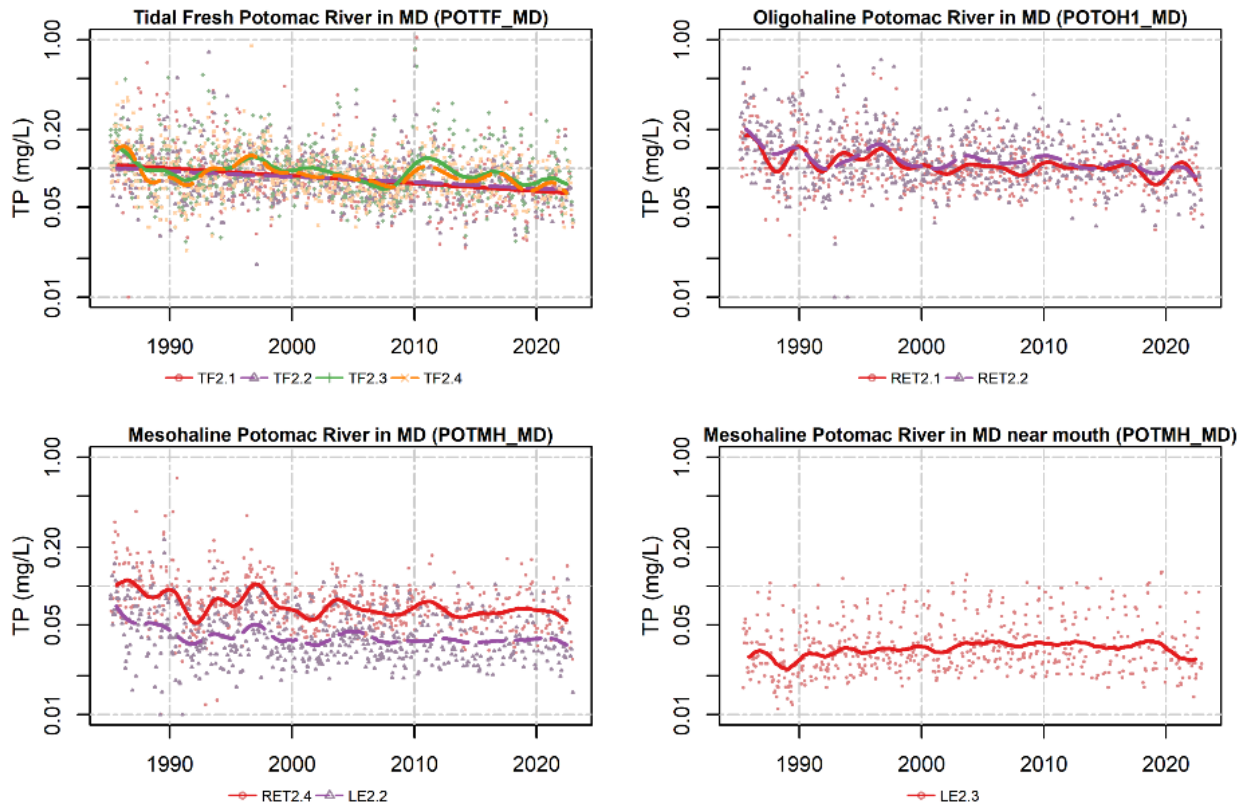


Figure A4. Annual bottom total phosphorus concentration data (dots) and average long-term pattern generated from non-flow adjusted Generalized Additive Models (GAMs). Colored dots represent data corresponding to the monitoring station shown indicated in the legend; colored lines represent mean annual GAM estimates for the noted monitoring stations.

- Surface Dissolved Inorganic Nitrogen

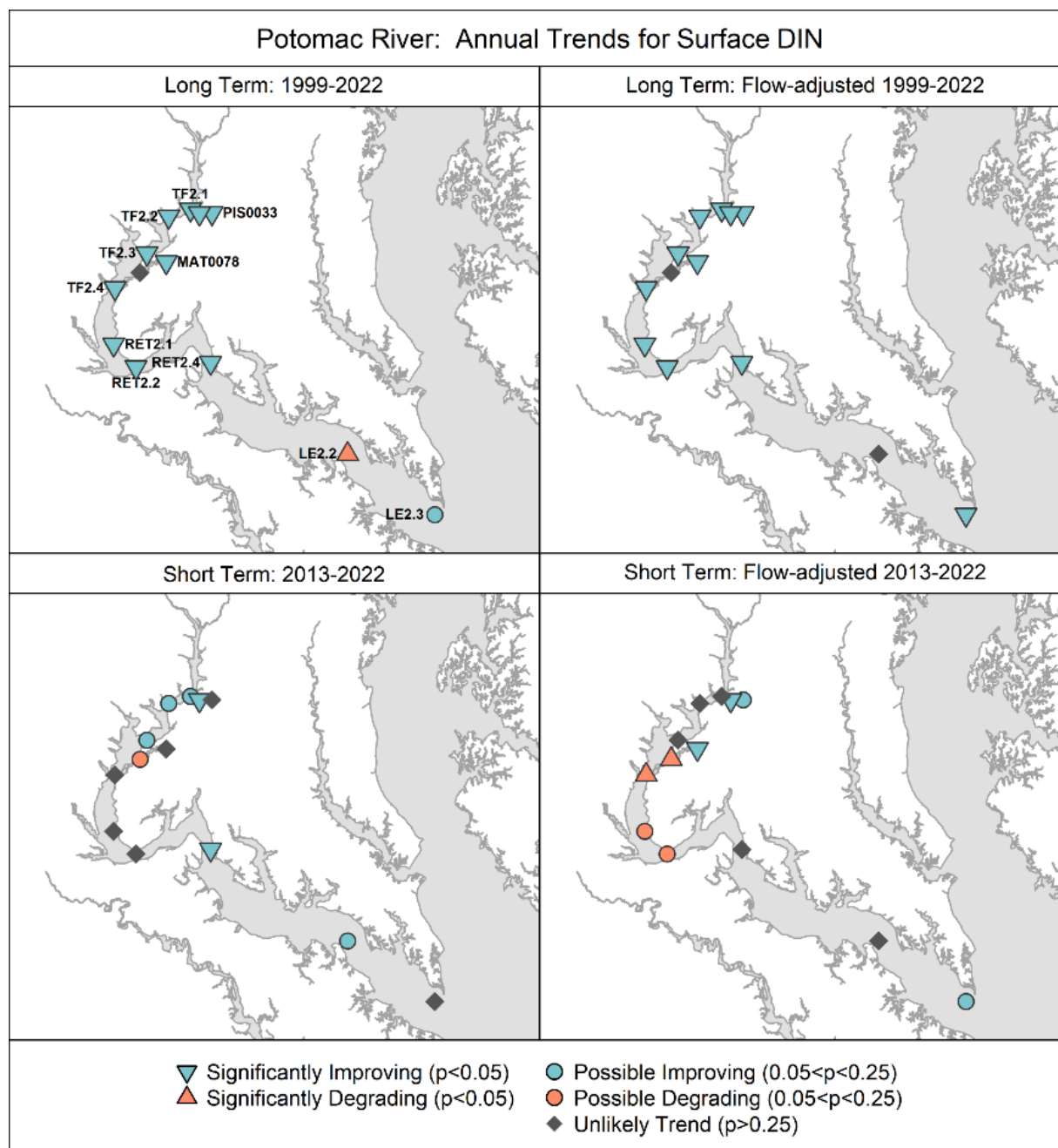


Figure A5. Annual flow-adjusted surface dissolved inorganic nitrogen concentration trends as calculated using Generalized Additive Models (Murphy et al. 2019). Base map credit Chesapeake Bay Program, [www.chesapeakebay.net](http://www.chesapeakebay.net), North American Datum 1983. For more information on the tidal stations and Chesapeake Bay tidal water quality monitoring, refer to <https://www.chesapeakebay.net/what/programs/quality-assurance/tidal-water-quality-monitoring>.

### Annual Surface Dissolved Inorganic Nitrogen Data and Average Predictions

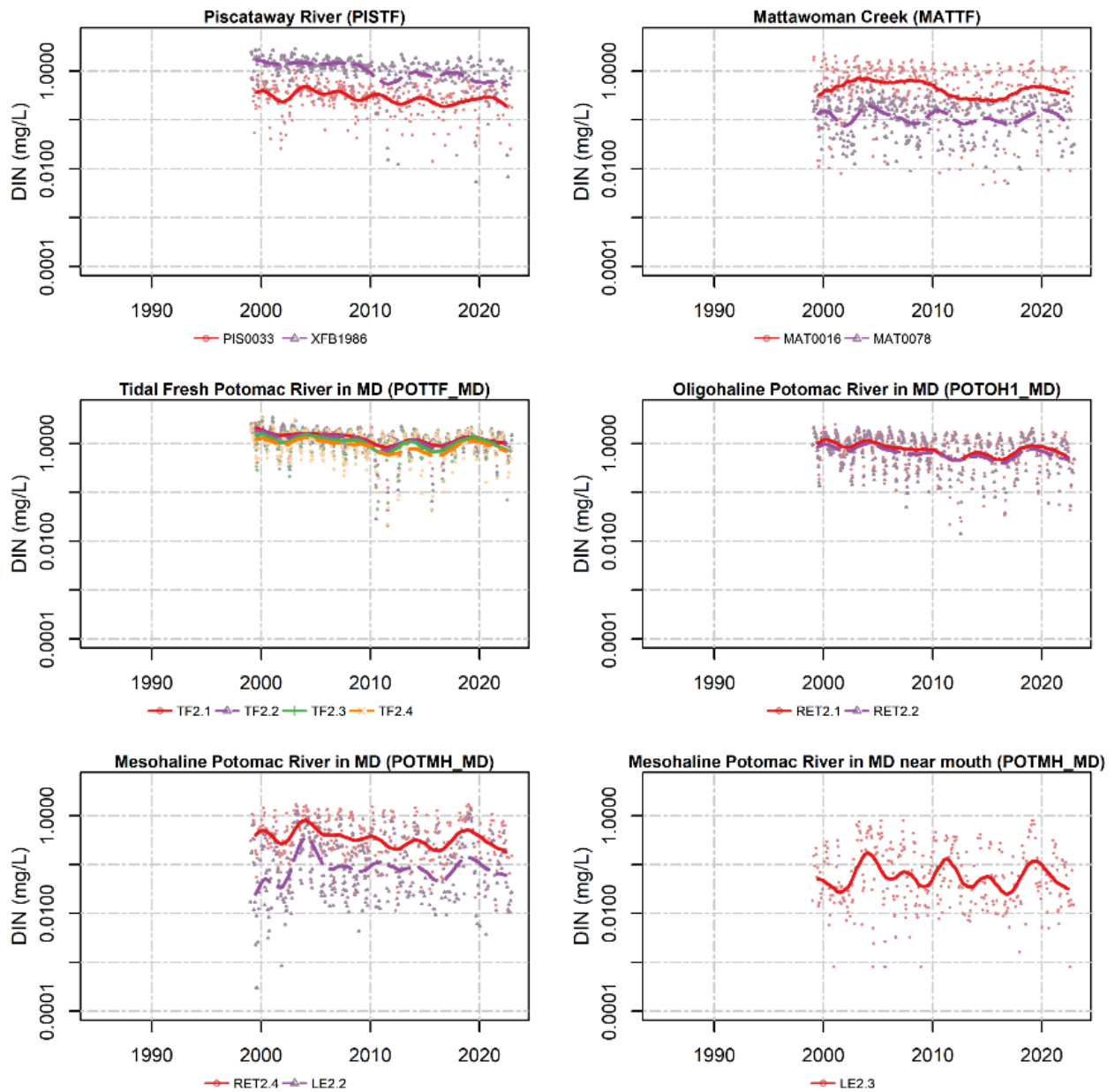


Figure A6. Annual surface dissolved inorganic nitrogen concentration data (dots) and average long-term pattern generated from non-flow adjusted Generalized Additive Models (GAMs). Colored dots represent data corresponding to the monitoring station shown indicated in the legend; colored lines represent mean annual GAM estimates for the noted monitoring stations.

- Surface Orthophosphate

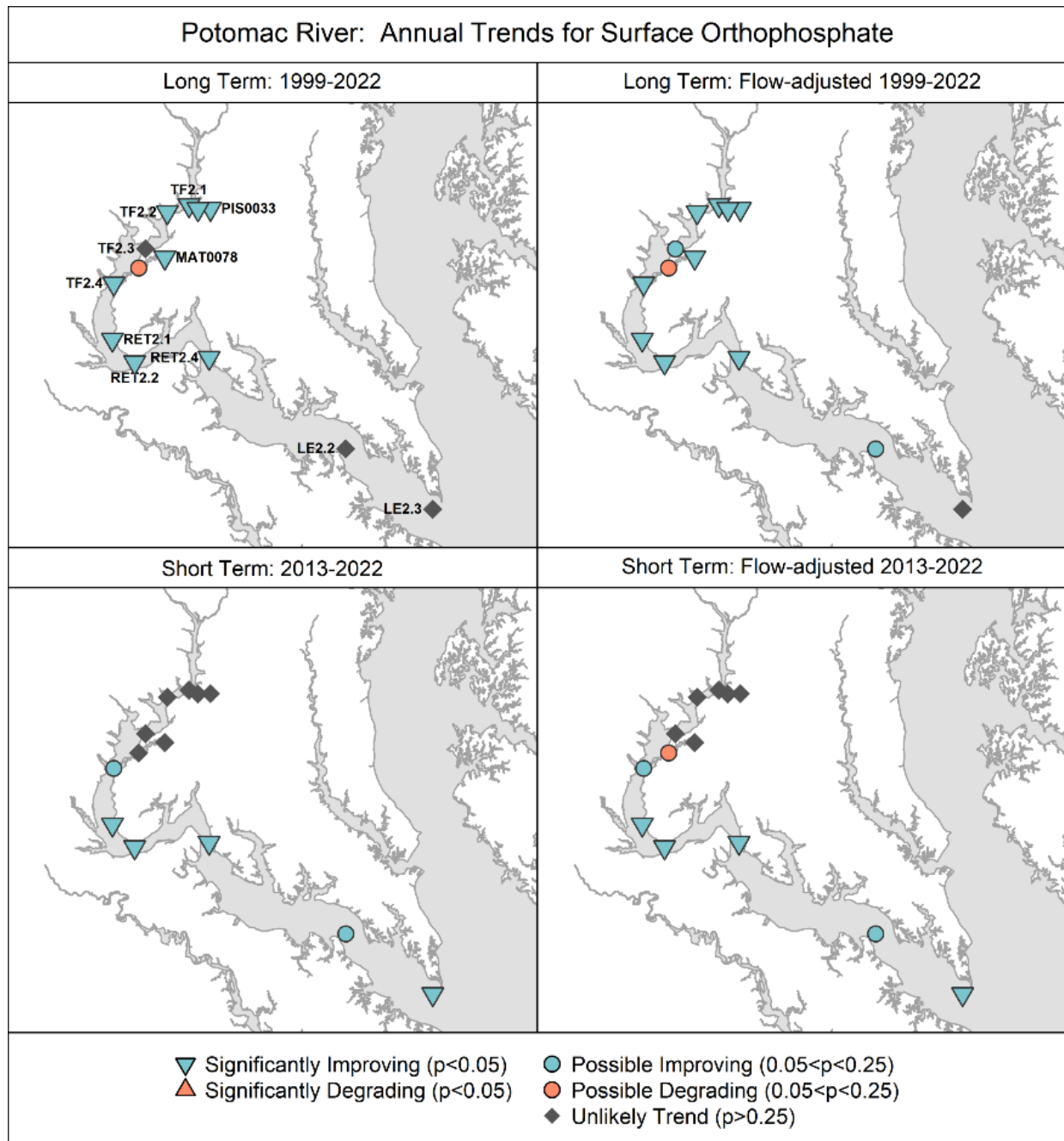


Figure A7. Annual flow-adjusted surface orthophosphate concentration trends as calculated using Generalized Additive Models (Murphy et al. 2019). Base map credit Chesapeake Bay Program, [www.chesapeakebay.net](http://www.chesapeakebay.net), North American Datum 1983. For more information on the tidal stations and Chesapeake Bay tidal water quality monitoring, refer to <https://www.chesapeakebay.net/what/programs/quality-assurance/tidal-water-quality-monitoring>.



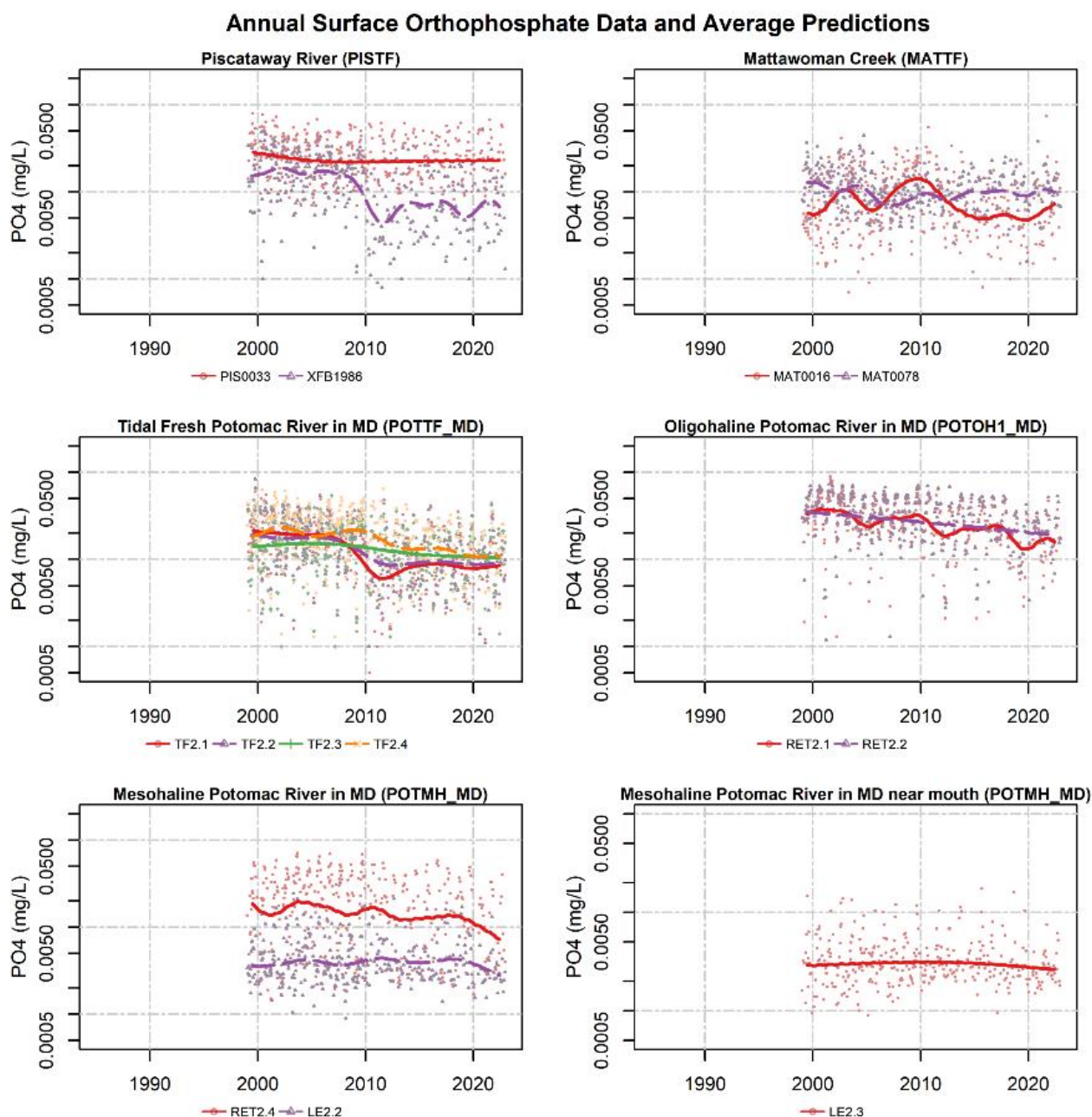


Figure A8. Annual surface orthophosphate concentration data (dots) and average long-term pattern generated from non-flow adjusted Generalized Additive Models (GAMs). Colored dots represent data corresponding to the monitoring station shown indicated in the legend; colored lines represent mean annual GAM estimates for the noted monitoring stations.



- Surface Total Suspended Solids

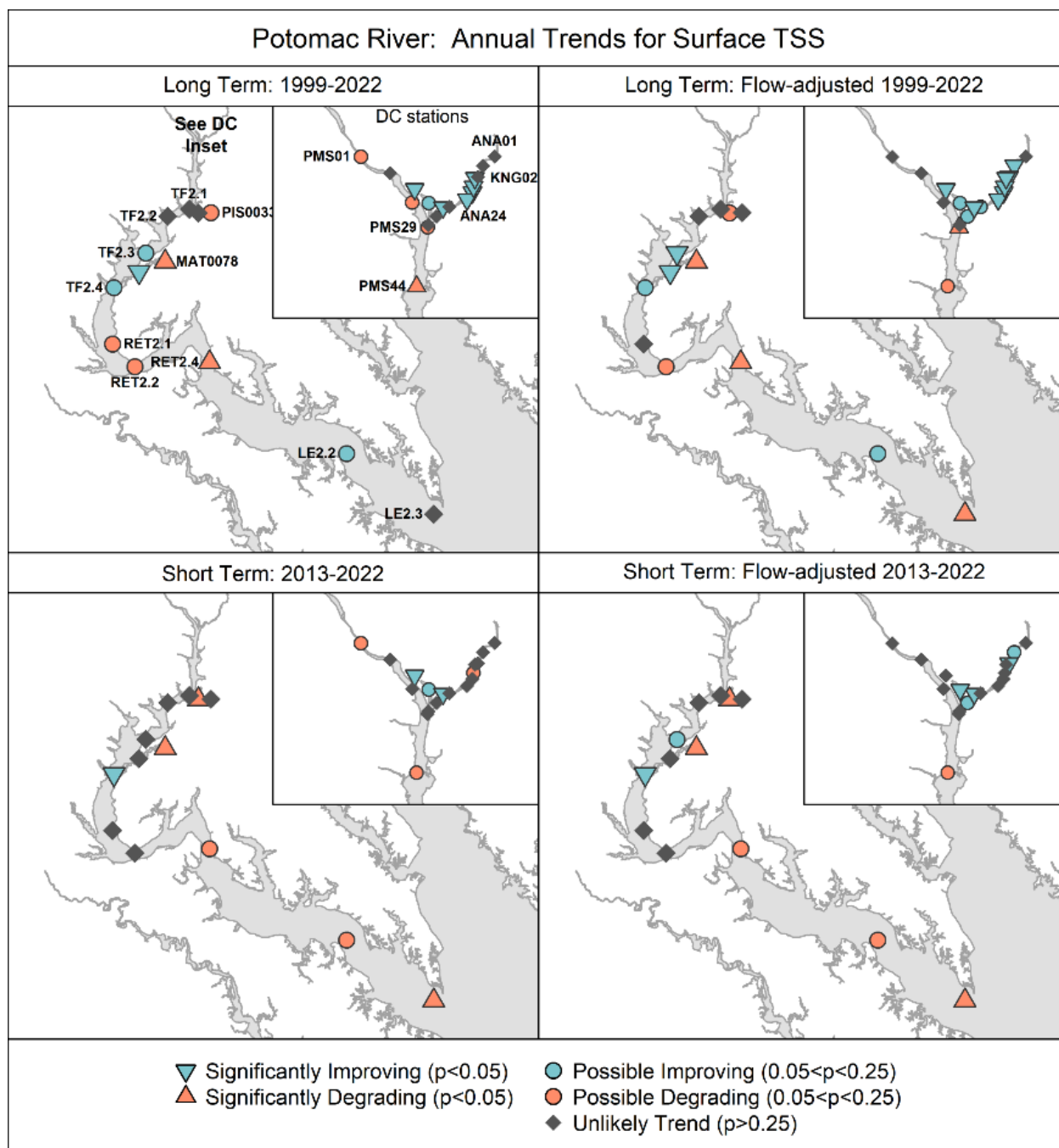


Figure A9. Annual flow-adjusted surface total suspended solids concentration trends as calculated using Generalized Additive Models (Murphy et al. 2019). Base map credit Chesapeake Bay Program, [www.chesapeakebay.net](http://www.chesapeakebay.net), North American Datum 1983. For more information on the tidal stations and Chesapeake Bay tidal water quality monitoring, refer to <https://www.chesapeakebay.net/what/programs/quality-assurance/tidal-water-quality-monitoring>.

### Annual Surface Total Suspended Solids Data and Average Predictions

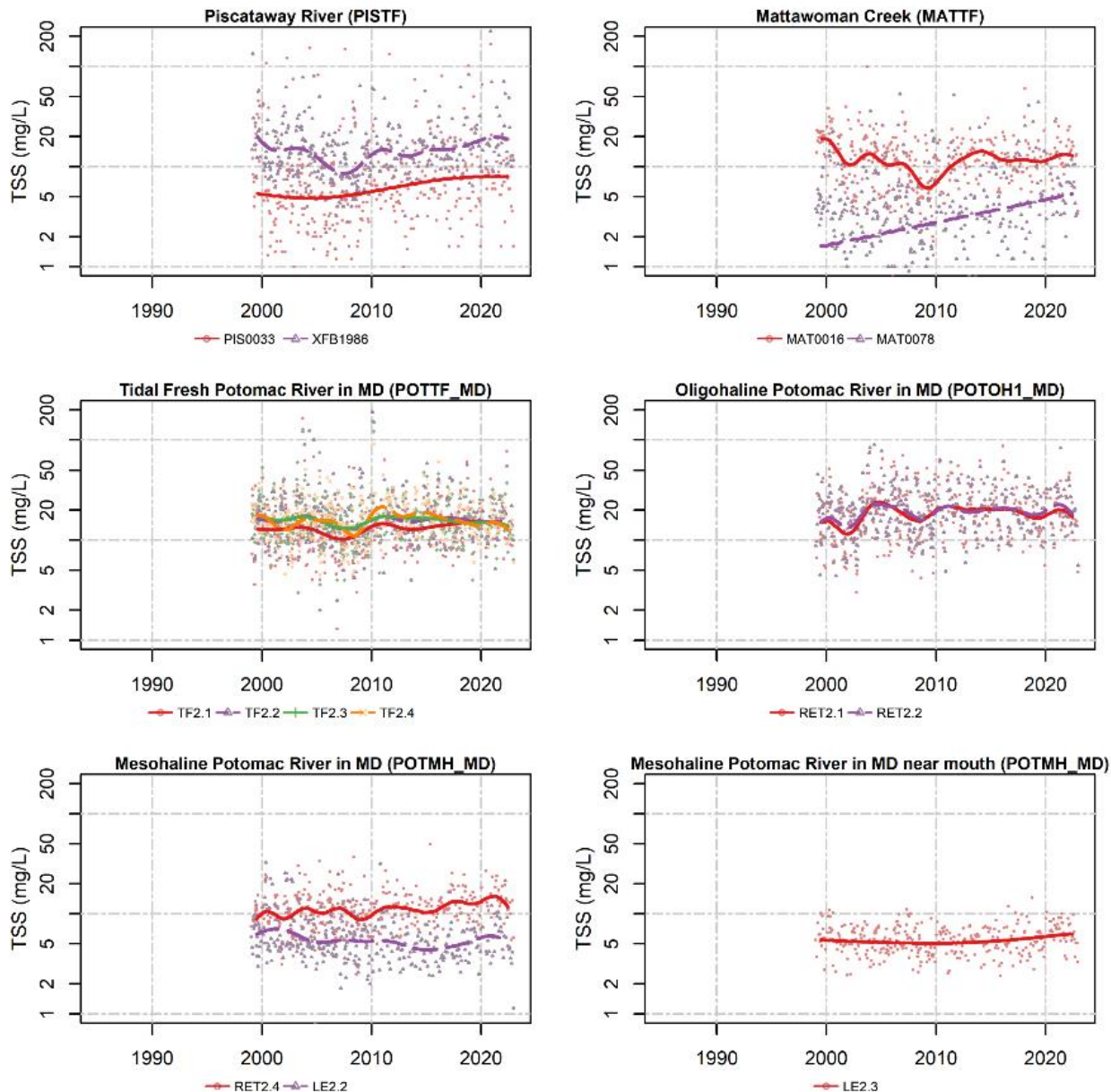


Figure A10. Annual surface total suspended solids concentrations (dots) and average long-term pattern generated from non-flow adjusted Generalized Additive Models (GAMs). Colored dots represent data corresponding to the monitoring station shown indicated in the legend; colored lines represent mean annual GAM estimates for the noted monitoring stations.

- Summer Surface Dissolved Oxygen

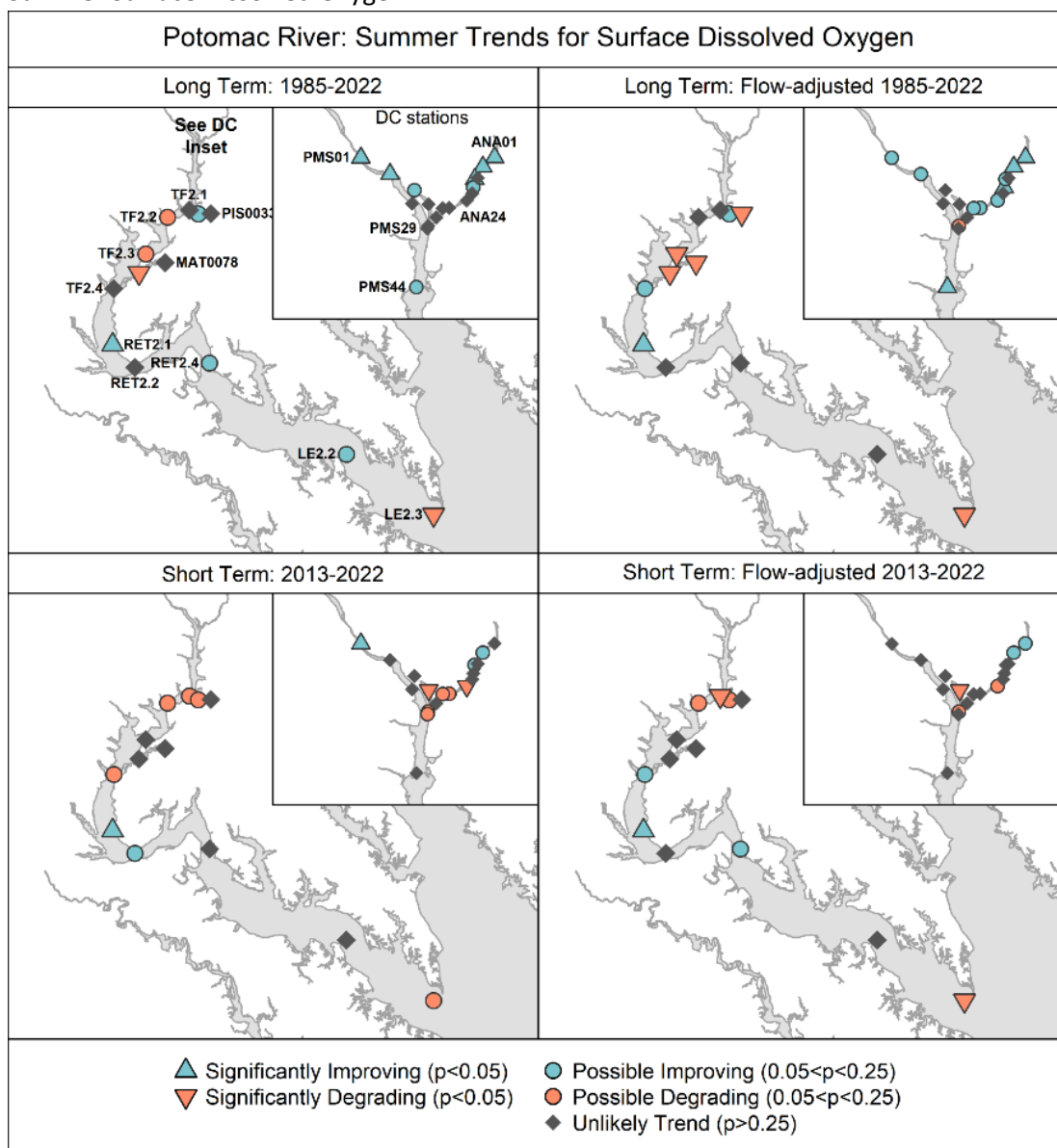


Figure A11. Annual flow-adjusted surface summer dissolved oxygen concentration trends as calculated using Generalized Additive Models (Murphy et al. 2019. Base map credit Chesapeake Bay Program, [www.chesapeakebay.net](http://www.chesapeakebay.net), North American Datum 1983. For more information on the tidal stations and Chesapeake Bay tidal water quality monitoring, refer to <https://www.chesapeakebay.net/what/programs/quality-assurance/tidal-water-quality-monitoring>.

### Summer (June-Sept) Surface DO Data and Average Predictions

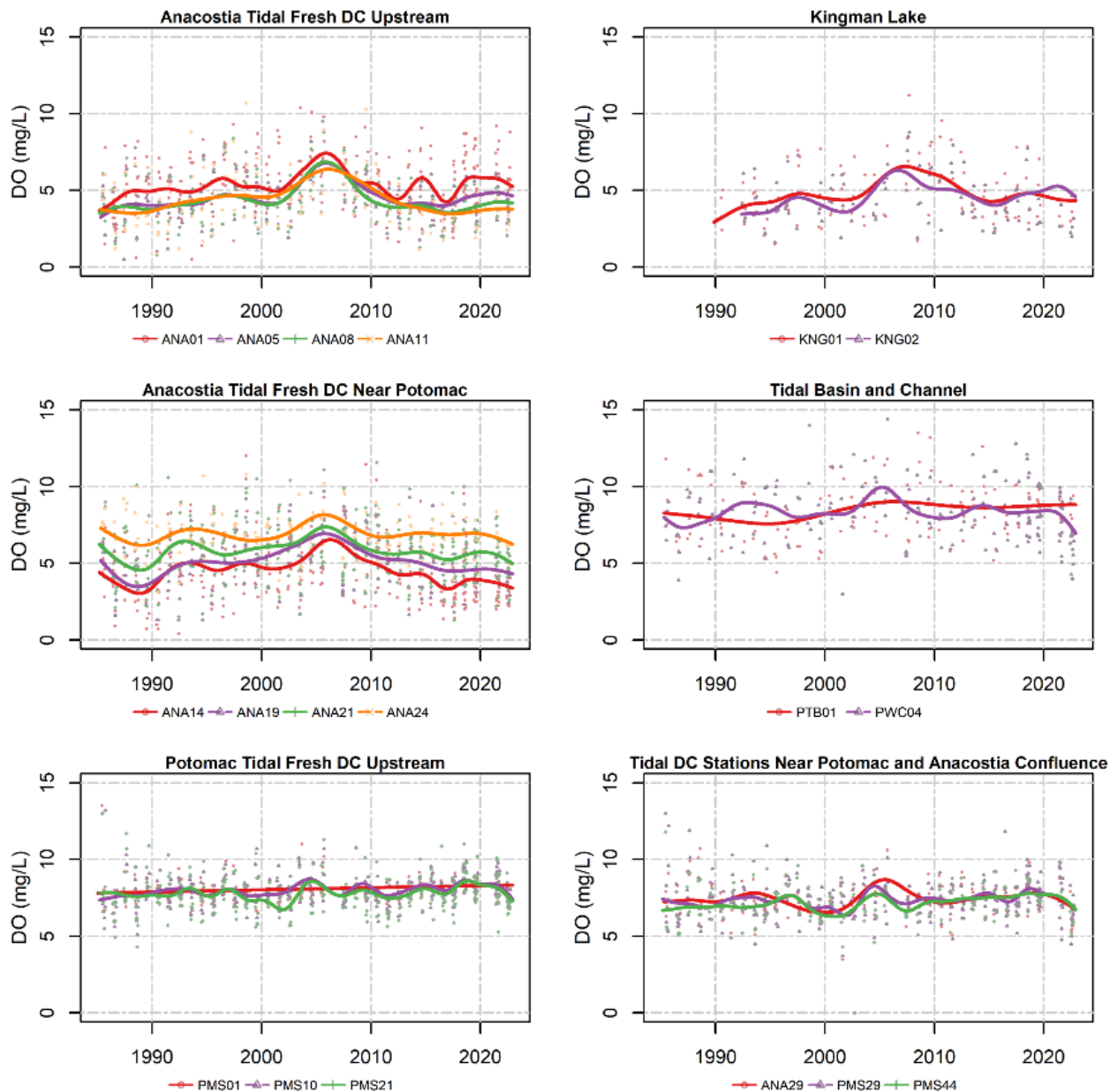


Figure A12. Annual surface dissolved oxygen concentration data (dots) and average long-term pattern generated from non-flow adjusted Generalized Additive Models (GAMs). Colored dots represent data corresponding to the monitoring station shown indicated in the legend; colored lines represent mean annual GAM estimates for the noted monitoring stations.